UNIVERSITÀ
DEGLI STUDI
DI PADOVA

UNIVERSITÀ DEGLI STUDI DI PADOVA

DIPARTIMENTO DI PEDIATRIA

SCUOLA DI DOTTORATO DI RICERCA
IN MEDICINA DELLO SVILUPPO E SCIENZE DELLA PROGRAMMAZIONE
INDIRIZZO: MALATTIE RARE; GENETICA, BIOLOGIA E BIOCHIMICA
CICLO XXIV

EXTRACELLULAR MATRIX-DEGRADING ENZYMES AND CONTROL OF FIBROBLAST GROWTH FACTOR-2 (FGF-2) SIGNALING IN PEDIATRIC GLIOMA CELL LINES

Direttore della Scuola: Ch.mo Prof. Giuseppe Basso
Coordinatore d'indirizzo: Ch.mo Prof. Giorgio Perilongo
Supervisore: Dott. Maurizio Onisto
Co-supervisore: Ch.mo Prof. Paolo Mignatti

Dottoranda: Evelyne Tassone

Table of contents

Summary

The main purpose of my research project was to investigate the role of two extracellular matrix-degrading enzymes, heparanase (HPSE) and membrane-type 1 matrix metalloproteinase (MT1-MMP), in pediatric gliomas. I spent the first two years of my PhD program in Dott. Maurizio Onisto's laboratory (University of Padua). Then I continued my work at New York University School of Medicine, under the supervision of Prof. Paolo Mignatti, whose experimental work focuses on the molecular mechanisms of proteolysis-independent signaling by MT1-MMP and its physiological inhibitor, tissue inhibitor of metalloproteinase-2 (TIMP-2).

Gliomas, the most common primary brain tumors, comprise a heterogeneous group of neoplasms that originate from glial cells. Despite recent advances in the management of these tumors, children affected by gliomas, particularly the more aggressive forms, have a poor prognosis. Gliomas can diffusely penetrate throughout the brain, even though they remain localized in this organ. One of the most important events during glioma cell invasion is extracellular matrix (ECM) degradation, a complex mechanism that involves both glycosidic and proteolytic enzymes. HPSE is an endo-β-D-glucuronidase secreted in the ECM, where it cleaves the heparan sulfate side chains of both soluble and membrane-bound proteoglycans. MT1-MMP, a cell membrane-bound proteinase with an extracellular catalytic domain and a short cytoplasmic tail, has been implicated in the proteolytic degradation of extracellular and transmembrane proteins. High levels of HPSE and MT1-MMP are present in a variety of aggressive malignancies, a finding that highlights their important role in cancer invasion and metastasis.

In this study we characterized pediatric glioma cell lines derived from different types of gliomas: two glioblastoma multiforme, one anaplastic astrocytoma, one diffuse astrocytoma and one pilocytic astrocytoma. In addition, we used human MCF-7 breast adenocarcinoma cells to examine the role of MT1-MMP, because these cells do not express this proteinase and thus represent an ideal model for the regulation of its expression.

The data reported show that MT1-MMP inhibits activation of intracellular signaling (ERK1/2) by fibroblast growth factor-2 (FGF-2) in MCF-7 cells. MT1-MMP does not degrade FGF-2 but reduces FGF-2 binding to the surface of MCF-7 cells. Since the biological effects of FGF-2 are mediated by its low- (heparan sulfate proteoglycans, HSPGs) and high-affinity receptors (FGFRs), we hypothesize that MT1-MMP controls FGF-2 interaction with these receptors.

In contrast, we found no clear correlation between HPSE, MT1-MMP or FGF-2 expression and the aggressiveness of the pediatric astrocytoma cells. The results show

that gene silencing of *HPSE* in a pediatric glioblastoma cell line does not affect vascular endothelial growth factor (*VEGF)* expression or cell proliferation, but upregulates matrix metalloproteinase-2 (*MMP-2)* and *MT1-MMP* expression. Moreover, ERK1/2 activation by FGF-2 inversely correlates with MT1-MMP expression in these pediatric glioma cells, although they express MT1-MMP in its inactive, proenzyme form. Unlike in MCF-7 cells, ERK1/2 activation by FGF-2 was decreased in the glioma cells by an MMP inhibitor, suggesting the involvement of MMPs other than MT1-MMP in pediatric astrocytoma activation of ERK1/2. No differences in ERK1/2 activation by FGF-2 were detected in glioma cells transfected with wt MT1-MMP, even though MT1-MMP was expressed in its active form. Finally, TIMP-2 induced ERK1/2 activation in all glioma cells irrespective of MT1-MMP expression. Because in the MCF-7 cells ERK1/2 activation by TIMP-2 is mediated by MT1-MMP, this finding indicates that in pediatric glioma cells TIMP-2 may have signaling functions independent of MT1-MMP.

Taken together, the results show that in MCF-7 cells MT1-MMP controls ERK1/2 activation by FGF-2 and FGF-2 interaction with its receptors. However, MT1-MMP does not have these effects in pediatric glioma cells, indicating a more complex control mechanism of intracellular signaling. This initial characterization of these unique pediatric astrocytoma cell lines provides new insights into the knowledge of this poorly studied group of tumors.

Riassunto

L'obiettivo principale del mio progetto di ricerca è stato analizzare il ruolo di due enzimi che degradano la matrice extracellulare, l'"heparanase" (HPSE) e la "membrane-type 1 matrix metalloproteinase" (MT1-MMP), nei gliomi pediatrici. Ho trascorso i primi due anni di Dottorato nel laboratorio del Dott. Maurizio Onisto (Università di Padova). Ho poi continuato il mio lavoro presso la New York University School of Medicine, sotto la supervisione del Prof. Paolo Mignatti, il cui lavoro sperimentale è focalizzato sull'approfondimento dei meccanismi molecolari alla base dell'attivazione del segnale intracellulare da parte di MT1-MMP e del suo inibitore fisiologico, il "tissue inhibitor of metalloproteinases-2" (TIMP-2).

I gliomi, i più comuni tumori cerebrali primari, comprendono un gruppo eterogeneo di neoplasie che originano dalle cellule gliali. Nonostante i recenti progressi raggiunti nel trattamento e nel controllo di tali tumori, la prognosi dei bambini affetti da glioma, ed in particolare dalle sue forme più aggressive, rimane tuttora infausta. Pur essendo confinati nell'organo nel quale originano, i gliomi posso invadere tutte le aree del cervello. Uno degli eventi più importanti che caratterizzano l'invasività dei gliomi è costituito dalla degradazione della matrice extracellulare, un complesso meccanismo che coinvolge enzimi sia glicosidici sia proteolitici. HPSE è una endo-β-D-glucuronidasi secreta nella matrice extracellulare, nella quale taglia le catene di eparan solfato dei proteoglicani solubili e legati alla membrana. MT1-MMP, una proteasi legata alla membrana e composta da un dominio catalitico extracellulare e da una piccola coda citoplasmatica, è coinvolta nella degradazione proteolitica di proteine extracellulari e di membrana. Elevati livelli di HPSE e MT1-MMP sono stati riscontrati in numerosi tipi di tumore e tale evidenza sottolinea il ruolo chiave che essi svolgono nell'invasività tumorale e nella formazione di metastasi.

In questo studio sono state caratterizzate cinque linee cellulari di glioma pediatrico derivanti da diversi tipi di glioma: due glioblastomi multiformi, un astrocitoma anaplastico, un astrocitoma diffuso ed un astrocitoma pilocitico. Con lo scopo iniziale di esaminare il ruolo di MT1-MMP nell'attivazione del segnale indotto dall'FGF-2, sono state inoltre utilizzate cellule di carcinoma mammario MCF-7, le quali non esprimono MT1-MMP e perciò rappresentano un modello ideale per studiare la regolazione della sua espressione.

I dati riportati mostrano che nelle cellule MCF-7 MT1-MMP inibisce l'attivazione del segnale intracellulare (ERK1/2) da parte del "fibroblast growth factor-2" (FGF-2). MT1-MMP non degrada l'FGF-2, ma riduce il legame di questo fattore di crescita alla superficie delle cellule. Poichè gli effetti biologici dell'FGF-2 sono mediati dai suoi

recettori a bassa e ad alta affinità (rispettivamente proteoglicani eparan solfato e recettori tirosin chinasici), ipotizziamo che MT1-MMP controlli l'interazione tra l'FGF-2 ed i suoi recettori.

Nelle cellule di astrocitoma pediatrico non è stata identificata alcuna chiara correlazione tra espressione di HPSE, MT1-MMP o FGF-2 ed aggressività tumorale. I risultati inoltre dimostrano che il silenziamento genico di HPSE in una linea cellulare di glioblastoma pediatrico non influenza l'espressione del "vascular endothelial growth factor" (VEGF) o la proliferazione cellulare, ma determina la sovraespressione della "matrix metalloproteinase-2" (MMP-2) e di MT1-MMP. Inoltre, nelle cellule di glioma, l'attivazione di ERK1/2 da parte di FGF-2 è inversamente correlata all'espressione di MT1-MMP, nonostante in queste cellule MT1-MMP sia espressa in forma di proenzima inattivo. Al contrario di quanto accade nelle cellule MCF-7, nelle cellule di glioma l'attivazione di ERK1/2 da parte dell'FGF-2 è inibita dal trattamento con un inibitore di MMP, suggerendo che in queste cellule MMP diverse da MT1-MMP possano essere coinvolte nell'attivazione di ERK1/2. Questa ipotesi è sostenuta anche dall'osservazione che nelle cellule di glioma trasfettate con MT1-MMP wt non si ottiene alcuna diminuzione dell'attivazione di ERK1/2 dall'FGF-2, anche se MT1-MMP è espressa in forma attiva. Infine, al contrario delle cellule MCF-7, in tutte le cellule di glioma, TIMP-2 induce l'attivazione di ERK1/2 indipendentemente dall'espressione di MT1-MMP. Poichè nelle cellule MCF-7 l'attivazione di ERK1/2 da parte di TIMP-2 è mediata da MT1-MMP, questa osservazione indica che nelle cellule di glioma pediatrico il TIMP-2 può attivare segnali intracellulari con un meccanismo indipendente da MT1-MMP.

In conclusione, i risultati ottenuti mostrano che nelle cellule MCF-7 MT1-MMP controlla l'attivazione di ERK1/2 da parte dell'FGF-2 e l'interazione di questo fattore di crescita con i suoi recettori. Al contrario, MT1-MMP non ha questi effetti nelle cellule di glioma pediatrico, indicando l'esistenza di un più complesso meccanismo di controllo del segnale intracellulare. La caratterizzazione delle linee cellulari di astrocitoma pediatrico presentata in questa tesi offre una più completa conoscenza di questo gruppo di tumori ancora poco studiati.

Chapter 1: Introduction

1.1 Primary central nervous system tumors

Primary central nervous system (CNS) tumors account for approximately 2-3% of all cancer types; in Western Europe, North America and Australia, the mortality rates for these tumors are 3 - 7 per 100,000 people per year [1]. CNS tumors, together with leukemia, are the leading cause of childhood cancer-related mortality [2]. These tumors comprise a heterogeneous group of benign and malignant neoplasms that originate from brain cells, the membranes around the brain (meninges), nerves, or glands. They can directly affect normal brain cells, but also produce inflammation and increase pressure in the brain. The causes of primary brain tumors are still unknown. Genetic predisposition to brain tumors appears relatively uncommon, although they may be inherited as a part of several familial diseases, such as neurofibromatosis; moreover, environmental factors associated with primary brain tumors are difficult to identify. Tumors may occur at any age, but most brain tumors are rare in the first year of life [3]. Over the past three decades, the management of brain tumors in children has positively evolved reflecting refinements in tumor classification, delineation of risk groups within histological subsets of tumors, and incorporation of recently developed molecular and imaging techniques. These advances have improved the outcome of some childhood brain tumors, even though the prognosis of other cancer types remains still very poor. Pediatric brain tumors are usually treated by different approaches involving surgery, radiation and chemotherapy. The specific modalities depend on tumor histology, location, patient's age, and risk factors of the individual tumor subgroups [4].

1.2 Pediatric gliomas

1.2.1 Definition and characteristics of gliomas

Histologically, human tumors are diagnosed and graded according to the World Health Organization (WHO) system, most recently published in 2007 [5], which firstly classifies brain tumors into glial and nonglial (neuronal) tumors.
As reported in the population-based study by Kaatsch and colleagues [6], glial tumors (or gliomas) comprise approximately 60% of pediatric brain tumors, whereas the remaining 40% are heterogeneous and consist of medulloblastomas and other embryonal tumors, craniopharyngiomas, pineal tumors, meningiomas, and others (Table 1.1) [7].

	Tumor Entity	World Health Organization Grade	Frequency (%)
Gliomas	Astrocytomas	1-4	41.7
	Ependymomas	1-3	10.4
	Gangliogliomas[a]	1	3.2
	Oligodendrogliomas	2-3	1.1
Nonglial tumors	Embryonal tumors	4	25.7
	Craniopharyngeomas	1	4.4
	Pineal tumors	1-4	1.3
	Meningeomas	1-3	1.2
	Others (eg, lymphomas, germ cell tumors, metastases)	NA	11.0

[a] Gangliogliomas are mixed neuronal-glial tumors.

Table 1.1. Main histological subtypes, WHO grade, and frequency of CNS tumors in children (data from Kaatsch *et al.*, 2001) [7].

A glial tumor is a primary brain tumor arising from the supportive cells of the brain, named glial or neuroglial cells, the most common cellular component of the brain. Glial cells surround and provide mechanical support and electrical insulation for the neurons in the CNS; together with neurons, they compose the tissue of the CNS. As shown in Fig. 1.1, different types of glial cells exist: astrocytes, microglial cells, ependymal cells, and oligodendrocytes.

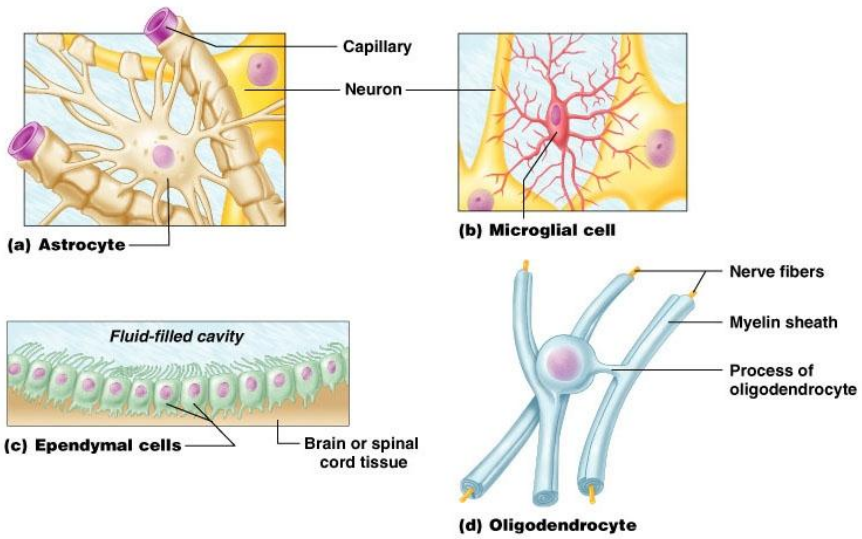

Figure 1.1. Neuroglial cells: (a) astrocyte; (b) microglial cell; (c) ependymal cell; (d) oligodendrocyte. Copyright © 2004 Pearson Education, Inc.

Astrocytes have a characteristic star-like morphology with long cytoplasmic processes that connect neurons and capillary endothelial cells. They provide both mechanical and metabolic support for neurons, regulating the environment where they function; they contribute to the blood-brain barrier structure, control the transport of different molecules from blood to neural tissue and coordinate nerve pathway development.
Microglial cells, easily recognized for their small size, provide a protective function to the nervous tissue.
Ependymal cells form the linings of the ventricles of the brain and the central canal of the spinal cord, and contribute to the production of cerebrospinal fluid (CSF).
The name of the fourth type of glial cells, the oligodendrocytes, derives from their limited number of dendritic processes, which provide electrical insulation for the adjacent neurons by forming a part of the myelin sheath, and thereby increasing the speed of transmission of action potentials along that axon (Fig. 1.1).
Gliomas diffusely penetrate throughout the brain, but they do not metastasize and remain localized in their organ compartment. In contrast to most other malignant tumors, gliomas grow in a terminally differentiated organ, the brain, with no regular and cyclical cell turnover, unlike epithelia or bone marrow. Although pools of cycling cells may be found in the brain, they are highly discrete, and their mitotic activity is expressed only under specific circumstances, such as following injury. Importantly, the CNS is protected by the blood-brain barrier, which prevents the entry of numerous drugs, including many systemically effective chemotherapeutic agents [8].

1.2.2 Classification by cell type and localization

The WHO system classifies gliomas mainly by their morphological resemblance to the respective normal glial cells from which they derive, cytoarchitecture and immunohistological marker profile. Gliomas arise from astrocytes (astrocytomas), oligodendrocytes (oligodendrogliomas) and ependymal cells (ependymomas). In some cases, gliomas can have mixed features and are therefore named mixed gliomas (for example, oligoastrocytoma) (Table 1.2).
Because the localization of brain tumors plays an important role in the overall prognosis, gliomas are further categorized by their anatomical site into the following groups: supratentorial (in the cerebrum), brain stem, and cerebellar gliomas [7].

Tumor Entity	World Health Organization Grade				Frequency[a] (%)
	1	2	3	4	
Astrocytic tumors					38.8
Subependymal giant cell astrocytoma	X				0.4
Pilocytic astrocytoma	X				14.8
Pilomyxoid astrocytoma		X			NA
Diffuse astrocytoma		X			2.2
Pleomorphic xanthoastrocytoma		X			0.4
Anaplastic astrocytoma			X		1.9
Glioblastoma				X	2.8
Giant cell sarcoma				X	0.1
Gliosarcoma				X	0.1
Astrocytoma, not otherwise specified					15.6
Oligodendroglial tumors					1.5
Oligodendroglioma		X			1.4
Anaplastic oligodendroglioma			X		0.1
Oligoastrocytic tumors					0.6
Oligoastrocytoma		X			NA
Anaplastic oligoastrocytoma			X		NA
Ependymal tumors					8.9
Subependymoma	X				0.1
Myxopapillary ependymoma	X				0.3
Ependymoma		X			5.3
Anaplastic ependymoma			X		3.3
Choroid plexus tumors					1.8
Choroid plexus papilloma	X				1.2
Atypical choroids plexus papilloma		X			NA
Choroid plexus carcinoma			X		0.6

[a] Frequency among pediatric central nervous system tumors excluding germ cell tumors.

Table 1.2. Gliomas, tumor grades, and frequency according to the WHO classification of CNS tumors [7].

1.2.3 Classification by grade

In addition to the classifications described above, there is also a WHO grading system that assigns a grade from I to IV to each type of tumor, with I being the least aggressive and IV the most malignant. The WHO grading scheme is determined by the pathologic evaluation of the tumor and the presence of specific factors, including atypia, mitosis, endothelial proliferation, and necrosis. Grade I and II tumors are also defined as low-grade gliomas, whereas grade III and IV are called high-grade gliomas. The system distinguishes four grades for astrocytomas (I, II, III and IV) and two grades (II and III) for oligodendrogliomas and oligoastrocytomas [5].

Although the WHO system is based only upon adult tumors, which share many morphological features with their pediatric counterparts, it is important to remember that this classification may not be strictly representative of the histopathological differences characteristic of childhood. Furthermore, recent molecular findings have shown that the

identified histological groups comprise several entities with morphological similarities but distinct pathways of tumorigenesis, and these molecular differences may play a key role in determining the appropriate therapeutic approach.

1.2.4 Astrocytomas

For the purposes of this thesis, only astrocytomas will be considered in the next paragraphs, and in particular a specific subtype for each grade of astrocytoma will be extensively examined, as reported in Table 1.3.

Tumor	Grade
Pilocytic astrocytoma	I
Diffuse astrocytoma	II
Anaplastic astrocytoma	III
Glioblastoma	IV

Table 1.3. Astrocytomas and tumor grade.

Pilocytic astrocytoma

This particular type of astrocytoma has been referred to as pilocytic - meaning "hair-like"- because its cells often show a biphasic, ''piloid'' pattern, with long and bipolar processes. Pilocytic astrocytoma is the most frequent pediatric glioma, with an incidence equal to 20% of all tumors in children up to 14 years of age, and 15% in teenagers aged 15 to 18 years. Pilocytic astrocytoma is a grade I glioma, usually well-circumscribed, slow-growing, with a morphologically benign appearance. It is usually associated with a favorable prognosis, as indicated by a 10-year survival rate of 96% [9]. It can be localized in the cerebellum, the hypothalamic/optic pathways, thalamic region, cerebral hemispheres, brain stem, and spinal cord. Microcystic regions and other regions with oligodendroglioma-like cells can be found in the tumor besides the typical compact ''piloid'' areas.

Diffuse astrocytoma

Diffuse astrocytoma is about 6 to 7 times less common in children than pilocytic astrocytoma. It is classified as a grade II glioma because of its tendency to be well differentiated and infiltrative, with increased cell density and some cellular anomalies or atypias. Tumor cells can generate a loosely structured, often microcystic tumor matrix. Diffuse astrocytoma can be located in any region of the CNS, with the most frequent location being the frontal and temporal lobes. Although this low-grade tumor presents specific genetic alterations (paragraph 1.2.6), and their accumulation may correlate with

tumor progression and malignancy, the evolution of the disease into anaplastic astrocytoma or secondary glioblastoma is only observed in about 10% of children with this tumor [7,10,11].

Anaplastic astrocytoma

Anaplastic astrocytoma principally arises in the cerebral hemispheres, with the same frequency in children as diffuse astrocytoma. As a grade III tumor, anaplastic astrocytoma is characterized by rapid and infiltrative growth, and shows signs of increased vessel density, cellular atypias, anaplasia, elevated mitotic activity and high cell density.

Glioblastoma

Glioblastoma, a grade IV astrocytoma typically located in the fronto-temporal region, occurs about 1.5 times more often than anaplastic astrocytoma in children, but is approximately 100 times less common in children than in adults, where it usually manifests. Glioblastoma, the most aggressive and diffusely infiltrating glioma, shows vascular endothelial proliferation, necrosis, very high cell density, nuclear atypias and mitotic activity. It mostly occurs *de novo* (primary glioblastoma), but can also evolve from a preceding low-grade astrocytoma (secondary glioblastoma) [7,8].

1.2.5 Clinical presentation

Because pediatric low-grade gliomas encompass a heterogeneous group of tumors with different histology and behavior, clinical presentation can vary accordingly. Almost 50% of children have symptoms for 6 months or longer prior to diagnosis. Patients usually show nonspecific symptoms due to increased intracranial pressure from obstruction of the ventricles, including headache (particularly in the morning), nausea, vomiting and lethargy. Physical examination findings include decreased upward gaze, sixth cranial nerve palsies, and papilledema. These are most often caused by tumors located in the cerebellum, optic chiasm/hypothalamus, dorsally exophytic brain stem, and tectum. Other symptoms are specific for tumor localization and include focal neurological findings, seizures and endocrinopathies [12].

Children with high-grade gliomas can also present with a variety of signs and symptoms that vary according to tumor localization and child’s age. In this case, the history is typically short, with an evolution of symptoms measured in a few months to weeks, sometimes even days. Patients with cortical tumors often show seizures as their first manifestation, but they also can experience hemiparesis, visual field deficits, and headache. A mass that obstructs cerebrospinal fluid’s flow and causes hydrocephalus often produces morning headache, vomiting, and papilledema. Very young children may

have nonspecific symptoms, such as irritability, lethargy, vomiting, failure to thrive, or macrocephaly [13].

1.2.6 Tumor biology

The tumorigenesis of pediatric gliomas is not well-understood. Typical cytogenetic and molecular abnormalities of adult gliomas occur less frequently and with different patterns in children, and to date only few of them have been identified as specific of children.
Studying tumors in children affected by genetic susceptibility syndromes improves the knowledge about the signal transduction pathways involved in the development of low-grade gliomas. In particular, in children with type 1 neurofibromatosis the inactivation of the tumor suppressor neurofibromin results in increased Ras activity and astrocyte proliferation. This aberrant activation is responsible for the formation of low-grade astrocytomas in 15% to 20% of type 1 neurofibromatosis patients [14]. Moreover, some type 1 neurofibromatosis children with pilocytic astrocytomas show frequent activation of the mammalian target of rapamycin (mTOR) pathway [15].
Activating mutations of KRAS, which also result in the activation of MAPK signaling, have been reported in a minor fraction of sporadic pilocytic astrocytomas [16].
Adult low-grade gliomas show frequent p53 mutations, which in children account for only 5% to 10% of low-grade gliomas [17].
Many studies have also revealed a balanced karyotype in a majority of pilocytic astrocytomas, although duplication of chromosomes 5 and 7 are the most frequently found chromosomal aberrations. A small nonrandom duplication in the 7q34 region can be present in pilocytic astrocytomas. This duplication involves the oncogene *BRAF* and causes the up-regulation of the RAS/RAF/MEK pathway [12,18]. Loss of heterozygosity of chromosomal regions 1p36 and 19q13 is a favorable prognostic factor in adults with oligodendrogliomas, but not in pediatric tumors [19].
The gain of chromosomal material at chromosome arm 1q is associated with a significantly shorter survival in pediatric anaplastic astrocytomas [20]. Other specific genomic aberrations of these tumors are gains of 5q and losses of 6q, 9q, 12q, and 22q. Mutations in the PTEN tumor suppressor gene at 10q23 are rarely observed in pediatric anaplastic astrocytoma (6%), and are associated with poor prognosis [21].
Although pediatric and adult glioblastomas are histologically very similar, the genetic and molecular analysis of these tumors suggests that most childhood lesions arise through molecular pathways distinct from those characteristic of adults.
TP53 mutations, always associated with secondary glioblastoma in adults, frequently occur in *de novo* (primary) pediatric glioblastomas [22].

Genomic amplification or rearrangement of the epidermal growth factor receptor (*EGFR*) gene are the most common genetic aberrations in adult primary glioblastoma, but they are rarely (less than 10%) observed in pediatric tumors [23].
Similarly, mutations of the PTEN tumor suppressor gene at 10q23 occur less frequently in pediatric glioblastomas than in adult tumors, and are associated with poor prognosis [21].
Some genetic aberrations, such as gains of 1q, 3q, and 16p, and losses of 8q, and 17p, are more frequent in the pediatric age group [20].
According to the activation status of the MAPK and AKT pathways, two subsets of pediatric glioblastomas with different prognosis can be defined. In particular, the activation of these intracellular signaling cascades correlates with poor prognosis [24].
Amplification of the platelet-derived growth factor receptor α (*PDGFRA*) gene has been detected in 15% of pediatric malignant gliomas, suggesting that the encoded protein may be a relevant target for some tumors [4].

1.2.7 Treatment and outcomes

The success of treatment of patients affected by gliomas is highly dependent on tumor localization.
Surgery alone can provide prolonged, disease-free survival for those pediatric low-grade lesions that can be completely removed. Total resection is associated with 10-year overall survival rates of 90% or greater and rare tumor relapses. Children can also undergo subtotal resection or biopsy, and in some cases surgery is not feasible because of the tumor proximity or invasion of vital structures. When progression occurs, adjuvant therapies are initiated [25]. Radiation therapy typically results in an appreciable tumor reduction in patients with low-grade gliomas, and may improve the time of disease-free survival in children with partially resected lesions. Despite these potential benefits, radiotherapy can have deleterious side effects on the developing nervous, endocrine, and vascular systems, particularly in young children. For these reasons, chemotherapy is often used as adjuvant therapy for children with progressive low-grade gliomas. The combination of carboplatin and vincristine results in tumor reduction or stable disease, but up to 40% of children experience hypersensitivity reactions. Alternative treatments with other chemotherapeutic agents can also be effective [26].
Despite improvements in neurosurgery, radiotherapy, and chemotherapy, children with pediatric high-grade gliomas are still difficult to treat, have a poor clinical outcome, and most of them die within a few years of diagnosis. These tumors are invasive, aggressive, and relatively rare in children, making large randomized clinical trials challenging. Since many standard adult therapies have displayed only few benefits in children, the genetic and molecular differences between pediatric and adult high-grade glial tumors could be potentially important for the choice of the correct therapy.

Pediatric patients who undergo a complete surgical resection have a better chance at long-term survival than those subjected only to biopsy and partial tumor resection. High-grade gliomas almost always show response to radiation therapy, but this effect is usually transient, and most patients experience recurrence or disease progression within 6-18 months of diagnosis. The addition of high-dose chemotherapy only provides a short interval of disease control, with good initial responses to some chemotherapeutic agents, but does not improve survival.

A better survival for pediatric high-grade gliomas has been recently achieved by using combined treatment, based on radiation therapy and/or chemotherapy together with agents that have shown promise in preclinical studies, such as radiosensitizers, anti-angiogenic molecules, growth factor receptor inhibitors, and others. Although, for example, survival does not appear to be improved when children are treated with chemoradiotherapy and adjuvant temozolomide, hypermethylation of the O6-methylguanine-DNA-methyltransferase (MGMT) promoter is predictive of greater sensitivity to alkylating agents. Because of these still controversial results, biomedical research efforts should be focused on the use of new multitherapeutic treatments that are well-tolerated and offer the greatest anti-tumor activity for pediatric high-grade gliomas [27].

1.3 The extracellular matrix in the central nervous system

Extracellular space accounts for approximately 20% of total volume in the mature brain, and is filled with a highly structured and organized extracellular matrix (ECM). The ECM components are synthesized by both neurons and glial cells, which can easily interact with each other. The polysaccharide hyaluronic acid, a basic constituent of the brain ECM, non-covalently binds to proteoglycans, such as chondroitin sulfate and heparan sulfate proteoglycans, and glycoproteins, like for example tenascins and laminins. These and other proteins contribute to the structural composition of the brain ECM [28].

ECM molecules are expressed in the developing embryo, and the ECM undergoes significant changes during CNS development. The ECM of the embryonic and young brain supports neurogenesis, gliogenesis, cell migration, axonal outgrowth, genesis and rearrangements of synapses. ECM molecules also have a key role in the adult CNS, where they are present in almost every structure of the brain and spinal cord; the adult ECM is non-permissive for axonal outgrowth and inhibits regeneration and major reorganization processes [29].

Despite its typical heterogeneity, the ECM functions as an extracellular presynaptic and synaptic scaffold that directs the clustering of neurotransmitter receptors in the postsynaptic compartment and as a barrier for reducing the diffusion of soluble and membrane-associated molecules away from synapses. The ECM also supports the

migration and differentiation of stem cells present in the nervous system, and helps the correct localization of ion channels and transporters between astrocytic processes and blood vessels. Furthermore, the growth factors present in the ECM can bind to their cognate receptors at the cell surface in both neurons and glial cells, thus contributing to the regulation of different intracellular signaling pathways [30].

1.4 Molecular biology of glioma cell invasion

The biological mechanisms that underlie glioma cell invasion are not completely understood. Single tumor cells can invade normal brain tissue, thus creating numerous neoplastic lesions distinct from the primary tumor. This phenomenon involves cell interactions with the ECM and adjacent cells, and active cell movement is supported by specific biochemical processes. As shown in Fig. 1.2, tumor cell invasion requires four different and sequential stages:

a) detachment of invading cells from the primary tumor mass,
b) adhesion to the ECM,
c) degradation of the ECM, and
d) cell movement and contraction.

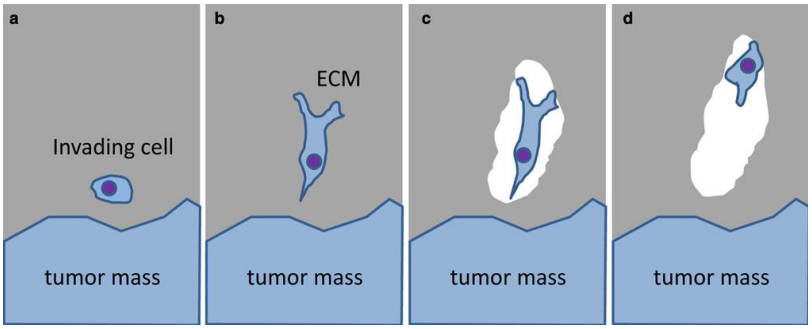

Figure 1.2. Schematic representation of the mechanism of glioma invasion [31].

The detachment of invading glioma cells from the primary tumor mass firstly involves the destabilization and disorganization of cadherin-mediated junctions that hold the primary mass together. After this event, decreased expression of connexin 43, an adhesion molecule primarily expressed in astrocytes, leads to a reduction in gap junction formation, which in turn facilitates uncontrolled cell division and de-differentiation. Finally, the hyaluronan receptor CD44, which normally anchors the primary mass to the ECM, is proteolytically cleaved.

Glioma cells adhere to the ECM by integrins, transmembrane glycoproteins that interact with numerous ECM proteins, such as fibronectin, vitronectin, fibrinogen, and cell surface molecules.

The degradation of different components of the ECM in order to allow the free movement of invading glioma cells is a complex mechanism that involves both proteolytic and glycosidic enzymes, such as the soluble and/or membrane-bound matrix metalloproteinases (MMPs and/or MT-MMPs) and the heparan sulfate-degrading enzyme heparanase, respectively. The expression and activity of these ECM-degrading enzymes will be discussed in the following paragraphs.

The migration of glioma cells, the last event of the invasion process, is characterized by the extension of a prominent leading cytoplasmic process followed by a forward movement of the cell body. Glioma cell motility and contractility requires many signaling molecules and cytoskeletal components, such as myosin II [31,32].

1.5 Matrix metalloproteinases (MMPs)

The ECM does not only provide a structural barrier to tissues or cells, but also actively participates in cell proliferation, motility, survival and apoptosis. Many extracellular and membrane-bound proteinases, such as the matrix metalloproteinases (MMPs), can regulate these physiological processes, and also mediate several changes in the microenvironment during tumor invasion and metastasis.

The MMPs belong to a family of zinc-dependent endopeptidases responsible for the degradation of numerous protein targets in the ECM. To date, 23 MMP members have been identified; they are divided in two groups based on their cellular localization (secreted and membrane-bound), or in five main groups according to their structure and substrate specificity: collagenases, gelatinases, membrane-type, stromelysins and matrilysins [33].

As shown in Fig. 1.3, the minimal common structural domains of all MMPs are:

1. an amino-terminal signal sequence (Pre), cleaved by the signal peptidase and necessary to direct the protein to the endoplasmic reticulum prior to its secretion,
2. a pro-domain (Pro) containing a thiol-group (-SH) and a furin cleavage site,
3. a catalytic domain with a zinc-binding site (Zn^{2+}).

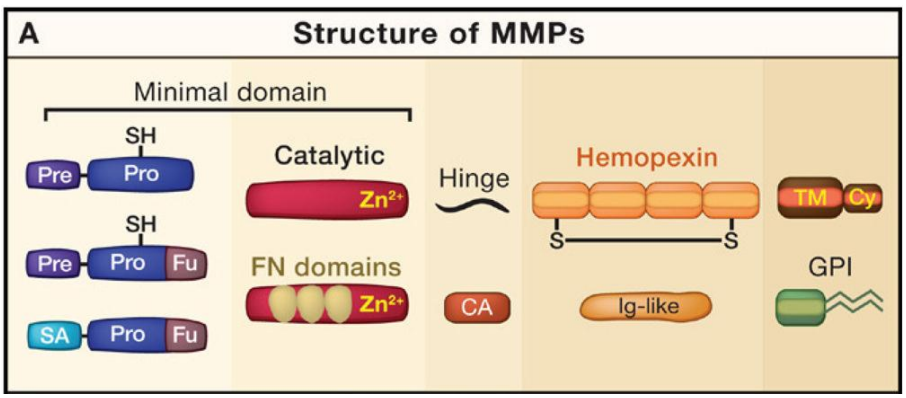

Figure 1.3. Structural domains of MMPs [33].

MMPs are synthesized as inactive proenzymes (proMMPs), in which the -SH group of the N-terminal cysteine residue of the prodomain interacts with the zinc ion of the catalytic site. Only after disruption of this interaction by a mechanism called cysteine switch, which is usually mediated by proteolytic removal of the prodomain or chemical modification of the cysteine residue, the enzyme becomes proteolytically active. The prodomain contains a consensus sequence for the activation of the protein; the proteolytic cleavage of the prodomain can occur intracellularly by furin or in the extracellular space by other MMPs or serine proteinases.

In addition to these minimal domains, most MMPs have a hemopexin-like region, o PEX domain, consisting of four repeats with sequence similarity to the heme-binding protein hemopexin. The PEX domain contains a disulfide bond (S-S) between the first and the last subdomains, and is linked to the catalytic domain via a flexible "hinge" region. The functions of the PEX domain are to provide substrate specificity and interaction with the physiological tissue inhibitors of metalloproteinases (TIMP). Within the PEX domain the gelatinases MMP-2 and -9 possess gelatin-binding repeats that resemble the collagen-binding type II motif of fibronectin (FN).

The membrane-bound MMPs (membrane-type MMP, or MT-MMP) also possess at the C-terminus either a transmembrane (TM) and a cytoplasmic domain (Cy), or a glycosylphosphatidylinositol (GPI) anchor. MMP-23 is unique in its structure as it is bound to the cell membrane through an N-terminal signal anchor (SA) and contains a unique cysteine array (CA) and an immunoglobulin (Ig)-like domain.

Because of their high proteolytic activity and potentially disastrous effects on the cell microenvironment, MMPs are tightly controlled at both transcriptional and post-transcriptional levels.

The net activity of MMPs in the tissue microenvironment depends on the local balance between active proteolytic enzymes and their physiological inhibitors. MMPs are firstly regulated by TIMPs, which are normally expressed in most normal and tumor tissues. TIMP-1, -2, -3, and 4 form reversible 1:1 stoichiometric complexes with active MMPs leading to inhibition of the proteolytic activity. Although both MMPs and TIMPs are expressed by cancer cells, they can also be synthesized and secreted by stromal cells infiltrating the tumor, such as inflammatory cells (neutrophils, macrophages, dendritic cells, lymphocytes, and mast cells), endothelial cells, fibroblasts, and hemopoietic progenitor cells.

MMPs can promote carcinogenesis and play a direct role in cell adhesion, migration, tumor angiogenesis, and proteolytic processing of cytokines, chemokines, growth factors or their receptors, underlying the complex nature of tumorigenesis [34].

1.6 MT1-MMP

1.6.1 Protein structure

Membrane-type 1 matrix metalloproteinase (MT1-MMP or MMP-14), the prototypical member of the MT-MMPs, is characterized by an overall protein structure similar to secreted MMPs with a catalytic domain, a flexible linker peptide and a hemopexin-like domain but, unlike its soluble counterparts, the enzyme is bound to the cell surface by a C-terminal transmembrane region that terminates in a short, 20-aminoacid cytoplasmic domain (Fig. 1.4).

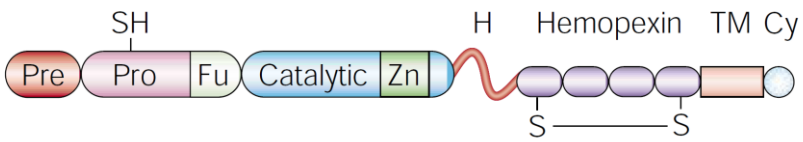

Figure 1.4. Protein structure of MT1-MMP [36].

In the human genome, MT1-MMP is encoded by a single gene located on chromosome 14. The first amino-terminal domain of the protein (Pre) is the signal peptide required to correctly direct MT1-MMP to the endoplasmic reticulum. The prodomain (Pro, M^{1}-R^{111}), which maintains the enzyme in an inactive form and is removed by proteolytic cleavage, contains a thiol-group (-SH) and a consensus sequence (Fu) for cleavage by the pro-hormone convertase furin. The Zn^{2+}-binding catalytic domain (Y^{112}-G^{285}) is responsible for substrate degradation and auto-catalysis. The hinge region (H, E^{286}-I^{318}), located between the catalytic and the hemopexin-like (PEX) domains, is a highly mobile peptide, which confers flexibility to the catalytic domain during its interactions with the different substrates. The PEX domain (C^{319}-C^{508}) is involved in substrate recognition and enzyme homo-dimerization; moreover, it participates in proMMP-2 activation and tumor invasion. MT1-MMP is also characterized by a hydrophobic transmembrane domain (TM, A^{539}-F^{562}). The short cytoplasmic tail (R^{563}-V^{582}) is essential for endocytosis, recycling and membrane localization of MT1-MMP, and is involved in the activation of intracellular signaling (see next paragraph).

This specific structure composed of an extracellular and an intracellular domain confers MT1-MMP with the unique ability to focalize the proteolytic activity to the pericellular microenvironment and closely interact with the intracellular transduction machinery involved in the cell response to extracellular signals [35,36].

1.6.2 Functions and regulation

MT1-MMP is widely expressed in a variety of cell types, where it plays an essential role in both physiological and pathological processes. The active enzyme can degrade numerous components of the ECM, such as collagen types I, II and III, fibrin, laminins-1 and -5, fibronectin, vitronectin, aggrecan, cell adhesion and signaling receptors [37]. In mice, MT1-MMP deficiency results in craniofacial dysmorphism, arthritis, osteopenia, dwarfism, fibrosis of soft tissues and premature death, thus highlighting the importance of MT1-MMP during postnatal development and in the correct turnover of the connective tissue [38].

MT1-MMP is spatially and temporally regulated at both transcriptional and post-transcriptional levels by tightly and well-coordinated mechanisms that control its expression, activity and subcellular localization. These mechanisms comprise activation of the MT1-MMP proenzyme, inhibition of MT1-MMP by TIMPs and autocatalytic inactivation, efficiency of trafficking to, and recycling from the plasma membrane. This multiple regulation mechanism is necessary for the preservation of normal cell functions, and its importance is well-illustrated by several studies that have described the effects of MT1-MMP overexpression in various human tumors, and shown the central role of MT1-MMP in ECM invasion by cancer cells [39].

MT1-MMP is synthesized as a latent proenzyme (60 kDa) that requires proteolytic cleavage of the propeptide for activation. Firstly, the prodomain sequence of MT1-MMP is proteolytically processed, resulting in the generation of an intermediate activation product. Subsequently, a proprotein convertase (such as furin) cleaves the inhibitory prodomain at the $R^{108}RKR^{111}\downarrow Y^{112}$ site in the trans-Golgi network. This two-step mechanism ends with the degradation of the inhibitory prodomain and release of the mature MT1-MMP enzyme (57 kDa), which traffics to the cell surface where the catalytic site is exposed to the extracellular space. The activation may also be mediated by other enzymes on the cell surface [40].

Current evidence suggests that the activity of MT1-MMP is short-lived and the half-life of active, mature MT1-MMP bound to the plasma membrane is approximately one hour [41]. During this time period, active MT1-MMP is either inactivated by TIMPs or autolytically degraded, or internalized with, partial recycling. TIMP-2, TIMP-3 and TIMP-4 are highly potent inhibitors of MT1-MMP, whereas TIMP-1 is a very poor inhibitor [35].

The expression of MT1-MMP at the cell surface and its activity in the pericellular space result in the modification of many tumor cell functions, including proliferation, migration, invasion and survival. The efficient penetration of the ECM is a complex phenomenon which involves not only the MT1-MMP-mediated proteolysis, but also the correct localization of the enzyme at the surface of migrating cells. Cell surface localization of

MT1-MMP is usually very weak in most cell types because of rapid endocytosis of the enzyme from the plasma membrane and its trafficking to early and late endosomes. The cytoplasmic domain plays an important role in the regulation of all these events, thus contributing to the pro-invasive properties of the enzyme. In addition, it activates intracellular signaling, such as the ERK pathway [42].

Furthermore, it has been shown that MT1-MMP – TIMP-2 interaction controls cell functions through a non-proteolytic mechanism. Although TIMP-2 is a powerful inhibitor of MT1-MMP activity, binding of physiological concentrations (10-100 ng/ml) of TIMP-2 to MT1-MMP causes rapid activation of the intracellular Ras-Raf-ERK signaling cascade, which leads to cancer cell proliferation and migration. This function is dependent on the presence of the cytoplasmic sequence of MT1-MMP [43].

Tumor cell migration is also enhanced by the cleavage of CD44, a membrane-associated glycoprotein and one of the targets of MT1-MMP proteolysis. MT1-MMP physically interacts with CD44 through its hemopexin domain, cleaving the protein and releasing the CD44 ectodomain. The association between MT1-MMP and CD44 results in downstream activation of the MAPK and PI3K signaling pathways involved in cell migration [44].

The hinge region is the main target for MT1-MMP auto-catalytic degradation, which results in the release of the catalytic domain into the extracellular space and the generation of an inactive membrane-tethered 44-kDa degradation product. The accumulation of the 44-kDa form regulates the endocytosis of the active protease to preserve a viable level of MT1-MMP on the cell surface, and it is associated with increased enzymatic activity [45].

MT1-MMP is the physiological membrane activator of the soluble MMP-2 and MMP-13. ProMMP-2, a secreted MMP that belongs to the gelatinase subfamily of MMPs, cleaves a variety of substrates, such as collagens IV and I and denatured collagen I. The extracellular activation of proMMP-2 by MT1-MMP requires the presence of TIMP-2. The C-terminal region of TIMP-2 binds to the PEX domain of proMMP-2, whereas the N-terminal interacts with the active site of MT1-MMP. MT1-MMP, TIMP-2 and proMMP-2 thus form a trimolecular complex at the cell surface that allows the activation of proMMP-2 by an adjacent TIMP-2-free MT1-MMP. ProMMP-2 (72 kDa) bound to the complex is cleaved by MT1-MMP, thus producing an intermediate form of 66 kDa, which is auto-catalytically processed to the fully active 62 kDa MMP-2 (Fig. 1.5).

The amount of proMMP-2 activation depends on several factors including the relative levels of TIMP-2 and active MT1-MMP. Low levels of TIMP-2 relative to MT1-MMP promote activation by generating the ternary complex leaving a sufficient amount of TIMP-2-free, active MT1-MMP able to cleave the prodomain of proMMP-2. On the contrary, high concentrations of TIMP-2, that inhibit all MT1-MMP molecules on the cell surface, block MT1-MMP activation. Therefore, optimum concentrations of MT1-MMP

and TIMP-2 are required for proMMP-2 activation, efficient tissue degradation and subsequent invasive growth [46].

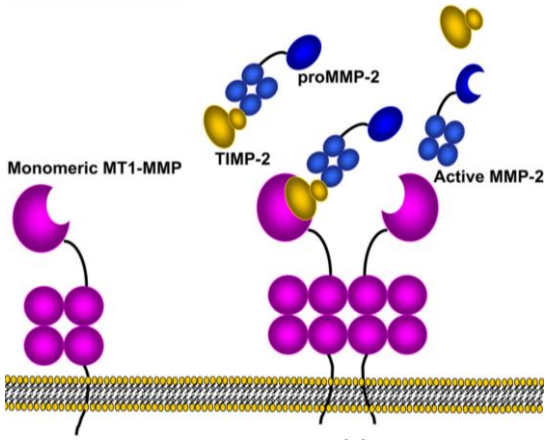

Figure 1.5. ProMMP-2 activation by MT1-MMP (Modified from Barbolina and Stack, 2008) [37].

The complete understanding of the molecular and cellular mechanisms involved in the up-regulation of MT1-MMP expression and activity by cancer cells can thus provide important new insights for the development of novel anticancer therapeutics to control tumor progression. In particular, this is a critical point in order to improve the outcome of childhood brain tumors, which still have a very poor prognosis. Recently published results by Xie and colleagues indicate that MT1-MMP expression and ERK1/2 phosphorylation levels positively correlate with the increasing pathological grades in adult brain glioma tissues [47]. With regard to the pediatric tumor counterparts, only few studies have been conducted so far. One of these has shown that tumor microinvasion into adjacent brain and expression of MMP-2 and MT1-MMP predict both overall and progression-free survival in pediatric ependymomas (WHO grade II and III gliomas), and that these are useful prognostic markers that may help stratify patients for adjuvant therapies [48].

1.7 Heparan sulfate proteoglycans

Heparan sulfate proteoglycans (HSPGs) are macromolecules abundantly associated with the cell surface and the ECM of a wide range of cells. The basic HSPG structure consists of a protein core to which several linear heparan sulfate (HS) chains are covalently O-linked. These polysaccharide chains can be modified by sulfation, epimerization, and N-acetylation. HSPGs are essential for normal cell growth and development, because they contribute to the self-assembly and integrity of the ECM and play an important role in cell-cell and cell-ECM interactions. HSPGs exert their multimodal functions by sequestering growth factors, chemokines and cytokines, providing a low-affinity reservoir

of these molecules and protecting them from proteolytic degradation. HSPGs also enhance cell adhesion through their interaction with the HS-binding domain of ECM proteins such as fibronectin, and act as co-receptors for many heparin-binding growth factors, such as fibroblast growth factor-2 (FGF-2 or basic FGF, bFGF), thus modulating their activity. For this reason, the cleavage of HS side chains not only alters ECM integrity but also releases HS-bound biological mediators [49].

Emerging evidence indicates that in tumor HS structure is altered, and some HSPGs possess a tumor-promoting effect. In particular, gliomas express significantly increased levels of HS compared with normal glial cells. This different expression of HSPGs in astrocyte-derived primary brain tumors can also be related to the malignant transformation or growth potential of glia-derived tumor cells [50,51].

1.8 Heparanase

1.8.1 Structure, functions and regulation

Heparanase, an endo-β-D-glucuronidase capable of cleaving HS side chains at a limited number of sites, is a protein encoded by a single gene located on chromosome 4 and named *HPSE* or *HPR-1* [52,53].

High levels of heparanase in many primary human tumors correlate with lymph node and distant metastasis, elevated microvessel density and reduced post-operative survival of cancer patients, a clinical observation that indicates pro-metastatic and pro-angiogenic roles of the enzyme. Heparanase is also involved in several other physiological and pathological processes, such as tissue morphogenesis, wound healing, hair growth, amyloidosis, bone remodeling, embryo implantation, and glomerular diseases [54,55].

Given the multitude of polypeptides associated with HS on the cell surface and ECM and their ability to strongly affect cell and tissue functions, heparanase activity and bioavailability is tightly regulated at transcriptional and post-translational levels. In particular, heparanase regulation is provided by its processing, cellular localization, and secretion.

Heparanase is synthesized as a pre-pro precursor, processed into an inactive form of 65 kDa after the cleavage of the signal peptide (M^{1}-A^{35}) necessary to direct the protein to the endoplasmic reticulum. Subsequently, the 6 kDa linker segment (S^{110}-Q^{157}) is excised by proteolysis, yielding the active enzyme. Active heparanase is a heterodimer consisting of a 50 kDa subunit (L^{158}-I^{543}) non-covalently linked to an 8 kDa peptide (Q^{36}-E^{109}) [56].

Pre-pro-heparanase is first targeted to the endoplasmic reticulum lumen via its own signal peptide, after which pro-heparanase is shuttled to the Golgi apparatus and secreted via vesicles that bud from the Golgi. Once secreted, heparanase interacts with cell membrane HSPGs, such as syndecan-family members, and the heparanase-HSPG complex is rapidly

endocytosed and accumulated in endosomes. The intracellular conversion of endosomes to lysosomes results in processing and activation of heparanase, which in turn participates in the turnover of HS side chains in the lysosome. This trafficking route may be bypassed by numerous potential ways, such as the direct conversion of secretory vesicles to endosomes. Lysosomal heparanase may translocate to the nucleus, where it affects gene transcription, or can be secreted in response to local or systemic signals. The latent secreted heparanase can also interact with heparanase-binding proteins and activate intracellular signaling pathways, leading to enhanced cell adhesion, migration, and angiogenesis [57].

1.8.2 Pro-metastatic and pro-angiogenic properties

Heparanase can enhance cell dissemination, and promote the formation of a vascular network that accelerates primary tumor growth and provides an access for the invading metastatic cells.

The systematic analysis of heparanase expression in primary human tumors has shown the clinical significance of this enzyme in tumor progression. Heparanase is up-regulated in many tumors, including the carcinomas of the colon, thyroid, liver, pancreas, bladder, cervix, breast, stomach, prostate, head and neck, salivary gland, nasopharynx, as well as leukemia, lymphoma, and multiple myeloma [58]. In all cases, the normal tissue surrounding the malignant lesion expresses little or no detectable levels of heparanase. In several carcinomas a more elevated heparanase expression is localized in the invasive front of the tumor, supporting its role in cell invasion. Furthermore, patients diagnosed as heparanase-positive exhibit a significantly higher rate of local and distant metastasis, along with reduced post-operative survival, compared with patients diagnosed as heparanase-negative. Patient survival is also associated with heparanase localization in tumor cells: nuclear localization correlates with maintained cellular differentiation and favorable outcome, suggesting that heparanase may affect gene regulation. In addition, heparanase up-regulation in primary human tumors correlates in some cases with increased tumor size and enhanced microvessel density, providing a clinical support for the pro-angiogenic function of the enzyme. The relationship between heparanase levels and patients' clinical status suggests that heparanase may be used as a diagnostic marker for the effectiveness of anti-tumor treatments [59].

HSPGs and HSPG-degrading enzymes are implicated in numerous and complex angiogenesis-related events, including cell invasion, migration, adhesion, differentiation, and proliferation. Because HSPGs are important components of blood vessels, heparanase activity on the sub-endothelial basement membrane can directly facilitate endothelial cells invasion. In addition, heparanase can also stimulate an indirect angiogenic response by releasing many HS-bound angiogenic growth factors from the ECM, such as FGF-2 and

vascular endothelial growth factor (VEGF), and by generating HS fragments that promote binding of receptors to FGF, dimerization, and signaling [60].

The involvement of heparanase in cancer metastasis and angiogenesis is not exclusively restricted to its HS-degrading activity in the ECM. Recent studies indicate that inactive heparanase can also exert non-enzymatic effects: it can bind to its putative cell-surface receptors and activate many intracellular signal transduction cascades, promoting cell adhesion and survival, up-regulation of VEGF [61] and tissue factor [62], and accelerating tumor growth.

In contrast to its widely reported overexpression in a variety of tumors, heparanase was found to be decreased in gliomas in one published study [63]. On the contrary, more recently, Hong and colleagues have described heparanase up-regulation in human gliomas [64]. Since the results of these few studies are still controversial, further experimental evidence is necessary to verify the correct level of expression and the potential role of heparanase in facilitating glioma tumor growth, particularly in the pediatric forms. However in spite of these uncertainties, these findings highlight heparanase as a potential therapeutic target in the treatment of malignant brain tumors.

1.9 Fibroblast growth factor-2 (FGF-2)

1.9.1 FGF-2 and FGF receptors (FGFRs)

Fibroblast growth factor-2 (FGF-2), formerly known as basic FGF (bFGF), is a member of a large family of 23 structurally related heparin-binding proteins (FGFs). FGF-2 is a ubiquitous growth factor implicated in a variety of physiological and pathological processes, such as cell survival, proliferation, migration, growth and differentiation [65].

The human *FGF-2* gene is located on chromosome 4. Alternative translation initiation of FGF-2 mRNA results in five biologically active proteins with different molecular weight, cellular localization and functions. Four high molecular weight (HMW) FGF-2 (34, 24, 22.5 and 22 kDa) forms are initiated by CUG start codons located upstream of the low molecular weight (LMW) FGF-2 (18 kDa) sequence, which starts at an AUG codon. Only 34 kDa HMW FGF-2 is translated by the conventional cap-dependent mechanism, whereas translation of all the other forms requires an internal ribosomal entry site (IRES) located between nucleotides 154 and 319 (Fig. 1.6).

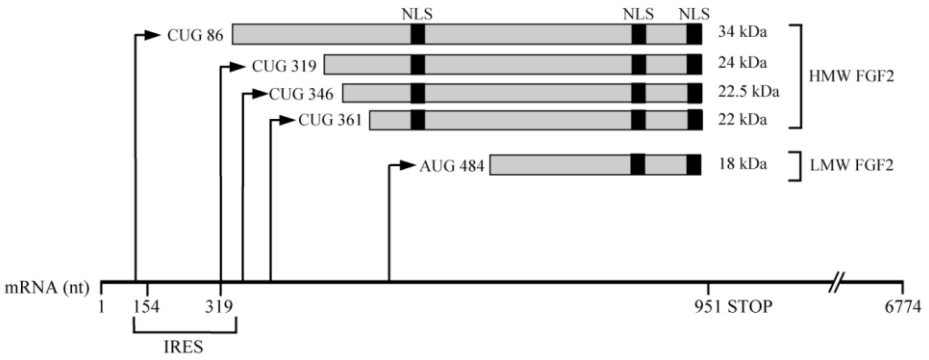

Figure 1.6. Schematic representation of human FGF-2 forms expression by alternative translation initiation [69].

All forms of FGF-2 contain a C-terminal bipartite nuclear localization sequence (NLS). The HMW isoforms also contain an N-terminal ER (glutamic acid - arginine) repeat that acts as an NLS. The 34 kDa isoform contains an additional NLS similar in structure to that of the human immunodeficiency virus (HIV) Rev protein (not shown in Fig. 1.6).

FGF-2 is a monomeric protein that lacks a conventional N-terminal signal sequence for secretion. LMW FGF-2 is secreted from cells through a non-classical secretory pathway independent of the endoplasmic reticulum/Golgi apparatus, but involving exocytosis, and requiring ATP [66,67]; in the extracellular space it can act as a paracrine or autocrine growth factor [68] by activating its cognate membrane receptors. Although HMW FGF-2 can also be released by cells - usually following cell lysis or damage - these forms are typically intracellular and accumulate in the nucleus and nucleolus after translation. The differences in the intracellular sorting of the various FGF-2 forms determine their functional diversity, with LMW FGF-2 being an extracellular signaling molecule that acts via activation of transmembrane receptors, and HMW FGF-2 having a nuclear, FGFR-independent intracrine function [69].

The biological effects of FGF-2 are mediated by high-affinity tyrosine kinase FGF receptors (FGFRs) and low-affinity receptors.

The four members of the FGFR family (FGFR-1, FGFR-2, FGFR-3 and FGFR-4) are encoded by different genes, and their structural heterogeneity is increased by alternative splicing.

The FGFRs have an overall structure similar to most receptor tyrosine kinases (RTKs). They are single-pass transmembrane proteins comprised of an extracellular region that binds FGF-2, a transmembrane domain and an intracellular tyrosine kinase domain. The extracellular part of the receptor is composed of three Ig-like domains (I-III) with an acidic, serine-rich region between domains I and II (acid box). The first Ig-like domain, together with the acid box, is important for receptor auto-inhibition. Domains II and III comprise the FGF-binding site. In FGFR-1, -2, and -3, alternative splicing in the Ig-like domain III generates isoforms with different ligand-binding specificities. The intracellular

tyrosine kinase domain, which relays the signal inside the cell, has an insert and is therefore referred to as a split kinase domain (Fig. 1.7).

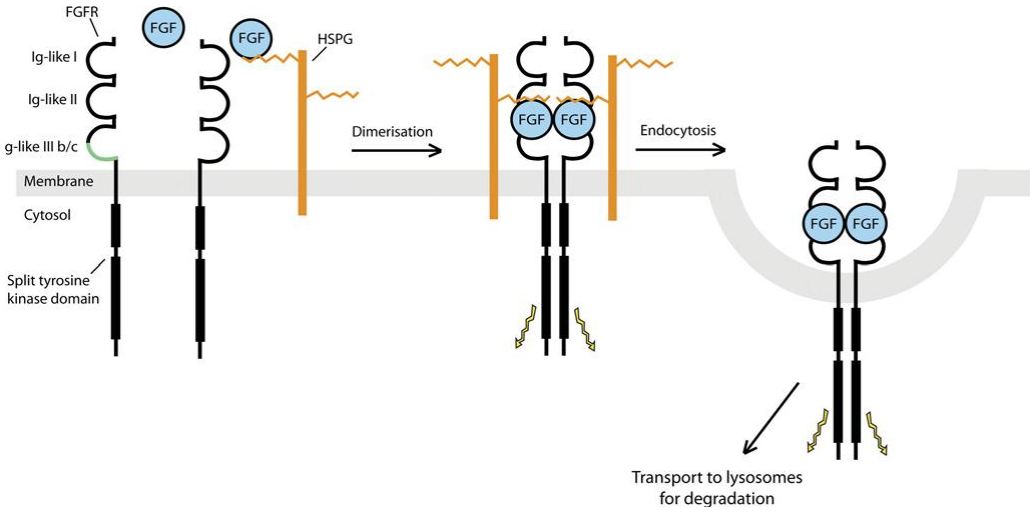

Figure 1.7. Schematic diagram of FGFR structure and FGF-2-FGFR-HSPG interactions [70].

FGF-2 can also bind to low-affinity receptors, HSPGs present in the ECM or bound to the cell membrane. A highly basic (i.e. positively charged) protein, FGF-2 interacts with the negatively charged polysaccharides, which protect it from degradation and participate in complex formation between FGF-2 and FGFRs. Binding of FGF-2 to the FGFRs determines the dimerization of a ternary complex consisting of two molecules of FGF-2, two FGFRs and two heparan sulfate chains. Formation of this complex results in activation of downstream signaling cascades, in particular the MAPK and the PI3K/Akt pathways. After activation, the complex is internalized by endocytosis and transported to lysosomes for degradation (Fig. 1.7) [70].

1.9.2 Role in angiogenesis and tumor growth

The intracellular signaling pathways activated by FGF-2 binding to FGFRs control a variety of biological processes.

Despite complex involvement of FGF-2 in embryonic development (brain, limbs, lung, heart, muscle, bone, blood, eye and skin), FGF-2 knockout mice are viable and have an apparently normal phenotype [71]. However, in the adult FGF-2 is implicated in controlling vascular tone, mediating cardiac hypertrophy, promoting the mobilization and differentiation of myocardial precursor cells, and facilitating wound healing. Importantly, FGF-2 is one of the most potent inducers of angiogenesis. Inhibition of angiogenesis through FGF-2 blockade is a critical step for limiting tumor metastases, as tumor growth

also depends on formation of a new capillary network from pre-existing blood vessels and circulating endothelial progenitor cells [72].

Because of its pleiotropic activity that affects both tumor vasculature and parenchyma, the FGF-2/FGFR system contributes to cancer progression not only by inducing neo-angiogenesis but also by directly acting on tumor cells. In particular, FGF-2 upregulation and release from tumor and/or stromal cells contributes to tumor proliferation, survival and migration. Several cancer types, including pancreatic, breast, non-small cell lung, and head and neck squamous carcinomas, are characterized by FGF-2 overexpression. Moreover, FGF-2 bound to the HS-chains in the ECM can be released very efficiently by both proteolytic and glycosidic enzymes, contributing to angiogenesis and tumor growth [73]. In addition to FGF-2, numerous alterations of FGFRs, such as inappropriate expression, activating point mutations, splice variations and genomic alterations, can also dysregulate FGF-2 signaling and promote tumorigenesis [74].

The clinical significance of FGF-2 is demonstrated by the findings that elevated levels in the serum of patients with breast, colorectal and renal cell carcinomas and other tumors inversely correlate with patients' survival [75,76].

FGF-2 also plays a critical role in nervous system development, and dysregulated expression has been implicated in the pathogenesis of glial tumors. FGF-2 is overexpressed in more than 90% of malignant gliomas and its level of expression correlates with tumor grade, extent of anaplasia, and clinical outcome [77,78].

Down-regulation of FGF-2 by antisense cDNA or oligonucleotides, neutralizing anti-FGF-2 antibody, or a peptide corresponding to the heparin-binding domain of FGF-2, and reduced expression of FGFR by antisense cDNA or oligonucleotides block angiogenesis and tumor growth *in vivo*, and therefore represent potential antineoplastic strategies [79].

Chapter 2: Project aims

Gliomas, the most frequent primary brain tumors, comprise a heterogeneous group of neoplasms that originate from glial cells. The biological mechanisms underlying glioma cell invasion in the normal brain tissue are numerous and complex. The degradation of different components of the extracellular matrix involves both proteolytic and glycosidic enzymes that modify the microenvironment during tumor invasion and metastasis. The majority of the studies conducted so far are focused on adult gliomas, which show different genetic, molecular and clinical features from their pediatric counterparts.
This study aimed to investigate the roles of heparanase (HPSE) and membrane-type 1 matrix metalloproteinase (MT1-MMP) by using cell lines derived from different types of pediatric gliomas: two glioblastoma multiforme (SF188 and KNS42), one anaplastic astrocytoma (UW479), one diffuse astrocytoma (Res259) and one pilocytic astrocytoma (Res186) cell line.

The following aims have been achieved in this experimental study:

1. Characterization of *HPSE* expression in pediatric glioma cells and analysis of the effects of *HPSE* gene silencing on the expression of matrix metalloproteinase-2 (*MMP-2*), *MT1-MMP* and vascular endothelial growth factor (*VEGF*), and on SF188 cell proliferation.

2. Analysis of activation of the ERK1/2 intracellular signaling pathway by fibroblast growth factor-2 (FGF-2) in human MCF-7 breast adenocarcinoma cells expressing MT1-MMP.

3. Analysis of the effects of MT1-MMP on FGF-2 interaction with the tumor cell surface.

4. Characterization of MT1-MMP, FGF-2, FGF receptors and tissue inhibitor of metalloproteinase-2 (TIMP-2) expression in pediatric glioma cells, and study of ERK1/2 activation by FGF-2 and by TIMP-2.

Chapter 3: Materials and Methods

3.1 Reagents

Rabbit anti-human MT1-MMP antibody (hinge region), rabbit anti-human TIMP-2 (C-terminus) antibody, Ilomastat (GM6001), and PVDF membranes were purchased from Millipore (Billerica, MA); mouse anti-human phospho-p44/42 MAPK (ERK1/2) (Thr^{202}/Tyr^{204}) was from Cell Signaling Technology (Danver, MA); doxycycline, 1,10-phenantroline, bovine serum albumin (BSA), puromycin, and mouse anti-human tubulin antibody were from Sigma-Aldrich (St. Louis, MO); donkey anti-mouse IgG antibody, donkey IgG anti-rabbit antibody, and streptavidin (all conjugated with horseradish peroxidase) from Jackson ImmunoResearch Laboratories (West Grove, PA); sulfosuccinimidyl-6-[biotin-amido]hexanoate (sulfo-NHS-LC-biotin), bicinchoninic acid (BCA) protein assay kit, and SuperSignal West Pico chemiluminescent substrate from Thermo Scientific (Rockford, IL); heparin-Sepharose beads from Reprokine Research Immunity (Valley Cottage, NY); protein A/G PLUS-agarose immunoprecipitation reagent was from Santa Cruz Biotechnology (Santa Cruz, CA); recombinant human basic FGF (155) from Akron Biotech (Boca Raton, FL); human recombinant TIMP-2 from PeproTech (Rocky Hill, NJ); CellTiter96 Aqueous One Solution Cell Proliferation (MTS) and GoTaq DNA Polymerase were from Promega (Madison, WI); MEM alpha medium, Lipofectamine 2000 Reagent, TRIzol Reagent, and SuperScript II Reverse Transcriptase from Invitrogen (Grand Island, NY); TransIT-LT1 transfection reagent was from Mirus (Madison, WI); HPSE gene-specific shRNA expression cassettes, and pRS plasmid (TR20003) from OriGene (Rockville, MD); complete mini protease inhibitor cocktail, PhosSTOP phosphatase inhibitor cocktail, and DNAse I from Roche (Indianapolis, IN); Dulbecco's modified Eagle's medium (DMEM), DMEM/F-12 Ham's medium, fetal bovine serum (FBS), L-glutamine, penicillin, and streptomycin from CellGro (Manassas, MA); Power SYBR Green master mix was from Applied Biosystem (Milan, Italy).

Wild-type and mutant MT1-MMP cDNAs cloned in pcDNA3 vectors, and mouse anti-human FGF-2 antibody were previously generated in Dr. P. Mignatti's laboratory (New York University School of Medicine).

3.2 Cell lines and culture media

The following human tumor cell lines were used:

Cell line	Tumor
MCF-7	Breast adenocarcinoma
SF188	Glioblastoma multiforme
KNS42	Glioblastoma multiforme
UW479	Anaplastic astrocytoma
Res259	Diffuse astrocytoma
Res186	Pilocityc astrocytoma

Table 3.1. Tumor cell lines.

MCF-7 cells, which do not express MT1-MMP, were obtained from ATCC. In addition, we used MCF-7 cells stably transfected with MT1-MMP cDNA under control by the tetracycline resistance transactivator in the Tet-Off conformation (MCF-7 clone 8) which had previously been generated in Dr. P. Mignatti's laboratory (New York University School of Medicine). In these cells addition to the culture medium of doxycycline (DOX), a stable analogue of tetracycline, prevents the expression of MT1-MMP.
The pediatric glioma cell lines were kindly provided by Dr. C. Jones (The Institute of Cancer Research, Sutton, UK) (Table 3.1).
Primary bovine capillary endothelial (BCE) cells, used as control in some experiments, were previously obtained from calf adrenal glands in Dr. P. Mignatti's laboratory.

MCF-7 and MCF-7 clone 8 cells were grown in DMEM supplemented with 10% (v/v) FBS, 2 mM L-glutamine, 100 U/ml penicillin, and 100 µg/ml streptomycin. SF188, KNS42, UW479, Res259 and Res186 cell lines were grown in DMEM/F12 Ham's medium supplemented with FBS, L-glutamine and antibiotics as above. BCE cells were grown in 0.1% gelatin-coated tissue culture plates in alpha MEM supplemented with 5% donor calf serum, L-glutamine and antibiotics. All the cells grew as monolayers, and were maintained at 37 ºC in a 5% CO_2 atmosphere saturated with H_2O.

3.3 Cell treatments

All the treatments described below were performed with medium containing 0.5% FBS.

3.3.1 FGF-2 treatment

Sub-confluent MCF-7 cells were serum-starved (0.5% FBS) and incubated for 24 h with or without 1 µg/ml DOX. Where indicated, cells were incubated for 15 min with medium containing either 50 µM Ilomastat or 500 µM 1,10-phenantroline before treatment with FGF-2 as indicated in Results. In some experiments serum-starved cells were treated with 30 ng/ml of FGF-2 for 15 min and subsequently washed 3 times with PBS followed by one washing with either 2 M NaCl in 20 mM HEPES, pH 7.5 or 2 M NaCl in 20 mM sodium acetate, pH 4.0. After treatment, cells and conditioned media were immediately collected for subsequent analysis (paragraphs 3.7 and 3.9). Alternatively, 8×10^3 MCF-7 clone 8 cells grown in 96-well culture plates and serum-starved were incubated overnight with or without DOX, and subsequently with or without 10 ng/ml FGF-2 for 1 to 3 days, and further analyzed for proliferation by the MTS assay (paragraph 3.10).

3.3.2 TIMP-2 treatment

Sub-confluent cells serum-starved (0.5% FBS) for 24 h were treated for 15 min with or without 50 µM Ilomastat, and subsequently with or without 100 ng/ml TIMP-2. Both Ilomastat and TIMP-2 were added directly to the medium in a volume of 1 ml of medium. Cells were immediately collected for subsequent analysis (paragraph 3.7).

3.4 RNA extraction and cDNA synthesis

Total RNA was extracted with the TRIzol Reagent including DNase I treatment. Yield and purity were checked by Nanodrop (EuroClone). One microgram of total RNA was reverse-transcribed using 500 ng of random primers and 200 U of SuperScript Reverse Transcriptase. All the protocols were performed following the manufacturer's instructions.

3.5 Semi-quantitative PCR and Real-Time quantitative PCR

Expression of *FGFR-1, -2, -3,* and *-4* was analyzed by semi-quantitative PCR. The reaction was performed with GoTaq polymerase using 5 µmoles of forward and reverse primers, denaturation at 95 ºC for 10 min, followed by 28 cycles of denaturation at 95 ºC for 30 sec, annealing at 58 ºC for 30 sec, and elongation at 72 ºC for 30 sec. *GAPDH,*

measured with 25 cycles of amplification under the same conditions, was used as loading control. PCR products were resolved in 2% agarose gels in 1X TAE buffer (50 mM Tris-HCl pH 8.0, 20 mM sodium acetate, 2 mM Na_2EDTA), and visualized under UV light.

Expression of *HPSE*, *MMP-2*, *MT1-MMP* and *VEGF* was analyzed by Real-Time quantitative PCR. The reaction was performed with the Power SYBR Green Master Mix using 5 µmoles of forward and reverse primers, denaturation at 95 ºC for 10 min, followed by 40 cycles of denaturation at 95 ºC for 30 sec, annealing and elongation at 60 ºC for 30 sec. *GAPDH* was used as loading control. Gene expression was quantified by the comparative Ct method (ΔΔCt), and the relative quantification was calculated as $2^{-\Delta\Delta Ct}$. Melting curve analysis was used to rule out the presence of non-specific amplification products.

The following primers were used:

Primer	PCR	Product length	Sequence (5' – 3')
FGFR-1_FOR	SQ	200 bp	ACCACCGACAAAGAGATGGA
FGFR-1_REV	SQ		GCCCCTGTGCAATAGATGAT
FGFR-2_FOR	SQ	247 bp	TCTAAAGGCAACCTCCGAGA
FGFR-2_REV	SQ		CTCTGGCGAGTCCAAAGTCT
FGFR-3_FOR	SQ	282 bp	CCACTGTCTGGGTCAAGGAT
FGFR-3_REV	SQ		CCAGCAGCTTCTTGTCCATC
FGFR-4_FOR	SQ	220 bp	TCATCAACCTGCTTGGTGTC
FGFR-4_REV	SQ		CGGGACTCCAGATACTGCAT
GAPDH_FOR	SQ	458 bp	AACATCATCCCTGCCTCTAC
GAPDH_REV	SQ		CCCTGTTGCTGTAGCCAAAT
HPSE_FOR	Q	136 bp	ATTTGAATGGACGGACTGC
HPSE_REV	Q		GTTTCTCCTAACCAGACCTTC
MMP-2_FOR	Q	71 bp	GCGGCGGTCACAGCTACTT
MMP-2_REV	Q		CACGCTCTTCAGACTTTGGTTCT
MT1-MMP_FOR	Q	131 bp	TGCCATGCAGAAGTTTTACGG
MT1-MMP_REV	Q		TCCTTCGAACATTGGCCTTG
VEGF_FOR	Q	81 bp	ATGACGAGGGCCTGGAGTGTG
VEGF_REV	Q		CCTATGTGCTGGCCTTGGTGAG
GAPDH_FOR	Q	112 bp	ACACCCACTCCTCCACCTTT
GAPDH_REV	Q		TCCACCACCCTGTTGCTGTA

Table 3.2. Type of PCR performed (SQ = semi-quantitative, Q = quantitative), product length, and primer sequences.

Primers were designed with Primer3 (v. 0.4.0) using default settings. Because different FGFR isoforms are generated by alternative splicing, Fast DB software was first used to identify the exons shared by all FGFR variants, and primers were subsequently designed with Primer3.

3.6 Transient and stable transfections

Wild-type and mutant MT1-MMP cDNAs in pcDNA3 were transiently transfected into sub-confluent cells in 6-well plates using 3 µg of plasmid and 7.5 µl of Lipofectamine, according to the manufacturer's instructions. In particular, the mutant MT1-MMP constructs contained MT1-MMP sequences either lacking the hemopexin domain (Δpex) or the cytoplasmic tail (Δcyt), or an alanine substitution of glutamic acid 240 in the catalytic domain (E240A). Twenty-four hours after transfection, cells were incubated with medium containing 0.5% FBS for additional 24 h, and immediately used for the experiments.

To obtain a stably *HPSE* silenced SF188 cell line, the following 29mer shRNAs targeting human heparanase were used:

shRNA	Sequence
pHPSE-1	TTATGTGGCTGGATAAATTGGGCCTGTCA
pHPSE-2	GTTCAAGAACAGCACCTACTCAAGAAGCT
pHPSE-3	GTGGTGATGAGGCAAGTATTCTTTGGAGC
pHPSE-4	TCGTTCCTGTCCGTCACCATTGACGCCAA

Table 3.3. ShRNA sequences of human *HPSE*.

Sub-confluent tumor cells in 6-well plates were transfected with 2 µg of each shRNA plasmid in serum-free medium using TransIT-LT1 according to the manufacture's instruction. Forty-eight hours after transfection, stable SF188 cell transfectants were grown for several weeks in medium containing 0.5 µg/ml puromycin. Six puromycin-resistant clones were selected for subsequent analysis.

3.7 Protein extraction and Western blotting

At the indicated times after FGF-2 or TIMP-2 treatment, cells were washed with ice-cold PBS and scraped in RIPA buffer (150 mM NaCl, 1% Igepal, 0.5% sodium deoxycholate, 0.1% SDS in 50 mM Tris-HCl, pH 8.0) containing protease (Complete) and phosphatase (PhosSTOP) inhibitors. Following centrifugation (14,000 rpm for 15 min at 4 º C) and sonication, the lysates were assayed for protein concentration by the BCA method, using BSA as standard.

Cell extract protein (20-40 µg) was diluted in reducing sample buffer (10% glycerol, 2% SDS, 80 mM Tris-HCl pH 6.8, 0.005% bromophenol blue, 10% β-mercaptoethanol) denatured for 10 min at 100 ºC, and electrophoresed in SDS/10-12% polyacrylamide gels. Proteins were transferred onto PVDF membranes; non-specific binding was blocked for 2 h at RT with 5% non-fat milk in Tris buffered saline (TBS) buffer. Membranes were

exposed to primary and secondary peroxidase-conjugated antibodies in TBS buffer containing 5% (w/v) non-fat milk. The working dilutions of the primary antibodies used in the experiments are listed in Table 3.4. The secondary antibodies were usually diluted 1:5,000 (2 h, RT), with the exception of the secondary antibody used to detect tubulin, which was diluted 1:20,000 (1 h, RT). The signal was detected with the SuperSignal West Pico Chemiluminescent substrate solution, according to the manufacturer's instructions.

In some experiments, the membranes were stripped by incubation in a mild stripping buffer (20 mM Glycine, 0.1% SDS, 1% Tween 20, pH 2.2) for 30 min at RT with gentle agitation, re-blocked and re-probed with other antibodies.

Since heparin shows high affinity for FGF-2, heparin-Sepharose beads were used to detect FGF-2 in cell conditioned medium or in the washing buffers used to remove FGF-2 from the cell surface. Heparin-Sepharose beads (20 µl) equilibrated with serum-free medium were incubated with 200 µl of the sample for 2 h at 4 ºC. Following centrifugation, the pelleted beads were resuspended in reducing sample buffer, denatured and loaded onto a SDS-polyacrylamide gel for Western blotting analysis as described above.

Primary antibody	Dilution and incubation time	Host
MT1-MMP	1:1,000; o/n, 4 ºC	Rabbit
P-ERK	1:1,000 in MCF-7 cells; 2 h, RT 1:5,000 in glioma cells; 1 h 30 min, RT	Mouse
FGF-2	1:3,000 in MCF-7 cells; 2 h, RT 1:5,000 in glioma cells; 1 h 30 min, RT	Mouse
TIMP-2	1:5,000; 2 h, RT	Rabbit
TUBULIN	1:25,000; 1 h, RT	Mouse

Table 3.4. Primary antibodies, dilutions, and incubation.

3.8 Biotinylation of soluble and cell surface associated FGF-2

Biotin, a small vitamin (244 Da) that binds the protein streptavidin with high affinity, can be conjugated to virtually all proteins without altering their biological activity. To label human recombinant FGF-2 we used sulfo-NHS-LC-biotin, which reacts with primary amino groups ($-NH_2$) in pH 7-9 buffers to form stable amide bonds.

Ten mM biotin reagent solution was added to 100 µg/ml FGF-2 in PBS, and incubated on ice for 2 h. The biotinylated FGF-2 was used for cell treatments, as described above, without purification, and detected by Western blotting with peroxidase-conjugated streptavidin.

Because Sulfo-NHS-LC-biotin is water soluble and charged by the sodium sulfoxide group on the succinimidyl ring, it cannot permeate cell membranes. Therefore, biotin can

also be used to label proteins localized on cell surface because as long as the cells remain intact, only primary amines exposed on the surface will be biotinylated. To biotinylate cell surface associated FGF-2 cell monolayers incubated with 30 ng/ml FGF-2 for 15 min were washed 3 times with ice-cold PBS, and incubated on ice for 30 min with 1 mM biotin (ice can reduce the active internalization of biotin). Following 3 washings with 100 mM glycine in PBS to quench and remove the excess of biotin reagent, the cells were lysed in RIPA buffer (50 mM Tris-HCl pH 8.0, 125 mM NaCl, 0.5% Igepal, 0.5% sodium deoxycholate, 0.1% SDS, 1 mM DTT) containing protease and phosphatase inhibitors. The cell lysate was centrifuged (14,000 rpm for 15 min at 4 ºC), sonicated, and assayed for protein concentration. Anti-FGF-2 antibody (1 µg) or mouse non-immune IgG (1 µg) was added to cell extract protein (1 mg), and incubated with protein A/G PLUS-agarose beads (30 µl) overnight at 4 ºC. Following centrifugation at 2000 rpm for 4 min at 4 ºC, the pelleted beads were resuspended in reducing sample buffer, loaded onto a SDS-polyacrylamide gel for Western blotting analysis, and the immunocomplexes were detected with peroxidase-conjugated streptavidin.

3.9 Gelatin zymography

MMP activities were studied by using zymography, which allows detection of both the proenzyme and active forms of MMP-2 and -9 [80]. Media (20 µl) conditioned by an equal number (5×10^5) of cells were electrophoresed in a SDS/8% polyacrylamide gel co-polymerized with 0.1% gelatin. Following electrophoresis, the gel was washed for 1 h at RT in 2.5% Triton X-100 and incubated overnight at 37 ºC in 100 mM Tris-HCl, 10 mM $CaCl_2$, pH 7.4. Finally, the gel was stained with 0.1% Coomassie Brilliant Blue R- 250, and destained with 30% methanol - 10% acetic acid. Gelatinolytic activities were detected as clear bands against the background of blue-stained gelatin.

3.10 Cell proliferation assay

Cell proliferation was measured by the MTS assay. FGF-2-treated or untreated cells were incubated with 3-(4,5-dimethylthiazol-2-yl)-5-(3-carboxy-methoxyphenyl)-2-(4-sulfophenyl)-2H-tetrazolium (MTS) for 1 h at 37 ºC, and the number of proliferating cells was evaluated by measuring optical density at 490 nm.

3.11 Statistical analysis

Differences between FGF-2-treated and untreated cells, and between wild-type and *HPSE* silenced cells were analyzed using the Students' *t* test. A p value ≤ 0.05 was considered as significant.

Chapter 4: Results

4.1 Pediatric glioma cell lines

All the pediatric glioma cell lines used in this study were derived from astrocytomas of differing grades arisen in patients aged 3-16 years. Established *in vitro* by other groups, these cell lines grow as monolayer cultures, with doubling times ranging between 24 and 48 h, and are characterized by a mixture of stellate and bipolar morphologies, with some cells being polygonal, cuboidal or flattened (Table 4.1; Fig. 4.1).

Cell line	WHO grade	Diagnosis	Age	Sex	Morphology	Doubling time
SF188	IV	Glioblastoma multiforme	8 yrs	male	stellate, polygonal, bipolar	26 hrs
KNS42	IV	Glioblastoma multiforme	16 yrs	male	cuboidal, polygonal, bipolar	48 hrs
UW479	III	Anaplastic astrocytoma	13 yrs	female	polygonal, stellate	28 hrs
Res259	II	Diffuse astrocytoma	4 yrs	female	polygonal, cuboidal, bipolar	24 hrs
Res186	I	Pilocytic astrocytoma	3 yrs	female	stellate, flattened, bipolar	46 hrs

Table 4.1. Characteristics of pediatric glioma cells (Modified from Bax *et al.*, 2009) [81].

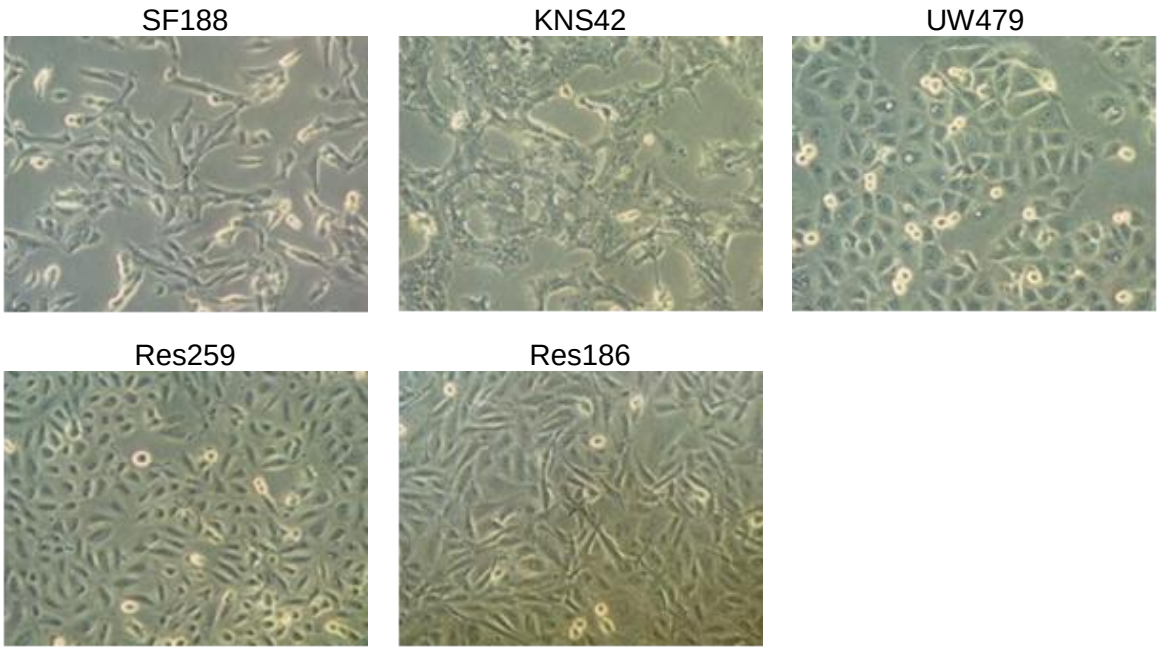

Figure 4.1. Representative images of pediatric glioma cells. All the cells grow as monolayer cultures, and are characterized by a mixture of stellate and bipolar morphologies, with some cells being polygonal, cuboidal or flattened. Original magnification × 200.

4.2 *HPSE* expression in pediatric glioma cells and *HPSE* silencing in SF188 cells

Preliminary experiments were performed to investigate the role of the heparan sulfate-degrading enzyme heparanase in glioma cell lines. Results from a quantitative Real-Time PCR assay showed different levels of *HPSE* expression in the different glioma cell lines, KNS42 cells having the highest levels and Res259 cells very low, almost undetectable levels (Fig. 4.2).

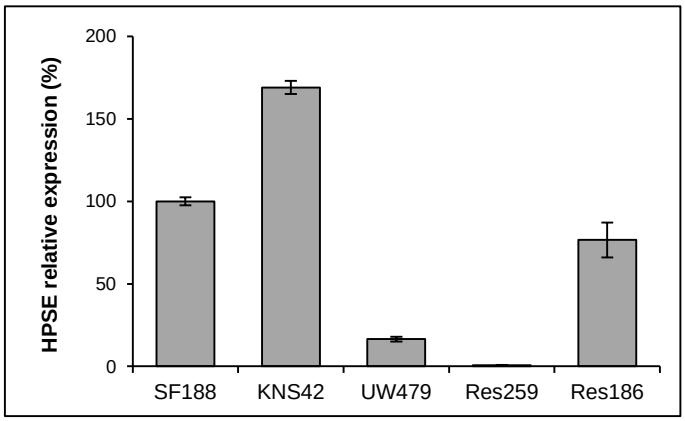

Figure 4.2. *HPSE* expression in pediatric glioma cells. *HPSE* mRNA levels in pediatric glioma cells were determined by quantitative Real-Time PCR. The results were normalized using *GAPDH* mRNA as an internal control and represent mean ± standard deviation of two different experiments performed with triplicate samples.

Since both SF188 and KNS42 cells showed high *HPSE* mRNA levels, these cell lines were subsequently used for *HPSE* downregulation. For this purpose cells were transfected with 29mer shRNAs to HPSE or with the corresponding empty vector as a negative control. Several clones of stable SF188 cell transfectants were obtained by selection with puromycin; however, KNS42 transfected cells died during the antibiotic selection.
HPSE mRNA expression was then measured in SF188 clones by quantitative Real-Time PCR. *HPSE* levels in non-transfected cells were comparable to those of cells transfected with the negative control plasmid. Among the 5 silenced clones, the one with the best silencing effect (73%) was chosen for subsequent experiments, and named pHPSE-3. In addition, a mixture of clones of SF188 cells transfected with all four 29mer shRNA plasmids together showed *HPSE* mRNA expression similar to that of the other clones (pHPSE-1, -2, -4) (Fig. 4.3).

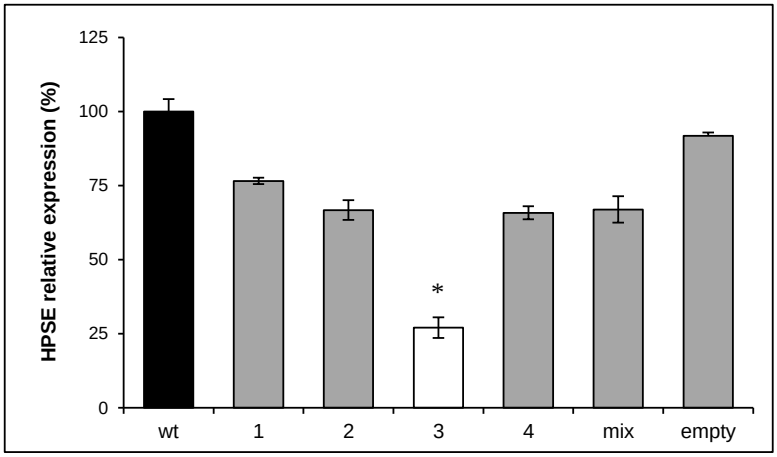

Figure 4.3. Stable silencing of *HPSE* in SF188 cells. SF188 cells were transfected with 29mer shRNAs to *HPSE* or with the empty vector as a negative control. Several clones of stable SF188 cell transfectants were obtained by selection with puromycin. *HPSE* mRNA levels in SF188 clones were determined by quantitative Real-Time PCR. The results were normalized using *GAPDH* mRNA as an internal control and represent mean ± standard deviation of two different experiments performed with triplicate samples. Clone 3 cells, which showed the strongest silencing effect (73%), were chosen for subsequent experiments, and named pHPSE-3 (wt, non-transfected cells, black bar; 1, 2, 4, cells transfected with the shRNA plasmid-1, 2, 4, respectively, gray bar; 3, cells transfected with shRNA plasmid-3, white bar; mix, cells transfected with all four shRNA plasmids, gray bar; empty, cells transfected with the empty vector, gray bar; * $p < 0.05$, SF188 wt *vs.* pHPSE-3 cells).

4.3 Effects of *HPSE* silencing on *MMP-2*, *MT1-MMP* and *VEGF* expression in SF188 cells

Given the close association existing between glycosidases and proteases in the ECM, *MMP-2* and *MT1-MMP* mRNA expression was then studied by quantitative Real-Time PCR in SF188 wt cells and pHPSE-3 cells. SF188 cells showed high *MMP-2* mRNA levels; these cells also synthesized the corresponding protein, which is released in the extracellular environment in its proenzymatic form (proMMP-2). Conversely, *MT1-MMP* mRNA levels were about 10 times lower relative to *MMP-2* expression (Fig. 4.4A).

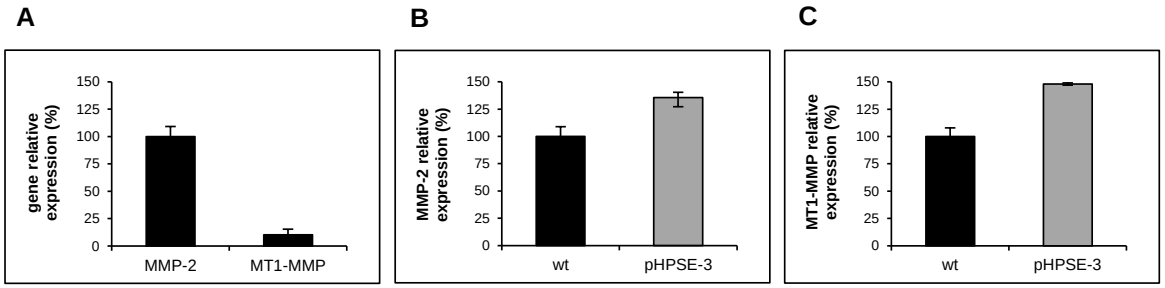

Figure 4.4. *MMP-2* and *MT1-MMP* expression in SF188 wt and silenced cells. *MMP-2* (A, B) and *MT1-MMP* (A, C) mRNA levels in SF188 wt (black bar) and silenced (gray bar) cells were determined by quantitative Real-Time PCR. The results were normalized to *GAPDH* mRNA as an internal control and represent mean ± standard deviation of two different experiments performed with triplicate samples.

MMP-2 and *MT1-MMP* mRNA levels were 35 and 50% higher, respectively, in pHPSE-3 cells than in SF188 wt cells (Fig. 4.4, B and C).

Since HPSE can also participate in the regulation of VEGF signaling [61], the mRNA expression of this growth factor was also analyzed by quantitative Real-Time PCR analysis in SF188 wt cells and pHPSE-3 cells. The results showed that *VEGF* mRNA levels were comparable in both cell lines. Interestingly, treatment of SF188 cells with FGF-2 (10 ng/ml) for 24 h increased *VEGF* expression about 2.5-fold relative to untreated cells (Fig. 4.5).

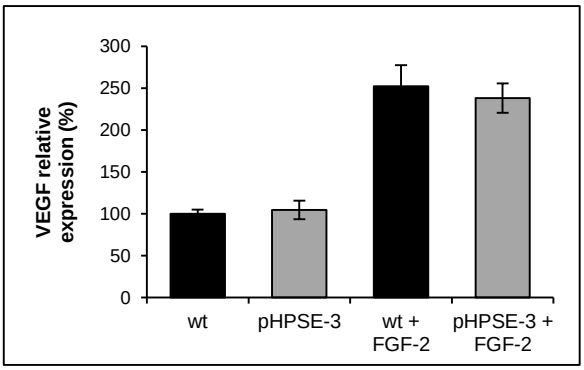

Figure 4.5. *VEGF* expression in SF188 wt and silenced cells. *VEGF* mRNA levels in SF188 wt (black bar) and silenced (gray bar) cells were determined by quantitative Real-Time PCR. SF188 wt and silenced cells were also treated with FGF-2 (10 ng/ml) for 24 h and *VEGF* mRNA levels measured. The results were normalized using *GAPDH* mRNA as an internal control and represent mean ± standard deviation of two different experiments performed with triplicate samples.

4.4 Effects of *HPSE* silencing on SF188 cell proliferation

In order to understand whether *HPSE* silencing altered FGF-2 effect on glioma cell proliferation SF188 wt cells and pHPSE-3 cells were treated with FGF-2 (10 ng/ml), and the cell number was measured by the MTS assay after 1 and 2 days.

At each time-point, no statistically significant difference in cell proliferation was observed between untreated wt cells and silenced cells. After 2 days FGF-2 induced a 25% and 20% increase in cell number in wt and silenced cells, respectively ($p < 0.05$, Fig. 4.6,A).

In these experiments we used bovine capillary endothelial (BCE) cells as a positive control for the activity of FGF-2 as an inducer of cell proliferation. Since BCE are normal primary cells, they grow more slowly than tumor cells, and under low serum conditions their growth is almost arrested. After 6 days of FGF-2 treatment, the number of BCE cells was more than 3 times higher than that of untreated cells ($p < 0.05$), showing that the FGF-2 we used was indeed active (Fig. 4.6,B).

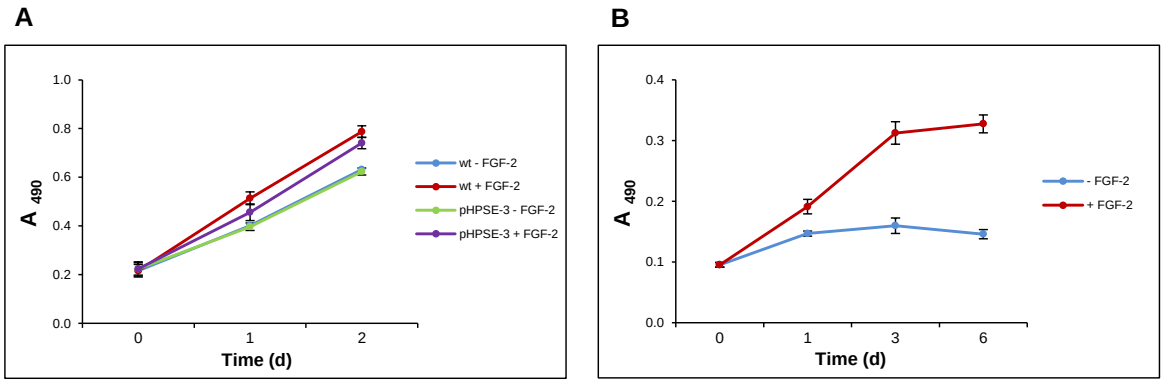

Figure 4.6. Effects of *HPSE* silencing on SF188 cell proliferation. SF188 wt and silenced cells grown in medium containing 0.5% FBS were treated with FGF-2 (10 ng/ml) for 1 and 2 days and cell number was measured by the MTS assay. BCE cells treated with FGF-2 (10 ng/ml) for 1, 3 and 6 days were used as positive control for FGF-2 activity. Each point represents mean ± standard deviation of a representative experiment performed with triplicate samples.

4.5 MT1-MMP, FGF-2 and *FGFRs* expression in MCF-7 cells

The following experiments were performed in the Prof. Mignatti's laboratory at New York University School of Medicine, where I spent the third year of my PhD program.
Before studying the involvement of MT1-MMP in the pediatric glioma cell lines, the role of MT1-MMP was first examined in the human MCF-7 breast adenocarcinoma cell line. MCF-7 cells, which do not express MT1-MMP, offer a useful model for studying this proteinase by transient transfection of plasmids encoding wild-type (wt) or mutant MT1-MMP cDNA.
Wild-type MT1-MMP is a 582-amino acid protein consisting of numerous domains:

- pre/propeptide $M^{1} – R^{111}$
- catalytic domain $Y^{112} – G^{285}$
- hinge region $E^{286} – I^{318}$
- hemopexin domain $C^{319} – C^{508}$
- transmembrane domain $A^{539} – F^{562}$
- cytoplasmic tail $R^{563} – V^{582}$.

In our study, we used three MT1-MMP mutants:

1. MT1-MMP devoid of the hemopexin domain (Δpex);
2. MT1-MMP devoid of the cytoplasmic tail (Δcyt);
3. MT1-MMP mutated in the catalytic site, with an alanine substitution of the glutamic acid in position 240 (E240A); this mutant is devoid of proteolytic activity.

The aminoacidic sequence of MT1-MMP is shown in Fig. 4.7.

```
1    MSPAPRPPRCLLLPLLTLGTALASLGSAQSSSFSPEAWLQQYGYLPPGDLRTHTQRSPQS  60
61   LSAAIAAMQKFYGLQVTGKADADTMKAMRRPRCGVPDKFGAEIKANVRRKRYAIQGLKWQ  120
121  HNEITFCIQNYTPKVGEYATYEAIRKAFRVWESATPLRFREVPYAYIREGHEKQADIMIF  180
181  FAEGFHGDSTPFDGEGGFLAHAYFPGPNIGGDTHFDSAEPWTVRNEDLNGNDIFLVAVHE  240
241  LGHALGLEHSSDPSAIMAPFYQWMDTENFVLPDDDRRGIQQLYGGESGFPTKMPPQPRTT  300
301  SRPSVPDKPKNPTYGPNICDGNFDTVAMLRGEMFVFKERWFWRVRNNQVMDGYPMPIGQF  360
361  WRGLPASINTAYERKDGKFVFFKGDKHWVFDEASLEPGYPKHIKELGRGLPTDKIDAALF  420
421  WMPNGKTYFFRGNKYYRFNEELRAVDSEYPKNIKVWEGIPESPRGSFMGSDEVFTYFYKG  480
481  NKYWKFNNQKLKVEPGYPKSALRDWMGCPSGGRPDEGTEEETEVIIIEVDEEGGGAVSAA  540
541  AVVLPVLLLLLVLAVGLAVFFFRRHGTPRRLLYCQRSLLDKV                    583
```

Figure 4.7. Amino acidic sequence of wt MT1-MMP protein, as reported in Ensembl Genome Browser. MT1-MMP hemopexin and cytoplasmic domains are highlighted in yellow and green, respectively; the glutamic acid (E) in position 240 of the E240A mutant is written in red and bold.

In addition, we used stable MCF-7 cells Tet-Off transfectants (clone 8 cells) in which expression of wt MT1-MMP is controlled by the tetracycline resistance transactivator, and can therefore be suppressed by addition of doxycycline (a tetracycline analog) to the culture medium.

MCF-7 cells do not express FGF-2; however, by semi-quantitative RT-PCR analysis they show high expression of *FGF-2 receptors* (*FGFR*) *1*, *2* and *4*, and low expression of *FGF receptor-3* (Fig. 4.8). For each FGFR, the forward and reverse primers used were designed to detect all the splicing variants.

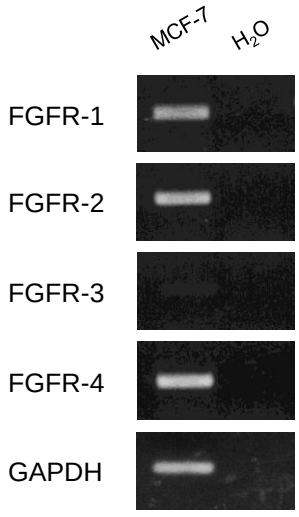

Figure 4.8. *FGFRs* expression in MCF-7 cells. *FGFRs* mRNA levels in MCF-7 cells were determined by semi-quantitative PCR. *GAPDH* mRNA was used as loading control (H_2O, negative control for PCR).

4.6 ERK1/2 activation by FGF-2 in MCF-7 cells expressing MT1-MMP

Since MCF-7 cells do not express FGF-2 but express 3 FGFRs, clone 8 cells grown in the presence or absence of DOX (i.e. without or with expression of MT1-MMP) were treated with human recombinant FGF-2 (0.75 ng/ml) for 15 min and ERK1/2 activation was analyzed by Western blotting.
As shown in Fig. 4.9, ERK1/2 activation by FGF-2 was lower in MT1-MMP expressing cells than in cells with no MT1-MMP expression.

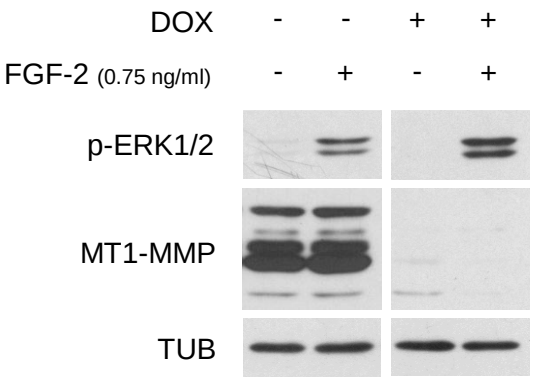

Figure 4.9. ERK1/2 activation by FGF-2 in MCF-7 cells. MT1-MMP Tet-Off MCF-7 cells (MCF-7 clone 8) grown for 24 h in the presence (no MT1-MMP expression) or absence (MT1-MMP expression) of 1 µg/ml DOX in medium containing 0.5% FBS were treated with 0.75 ng/ml FGF-2 for 15 min. Active ERK1/2 (p-ERK1/2) and MT1-MMP were detected by Western blotting. Tubulin was used as a loading control.

We next performed experiments to identify the optimal FGF-2 concentration and time of treatment to detect the different activation of ERK1/2. Addition of increasing concentrations of FGF-2 (from 0.25 ng/ml to 0.75 ng/ml for 15 min) and time-course experiments (from 15 min to 60 min with 0.75 ng/ml FGF-2) showed that the difference in ERK1/2 activation between MT1-MMP expressing and non-expressing cells was most evident after FGF-2 treatment with 0.75 ng/ml for 15 min (Fig. 4.10, A and B). Therefore, all subsequent experiments were performed with 0.75 ng/ml FGF-2 and 15 min incubation, except where indicated otherwise.
To confirm this result and understand which domain of MT1-MMP is responsible for the different ERK1/2 activation, MCF-7 cells transiently transfected with wt or mutant MT1-MMP cDNAs were treated with FGF-2 (0.75 ng/ml for 15 min).

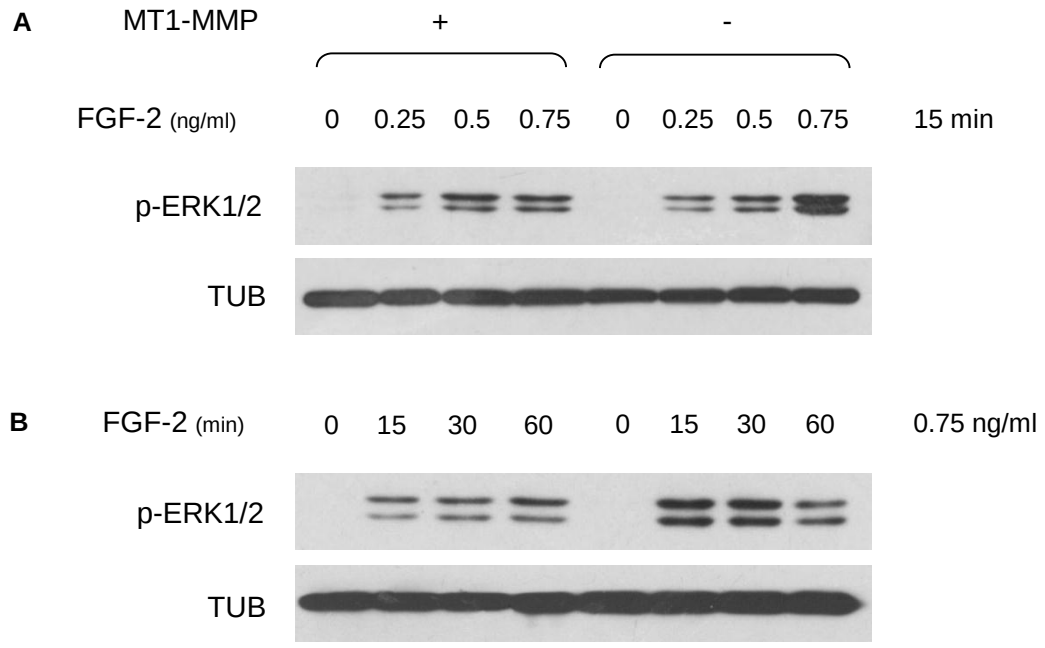

Figure 4.10. ERK1/2 activation by FGF-2 in MCF-7 cells. MCF-7 cells grown for 24 h in the presence or absence of DOX in medium containing 0.5% FBS were treated with increasing concentrations of FGF-2 (A) (0.25 ng/ml to 0.75 ng/ml) for 15 min or with 0.75 ng/ml FGF-2 for increasing times (B) (15 min to 60 min). ERK1/2 phosphorylation was detected by Western blotting. Tubulin was used as a loading control.

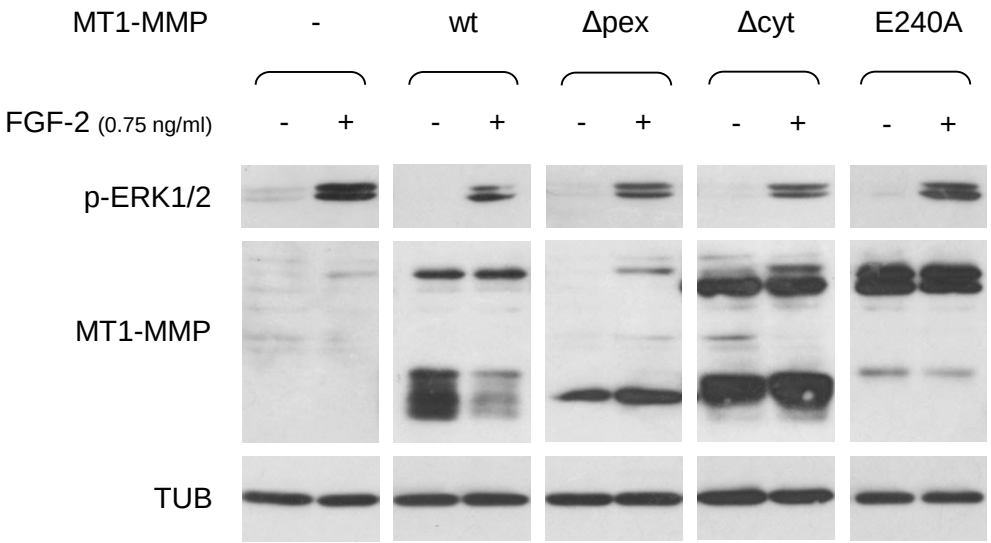

Figure 4.11. ERK1/2 activation by FGF-2 in MCF-7 cells transiently transfected with MT1-MMP. MCF-7 cells transiently transfected with wt or mutant MT1-MMP cDNAs were grown for 24 h in medium containing 0.5% FBS and treated with FGF-2 (0.75 ng/ml for 15 min). ERK1/2 phosphorylation and MT1-MMP expression were detected by Western blotting. Tubulin was used as a loading control (-, empty vector; Δpex, Δcyt, MT1-MMP devoid of the hemopexin domain or the cytoplasmic tail, respectively; E240A, MT1-MMP mutated in the catalytic site, with an alanine substitution of the glutamic acid in position 240).

As shown in Fig. 4.11, cells transfected with the control empty vector revealed no MT1-MMP expression. Conversely, in cells transfected with wt MT1-MMP, Western blotting analysis showed one 57 kDa band corresponding to active MT1-MMP, in addition to low molecular weight bands that represent MT1-MMP degradation products generated by auto-catalysis. Since the hemopexin domain accounts for 189 of 472 amino acids of active MT1-MMP, cells transfected with mutant MT1-MMP devoid of this domain (Δpex) showed a band of approximately 40 kDa. In contrast, mutant MT1-MMP lacking the short (20 amino acids) cytoplasmic tail (Δcyt) migrated in the gel as a band with a molecular weight similar to that of wt MT1-MMP. MCF-7 cells transfected with MT1-MMP mutated in the catalytic site (E240A) expressed a full-length protein, but no degradation products were detectable.

The level of ERK1/2 activation by FGF-2 in cells transfected with the empty vector was comparable to that obtained with the E240A mutant, and more elevated than the one observed in cells transfected with wt MT1-MMP. MCF-7 cells expressing either Δpex or Δcyt MT1-MMP, which are both proteolytically active, showed levels of ERK1/2 activation similar to that of cells expressing wt MT1-MMP (Fig. 4.11). These results therefore indicate that MT1-MMP decreases activation of ERK1/2 by a mechanism mediated by its catalytic domain.

To confirm this indication clone 8 cells were pre-treated with Ilomastat, a potent inhibitor of the catalytic activity of MMPs, and incubated with FGF-2. Consistent with the previous results, ERK1/2 activation by FGF-2 was lower in clone 8 cells expressing catalytically active MT1-MMP than in cells where the enzymatic activity was inhibited by Ilomastat (Fig. 4.12,A).

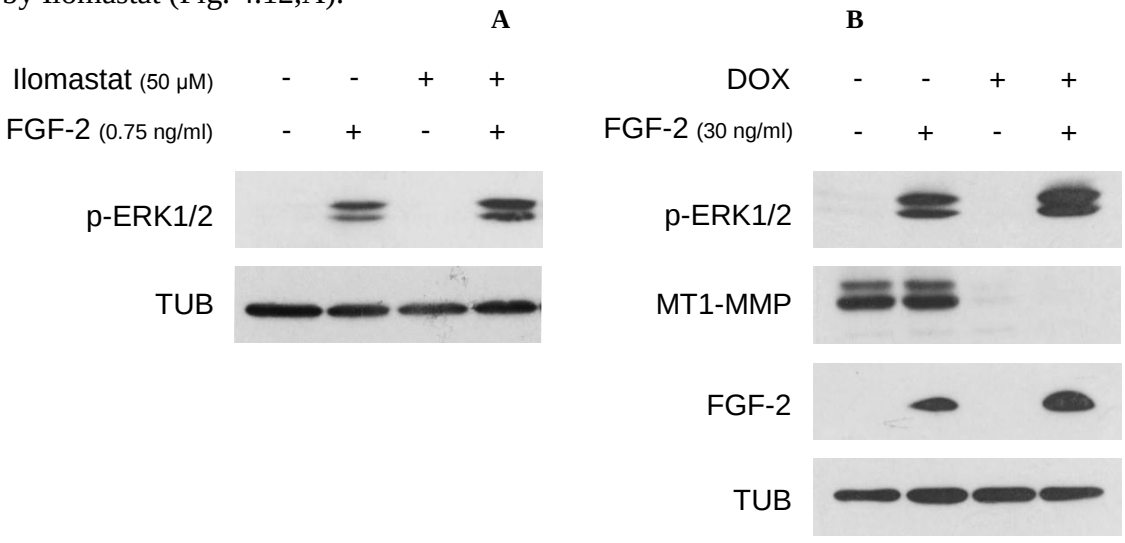

Figure 4.12. ERK1/2 activation by FGF-2 in MCF-7 cells. (A) MCF-7 cells grown for 24 h in medium containing 0.5% FBS were treated with Ilomastat (50 μM), a potent inhibitor of the catalytic activity of MMPs, and FGF-2 (0.75 ng/ml for 15 min). (B) MCF-7 cells grown for 24 h in the presence or absence of DOX in medium containing 0.5% FBS were treated with FGF-2 (30 ng/ml for 15 min). ERK1/2 phosphorylation, MT1-MMP expression and cell-associated FGF-2 were detected by Western blotting. Tubulin was used as a loading control.

The same effect was observed in other experiments in which MCF-7 cells expressing MT1-MMP were treated with 30 ng/ml FGF-2, a saturating concentration. In these experiments we also observed that the level of cell-associated FGF-2 was lower in cells that expressed than in cells that did not express MT1-MMP (Fig. 4.12,B).
These findings indicated that the proteolytic activity of MT1-MMP controls FGF-2 signaling by regulating the amount of FGF-2 that binds to the cells.

4.7 Effects of MT1-MMP on cell-associated FGF-2

To test the hypothesis of the possible regulation of FGF-2 signaling by active MT1-MMP we performed a series of experiments. In the first set of experiments, clone 8 cells grown in the presence of DOX (i.e. not expressing MT1-MMP) were treated with FGF-2 (30 ng/ml) for increasing lengths of time (5 min to 30 min), and ERK1/2 activation and cell-associated FGF-2 were analyzed by Western blotting analysis.

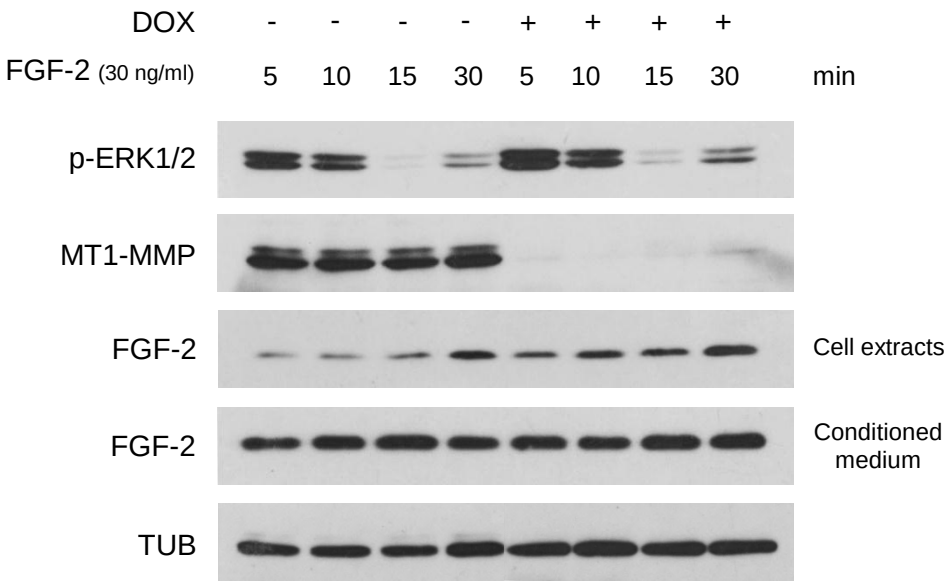

Figure 4.13. ERK1/2 activation by FGF-2 in MCF-7 cells. MCF-7 cells grown for 24 h in the presence or absence of DOX in medium containing 0.5% FBS were treated with FGF-2 (30 ng/ml) for increasing times (from 5 min to 30 min). ERK1/2 phosphorylation, MT1-MMP expression and cell-associated or soluble FGF-2 in the conditioned medium were detected by Western blotting. Tubulin was used as a loading control.

As shown in Fig. 4.13, maximum ERK1/2 activation occurred after 5 min of FGF-2 treatment and rapidly decreased, whereas the amount of cell-associated FGF-2 increased in a time-dependent manner, and only one band with a molecular weight equal to 17 kDa - corresponding to the recombinant exogenous FGF-2 - was detected in the cell extracts. At each time-point, both ERK1/2 phosphorylation and cell-associated FGF-2 were lower in MT1-MMP expressing cells than in cells devoid of this proteinase. In contrast, no

differences were detected in FGF-2 levels in the conditioned medium of cells that expressed *vs*. cells that did not express MT1-MMP (Fig. 4.13).
Since the quantity of FGF-2 observed in the conditioned medium was too high to appreciate potential differences, the experiment was repeated with 3 ng/ml FGF-2. However, with the exception of the 5 min time-point, also this experiment did not show any MT1-MMP-dependent differences in the levels of FGF-2 (Fig. 4.14).

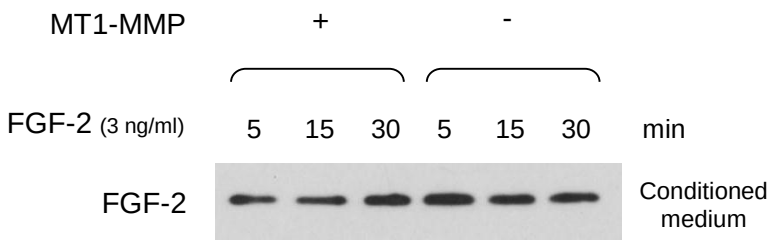

Figure 4.14. FGF-2 amount in MCF-7 cell conditioned medium. MCF-7 cells grown for 24 h in the presence or absence of DOX in medium containing 0.5% FBS were treated with FGF-2 (3 ng/ml) for increasing times (5 min to 30 min). FGF-2 was detected in the conditioned medium by Western blotting.

To investigate whether MT1-MMP affects FGF-2 binding to its low- (heparan sulfate proteoglycans, HSPGs) and/or high-affinity receptors (FGFRs), clone 8 cells were treated with 30 ng/ml of FGF-2 for 15 min, and subsequently washed 3 times with PBS alone or with PBS followed by a buffer containing either 2 M NaCl at pH 7.5 (2 M NaCl in 20 mM HEPES, pH 7.5) or 2 M NaCl at pH 4.0 (2 M NaCl in 20 mM sodium acetate, pH 4.0). Because of their different ionic strength (pH), these two buffers remove FGF-2 from the HSPGs or the FGFRs, respectively [82]. The amount of FGF-2 was finally detected in both cell extracts and washing buffers by Western blotting.
As shown in Fig. 4.15, consistent with previous results, in the control cells washed with PBS alone a lower amount of FGF-2 was present in extracts of MT1-MMP expressing cells than in cells without MT1-MMP. The detachment of FGF-2 from the cell surface was demonstrated by the presence of very faint bands corresponding to FGF-2 in extracts of the cells after the 2 M NaCl washings. Only in MT1-MMP non-expressing cells washed with 2.0 M NaCl at pH 7.5, FGF-2 was detected in the washing buffers, indicating that the amount of FGF-2 bound to the HSPGs in these cells was higher than in MT1-MMP expressing cells. In cells washed with 2 M NaCl at pH 4.0, no FGF-2 was identified (Fig. 4.15).

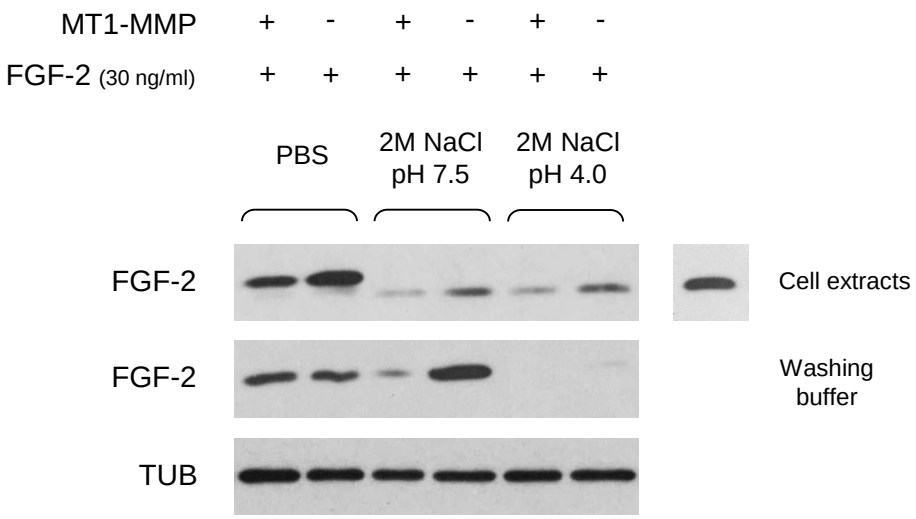

Figure 4.15. FGF-2 binding to low- and high-affinity receptors. MCF-7 cells grown for 24 h in the presence or absence of DOX in medium containing 0.5% FBS were treated with FGF-2 (30 ng/ml for 15 min) and then washed with PBS alone or with a buffer containing either 2 M NaCl at pH 7.5 or 2 M NaCl at pH 4.0. FGF-2 was detected in both cell extracts and washing buffers by Western blotting. One nanogram of the recombinant FGF-2 was also loaded to verify the molecular weight of cell-associated and detached FGF-2. Tubulin was used as a loading control.

4.8 Characterization of cell-associated FGF-2

To confirm that MT1-MMP does not degrade FGF-2 we used recombinant human FGF-2 labeled with biotin. This approach is preferable to Western blotting analysis to detect FGF-2 degradation. Indeed, monoclonal anti-FGF-2 antibody interacts with a specific region of FGF-2; if this region is cleaved from the protein the cleavage product may be impossible to detect.

Recombinant FGF-2 is a small protein with a molecular weight of 17 kDa, and composed of 155 amino acids. Biotin reacts chemically with the primary amino groups (-NH_2) of lysine (K), arginine (R), and the N-terminus of proteins, and these amino acid residues are numerous and well-distributed in FGF-2 (Fig. 4.16).

```
1     MAAGSITTLPALPEDGGSGAFPPGHFKDPKRLYCKNGGFFLRIHPDGRVDGVREKSDPHI   60
61    KLQLQAEERGVVSIKGVCANRYLAMKEDGRLLASKCVTDECFFFERLESNNYNTYRSRKY  120
121   TSWYVALKRTGQYKLGSKTGPGQKAILFLPMSAKS                           155
```

Figure 4.16. Amino acidic sequence of recombinant FGF-2 protein, as reported in Ensembl Genome Browser. Lysine (K) and arginine (R) residues are highlighted in yellow and light blue respectively.

Since the specific biotin used in this study was conjugated to a sulfated group, the biotinylated-FGF-2 could not permeate cell membranes, and only ECM- and/or membrane-bound FGF-2 could be detected.

After biotinylation, FGF-2 could be detected by both anti-FGF-2 antibody and streptavidin (Fig. 4.17,A). We then treated clone 8 cells with both unlabeled and biotinylated FGF-2, and analyzed ERK1/2 activation. The results showed that biotinylated FGF-2 was less effective in activating ERK1/2 than unlabeled FGF-2. Importantly, ERK1/2 phosphorylation levels induced by biotin alone were comparable to those obtained by biotinylated FGF-2, a limitation that prevented us from using biotinylated FGF-2 for the planned experiments (Fig. 4.17,B).

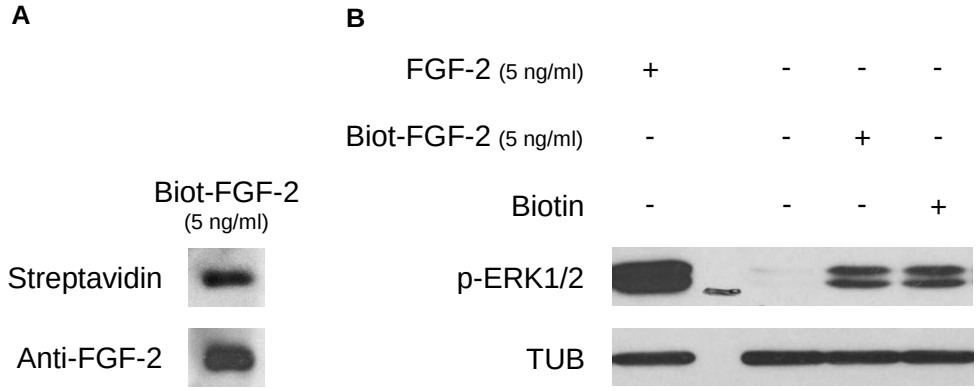

Figure 4.17. Biotinylation of soluble FGF-2. (A) Recombinant human FGF-2 labeled with biotin (5 ng/ml) was detected by Western blotting with streptavidin or with anti-FGF-2 antibody. (B) MCF-7 cells were treated with unlabeled FGF-2 (5 ng/ml), biotinylated FGF-2 (5 ng/ml) or biotin alone for 15 min. ERK1/2 activation was detected by Western blotting. Tubulin was used as a loading control.

Therefore, we adopted an alternative strategy. We first treated clone 8 cells with unlabeled FGF-2 (30 ng/ml for 15 min), and then biotinylated the proteins associated with the cell surface. These proteins included the exogenous FGF-2 bound to the FGFRs and to the HSPGs. The biotinylated FGF-2 was then immunoprecipitated with anti-FGF-2 antibody, and the immunocomplex detected by Western blotting using streptavidin.

As shown in Fig. 4.18, consistent with the previous results the amount of biotinylated FGF-2 was lower in MT1-MMP-expressing cells than in cells with no MT1-MMP. Indeed this difference was more evident than the one detected with anti-FGF-2 antibody, as this also detects intracellular, i.e. unlabeled, FGF-2 (Fig. 4.18).

Taken together, these experiments showed that catalytically active MT1-MMP reduces FGF-2 binding to the cell surface, but does not degrade it.

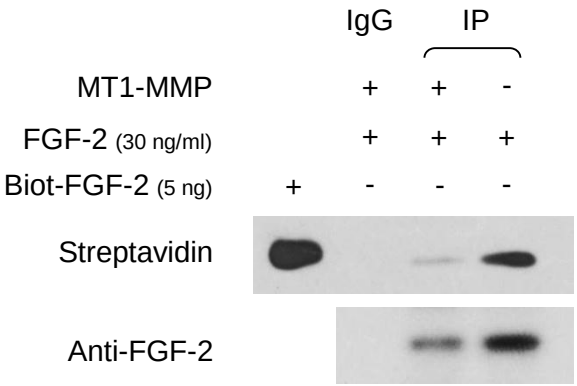

Figure 4.18. Biotinylation of cell surface-associated FGF-2. MCF-7 cells grown for 24 h in the presence or absence of DOX in medium containing 0.5% FBS were treated with unlabeled FGF-2 (30 ng/ml for 15 min) and cell surface-associated proteins, including FGF-2, were biotinylated. The biotinylated FGF-2 was immunoprecipitated with anti-FGF-2 antibody, and the immunocomplex detected by Western blotting using streptavidin. Five nanograms of the biotinylated FGF-2 were also loaded as a control for streptavidin binding to biotin.

4.9 Effects of decreased FGF-2 binding on MCF-7 cell proliferation

Since in MCF-7 cells expressing a catalytically active MT1-MMP both ERK1/2 activation by FGF-2 and the total amount of cell-associated FGF-2 were reduced, we investigated whether these effects affected cell proliferation. To test this hypothesis, clone 8 cells grown in the presence of DOX (i.e. without MT1-MMP expression) were treated with FGF-2 (10 ng/ml) and proliferation was analyzed by the MTS assay after 1, 2 and 3 days. Although these experiments were done in the presence of low serum concentration (0.5% FBS), the cells showed a very rapid growth rate. Cells treated with FGF-2 for 3 days showed a 50% increase in proliferation relative to untreated cells ($p < 0.05$). No statistically significant differences in cell proliferation were observed between MT1-MMP-expressing and non-expressing cells (Fig. 4.19).

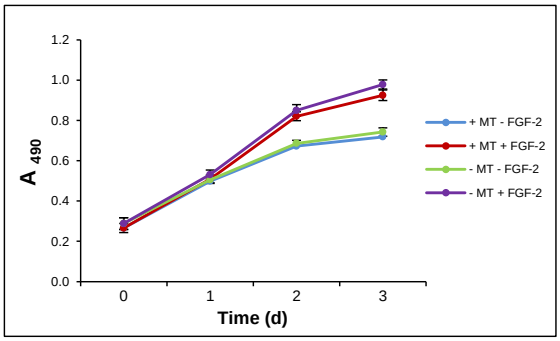

Figure 4.19. Effects of decreased FGF-2 binding on MCF-7 cell proliferation. MCF-7 cells grown for 24 h in the presence or absence of DOX in medium containing 0.5% FBS were treated with FGF-2 (10 ng/ml) for 1, 2 and 3 days and cell number was measured by the MTS assay. Each point represents mean ± standard deviation of a representative experiment performed with triplicate samples (MT, MT1-MMP).

4.10 MT1-MMP, FGF-2 and *FGFRs* expression in pediatric glioma cells

We further investigated whether the novel mechanism of FGF-2 control by MT1-MMP observed in MCF-7 cells was also effective in the pediatric glioma cell lines.
In order to evaluate MT1-MMP and FGF-2 expression in these cells, a preliminary Western blot analysis was performed. The results showed that two of the five cell lines (UW479 and Res186) express high levels of MT1-MMP, two (SF188 and Res259) have moderate expression levels, and one (KNS42) expressed no MT1-MMP. In all MT1-MMP-expressing cells, MT1-MMP appeared in the gel as a single band and no degradation products were detected.
Res186 cells exhibited high expression of both low- (17 kDa) and high-molecular weight (22 kDa) FGF-2. KNS42 cells expressed low levels of FGF-2, whereas the other cell lines showed no FGF-2 expression (Fig. 4.20,A).

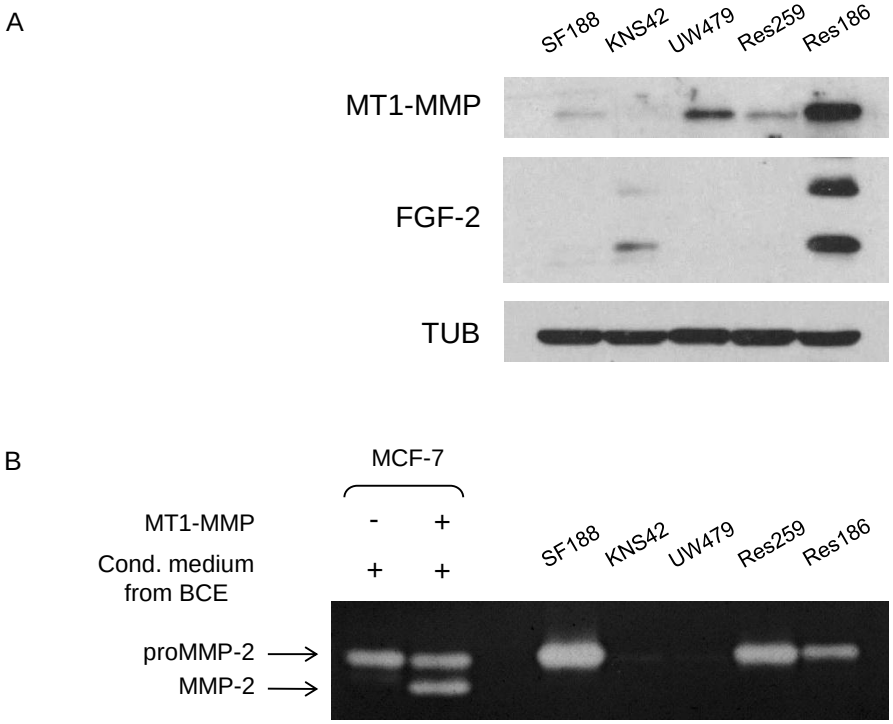

Figure 4.20. MT1-MMP and FGF-2 expression and MMP-2 activity in pediatric glioma cells. (A) MT1-MMP and FGF-2 expression was analyzed by Western blotting of pediatric glioma cell extracts. Tubulin was used as a loading control. (B) Glioma cell-conditioned medium was analyzed by gelatin zymography. As a positive control, BCE cell-conditioned medium containing proMMP-2 was incubated for 24 h with MCF-7 cells transfected with wt MT1-MMP. Both proMMP-2 and MMP-2 are visible.

Since proMMP-2 activation is a simple and indirect method to understand whether MT1-MMP is expressed in its activated form, we analyzed glioma cell-conditioned medium by gelatin zymography. As a positive control, BCE cell-conditioned medium, which contains proMMP-2, was incubated for 24 h with MCF-7 cells transfected with wt MT1-MMP.

MCF-7 cells do not express proMMP-2 or MMP-2 (not shown), but the transfected cells produce active MT1-MMP, which activates the proMMP-2 secreted from the BCE cells. Both proMMP-2 and MMP-2 were indeed detected in this control sample by zymography. Among the pediatric glioma cell lines, SF188, Res259 and Res186 cells showed only one band corresponding to the proMMP-2, whereas no MMP was detected in the other cell lines (Fig. 4.20,B).

UW479 and Res186 cells, which express MT1-MMP, were then incubated with BCE cell-conditioned medium, and, as shown in Fig. 4.21, in both cell lines only proMMP-2 was detected (Fig. 4.21). This finding indicated that the MT1-MMP expressed by these cells is not active.

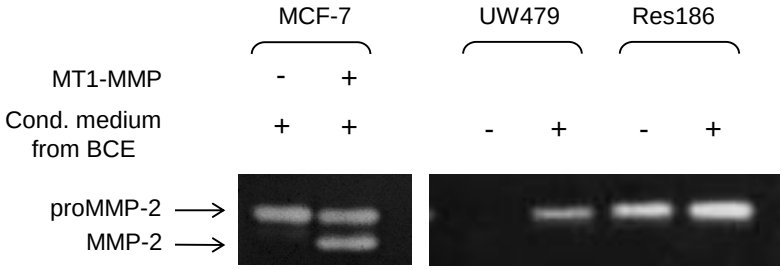

Figure 4.21. MMP-2 activity in UW479 and Res186 cells. BCE cell-conditioned medium incubated for 24 h with UW479 and Res186 cells and with MCF-7 cells transfected with wt MT1-MMP, as a positive control, was analyzed by gelatin zymography.

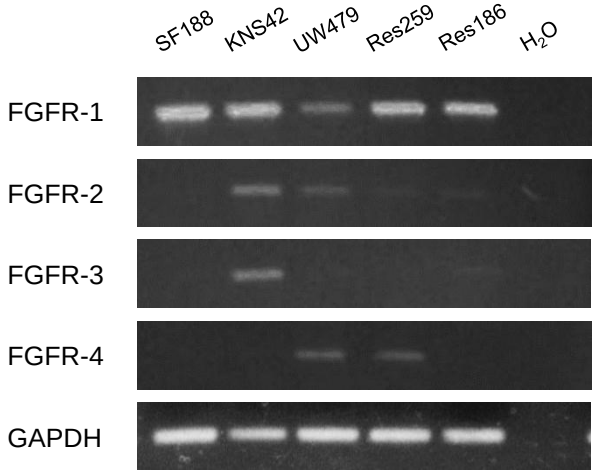

Semi-quantitative PCR analysis was then carried out to characterize the expression of the *FGFRs* in the pediatric glioma cell lines. Each cell line expressed at least one of the four *FGFRs* mRNA; *FGFR-1* being expressed in all cell lines (Fig. 4.22).

Figure 4.22. *FGFRs* expression in pediatric glioma cells. *FGFRs* mRNA levels in pediatric glioma cells were determined by semi-quantitative PCR. *GAPDH* mRNA was used as loading control (H_2O, negative control for PCR).

4.11 ERK1/2 activation by FGF-2 in pediatric glioma cells

Given the heterogeneity in the expression of MT1-MMP, FGF-2 and FGFRs, all the pediatric glioma cell lines were treated with recombinant FGF-2 (10 ng/ml for 15 min) to analyze ERK1/2 activation and understand whether a correlation between ERK1/2 activation and MT1-MMP expression also exists in these tumor cells.
In SF188, KNS42 and Res259 cells FGF-2 induced stronger ERK1/2 phosphorylation than in the other cell lines. In particular, under these experimental conditions, no ERK1/2 activation was induced by FGF-2 in UW479 cells, whereas Res186 cells showed constitutive ERK1/2 activation, even without FGF-2 treatment. In agreement with the results previously obtained with MCF-7 cells, ERK1/2 activation seemed to inversely correlate with MT1-MMP expression (Fig. 4.23).

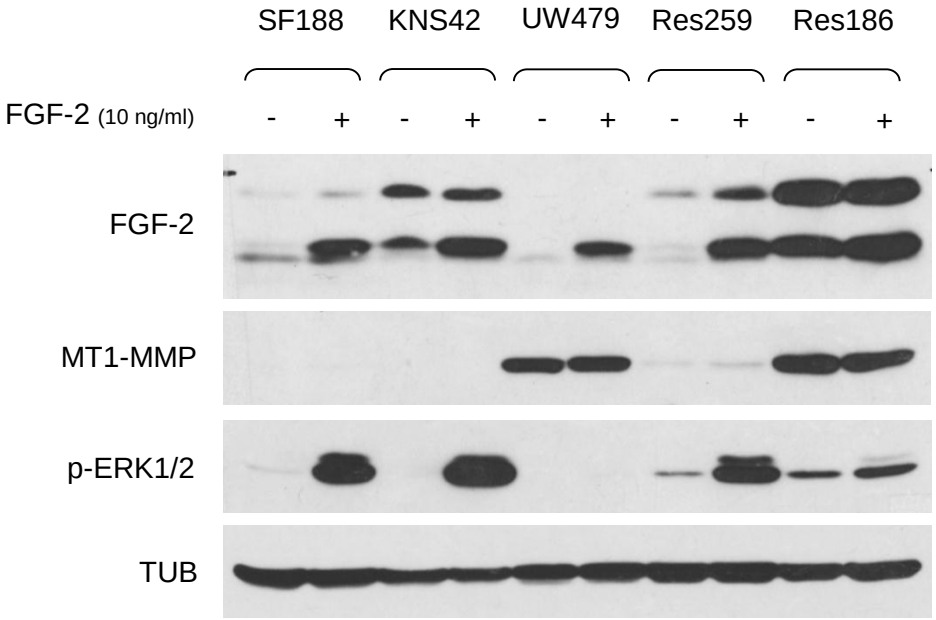

Figure 4.23. ERK1/2 activation by FGF-2 in pediatric glioma cells. Pediatric glioma cells grown for 24 h in medium containing 0.5% FBS were treated with FGF-2 (10 ng/ml for 15 min). ERK1/2 activation, FGF-2 and MT1-MMP were detected by Western blotting. Tubulin was used as a loading control.

Since SF188 cells were one of the most responsive to FGF-2 treatment, subsequent dose-response and time-course analyses of ERK1/2 activation were performed with these cells. Addition of increasing concentrations of FGF-2 (from 0.1 to 10 ng/ml for 15 min) showed that maximum ERK1/2 phosphorylation occurred with 1.0 ng/ml of FGF-2 and was very rapid (5-15 min) (Fig. 4.24).

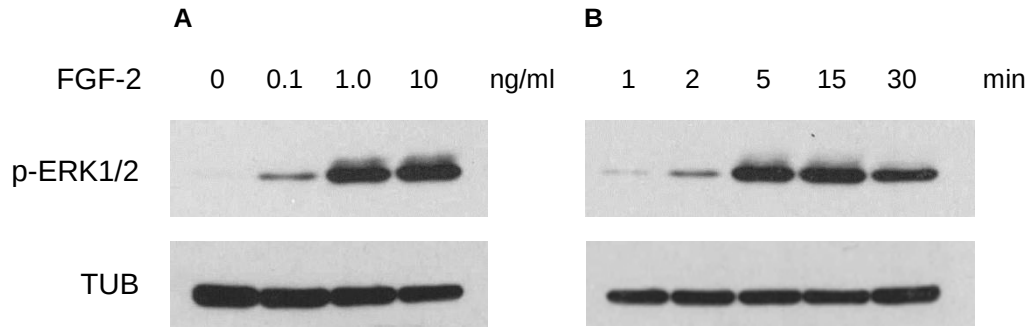

Figure 4.24. ERK1/2 activation by FGF-2 in SF188 cells. SF188 cells grown for 24 h in medium containing 0.5% FBS were treated with increasing concentrations of FGF-2 (A) (0.1 ng/ml to 10 ng/ml) for 15 min, or with 1 ng/ml FGF-2 for increasing times (B) (1 min to 30 min). ERK1/2 activation was detected by Western blotting. Tubulin was used as a loading control.

In order to investigate the existence of a potential common mechanism through which MT1-MMP could regulate intracellular signaling by FGF-2 in different tumor cells, glioma cells were pre-treated with the MMP inhibitor Ilomastat, and then incubated with FGF-2 (10 ng/ml for 15 min) (Fig. 4.25).

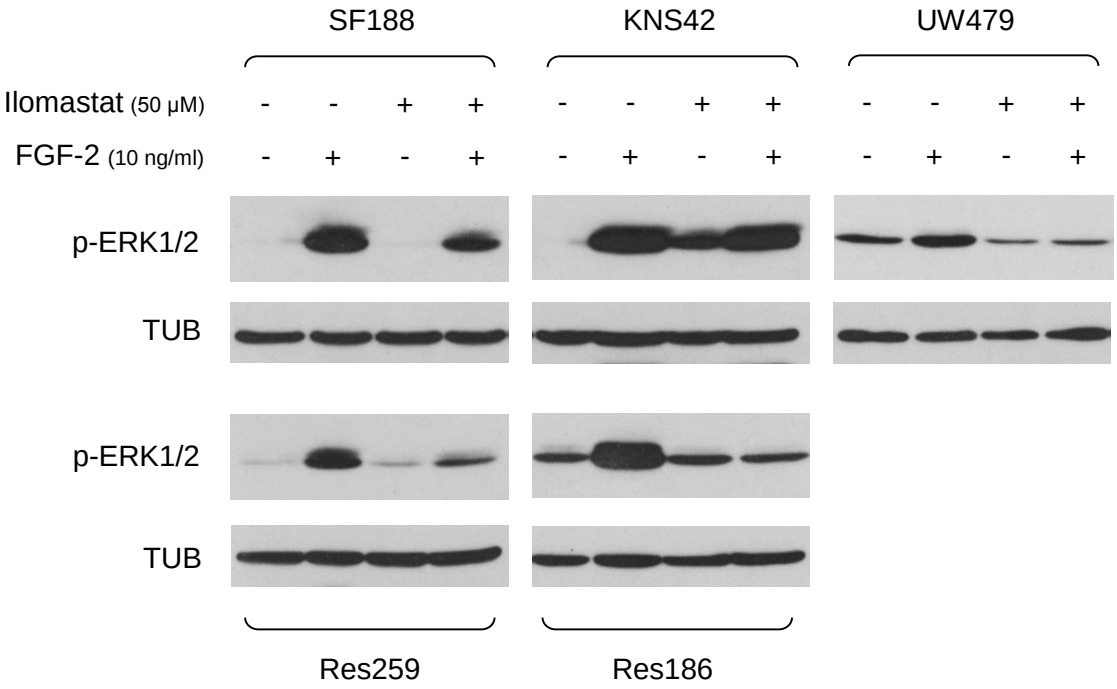

Figure 4.25. ERK1/2 activation by FGF-2 in pediatric glioma cells treated with Ilomastat. Pediatric glioma cells grown for 24 h in medium containing 0.5% FBS were treated with Ilomastat (50 µM) and FGF-2 (10 ng/ml) for 15 min. ERK1/2 activation was detected by Western blotting. Tubulin was used as a loading control.

In contrast to that observed with clone 8 cells, in all glioma cell lines ERK1/2 phosphorylation levels by FGF-2 were higher in cells expressing catalytically active MT1-MMP (and possibly other MMPs) than in cells where MT1-MMP activity was inhibited by Ilomastat. Moreover, in KNS42 and UW479 cells, ERK1/2 activation also occurred in cells treated with Ilomastat alone (Fig. 4.25).

To make sure that this finding did not result from a nonspecific effect of Ilomastat but was a consequence of MMP inhibition, SF188 cells were incubated with 1,10-phenantroline, another MMP inhibitor, and then treated with FGF-2 (10 ng/ml for 15 min). As shown in Fig. 4.26, the results obtained with this inhibitor confirmed that ERK1/2 activation by FGF-2 was more elevated in SF188 cells expressing catalytically active MMPs than in cells where MMP activities were inhibited (Fig. 4.26).

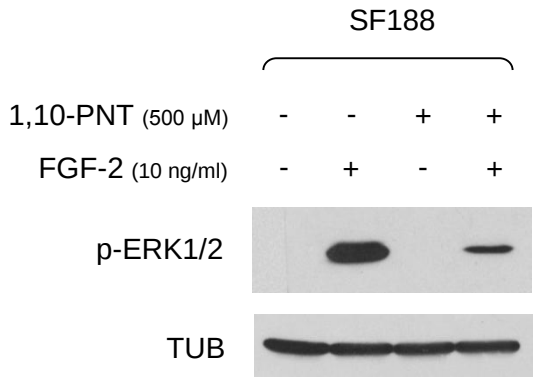

Figure 4.26. ERK1/2 activation by FGF-2 in SF188 cells treated with 1,10-phenantroline. SF188 cells grown for 24 h in medium containing 0.5% FBS were treated with 1,10-phenantroline (500 µM), an inhibitor of the catalytic activity of MMPs, and FGF-2 (30 ng/ml) for 15 min. ERK1/2 activation was detected by Western blotting. Tubulin was used as a loading control.

In a similar experiment, UW479 and Res186 cells were incubated with Ilomastat and 30 ng/ml of FGF-2 (15 min), and both ERK1/2 activation and cell-associated FGF-2 were analyzed by Western blotting. In UW479 cells, ERK1/2 activation by FGF-2 was either not measureable (Fig. 4.23), or sometimes very faint; low levels of constitutive ERK1/2 activation were observed both in the presence and absence of FGF-2 (Fig. 4.27). UW479 cells showed increased ERK1/2 phosphorylation in the presence of Ilomastat, which was reduced by FGF-2 treatment. No differences in the amount of cell-associated FGF-2 were found between UW479 cells in the presence or absence of Ilomastat. Consistent with ERK1/2 activation, in Res186 cells the amount of FGF-2 was decreased in the presence of Ilomastat. This reduction affected both endogenous FGF-2 (22 and 24 kDa) and exogenous recombinant FGF-2 (17 kDa) (Fig. 4.27).

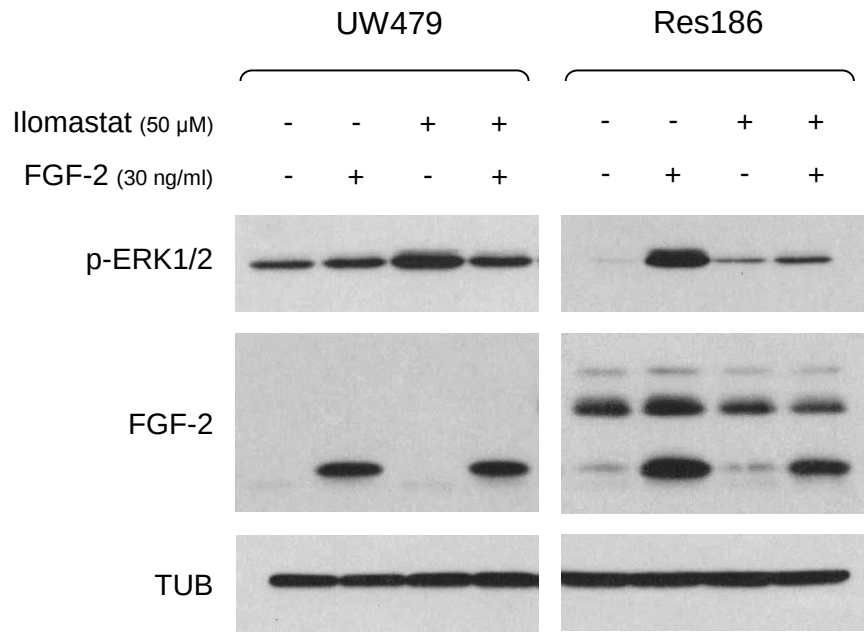

Figure 4.27. ERK1/2 activation by FGF-2 in UW479 and Res186 cells treated with Ilomastat. UW479 and Res186 cells grown for 24 h in medium containing 0.5% FBS were treated with Ilomastat (50 µM) and FGF-2 (30 ng/ml) for 15 min. ERK1/2 activation and FGF-2 were detected by Western blotting. Tubulin was used as a loading control.

As shown before, both UW479 and Res186 cells express MT1-MMP but do not activate proMMP-2 form, indicating that MT1-MMP is not activated (proMT1-MMP).

To understand what mechanism(s) could explain the differences in ERK1/2 activation and FGF-2 amount in these cells, KNS42 and Res259 cells, which do not express MT1-MMP, were transiently transfected with plasmids encoding wt or catalytically inactive MT1-MMP (E240A MT1-MMP), or with the control empty vector. KNS42 cells were then incubated for 24 h with SF188 cell-conditioned medium, which contains proMMP-2. Conversely, Res259 cells, which express proMMP-2, were incubated with plain medium. MT1-MMP expression and proMMP-2 activation were then analyzed by Western blotting and gelatin zymography, respectively.

As shown in Fig. 4.28, in KNS42 and Res259 cells transfected with wt MT1-MMP, MT1-MMP was expressed both as a full-length protein and as degradation products generated by auto-catalysis. However, MT1-MMP degradation products were not observed in KNS42 cells transfected with the catalytically inactive MT1-MMP E240A mutant; in contrast, they were present in Res259 E240A cells, probably resulting from proteolytic cleavage by other MMPs or other proteinases. In addition, transfection efficiency was higher in KNS42 than in Res259 cells (Fig. 4.28,A). In the conditioned medium collected from cells transfected with wt MT1-MMP we observed partial activation of proMMP-2 with generation of 62 kDa MMP-2 (Fig. 4.28,B).

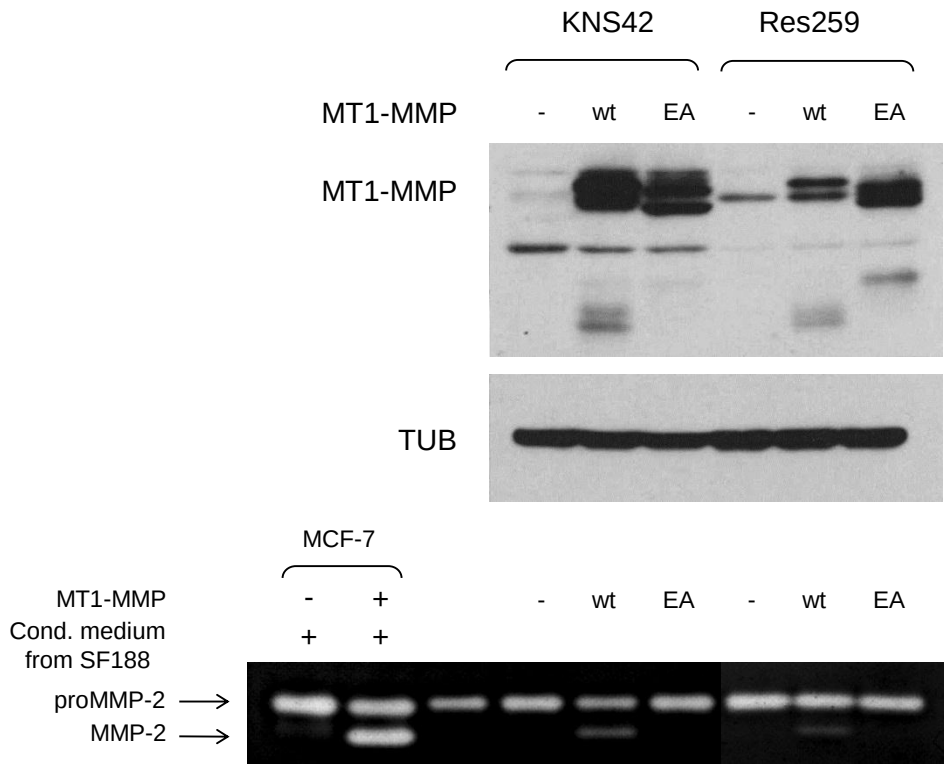

Figure 4.28. MT1-MMP expression and MMP-2 activity in KNS42 and Res259 transiently transfected cells. KNS42 and Res259 cells were transiently transfected with wt or mutant MT1-MMP cDNA. KNS42 cells were then incubated for 24 h with SF188 cell-conditioned medium, which contains proMMP-2, whereas Res259 cells, which express proMMP-2, were incubated with plain medium containing 0.5% FBS. (A) MT1-MMP expression was detected by Western blotting. Tubulin was used as a loading control (-, empty vector; EA, MT1-MMP mutated in the catalytic site). (B) Glioma cell-conditioned medium was analyzed by gelatin zymography. As a positive control, SF188 cell-conditioned medium was incubated for 24 h with MCF-7 cells transfected with wt MT1-MMP, and both proMMP-2 and MMP-2 were detected by zymography.

Subsequently, these cells were transiently transfected with the same plasmids and, 48 h after transfection, treated with FGF-2 (1 ng/ml for 15 min). In both cell lines no differences in ERK1/2 activation were detected between cells transfected with wt or catalytically inactive MT1-MMP. In contrast, in KNS42 cells transfected with E240A MT1-MMP, the level of cell-associated FGF-2 was higher than in cells transfected with wt MT1-MMP, consistent with the result previously obtained with MCF-7 cells. However, in Res259 cells the amount of cell-associated FGF-2 was higher in cells that expressed wt MT1-MMP than in cells with proteolytically inactive MT1-MMP (Fig. 4.29).

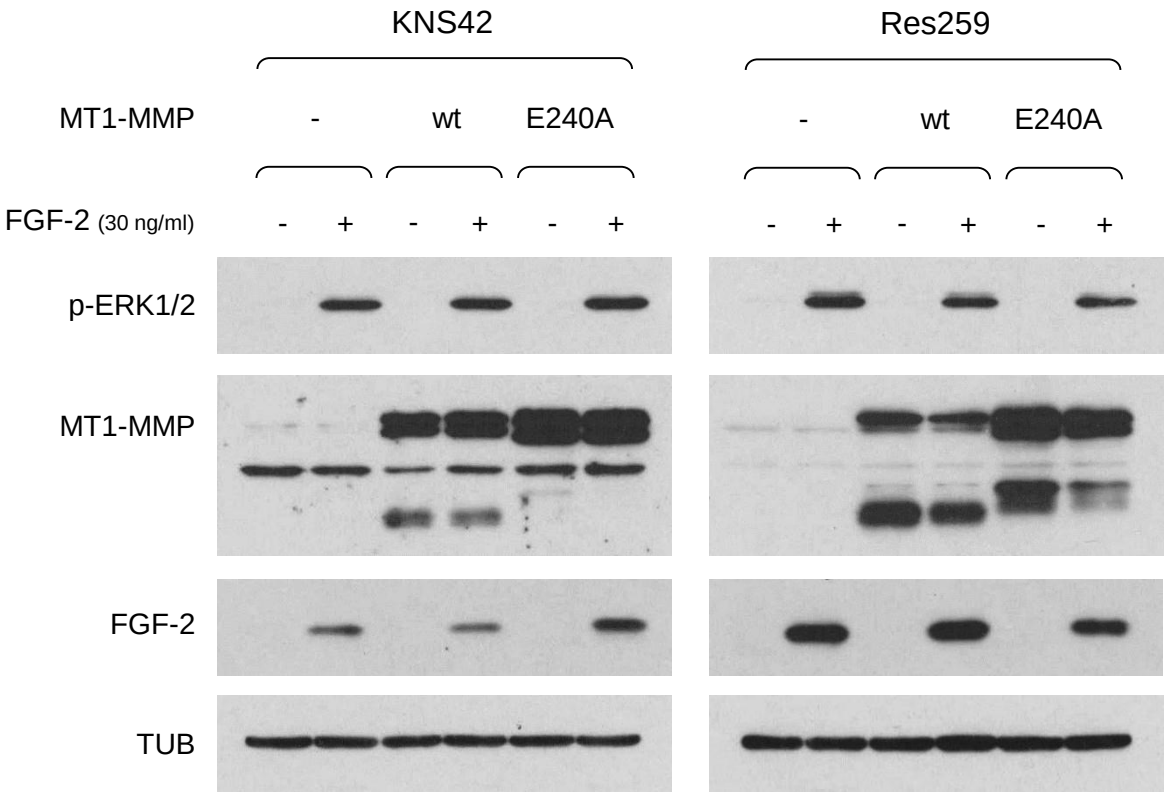

Figure 4.29. ERK1/2 activation by FGF-2 in KNS42 and Res259 cells transiently transfected with MT1-MMP. KNS42 and Res259 cells transiently transfected with wt or mutant MT1-MMP cDNA were grown for 24 h in medium containing 0.5% FBS and treated with FGF-2 (30 ng/ml for 15 min). ERK1/2 activation, and MT1-MMP and FGF-2 were detected by Western blotting. Tubulin was used as a loading control (-, empty vector; E240A, MT1-MMP mutated in the catalytic site).

4.12 Effects of FGF-2 on pediatric glioma cell proliferation

To understand whether the effects of FGF-2 on glioma cell proliferation correlated with MT1-MMP expression, all glioma cell lines were treated with FGF-2 (10 ng/ml), and proliferation was measured by the MTS assay after 1, 2 and 3 days.

All glioma cell lines showed a very rapid growth rate, both in the presence and absence of FGF-2. SF188 and KNS42 cells were the most responsive to FGF-2, showing a 35% and 70% increase in cell number, respectively, relative to untreated cells after 3 days ($p < 0.05$). At the same time-point, the effect of FGF-2 on UW479 and Res259 cell proliferation was moderate (10 and 15%, respectively). In contrast, Res186 cell proliferation was not affected by FGF-2 (Fig. 4.30).

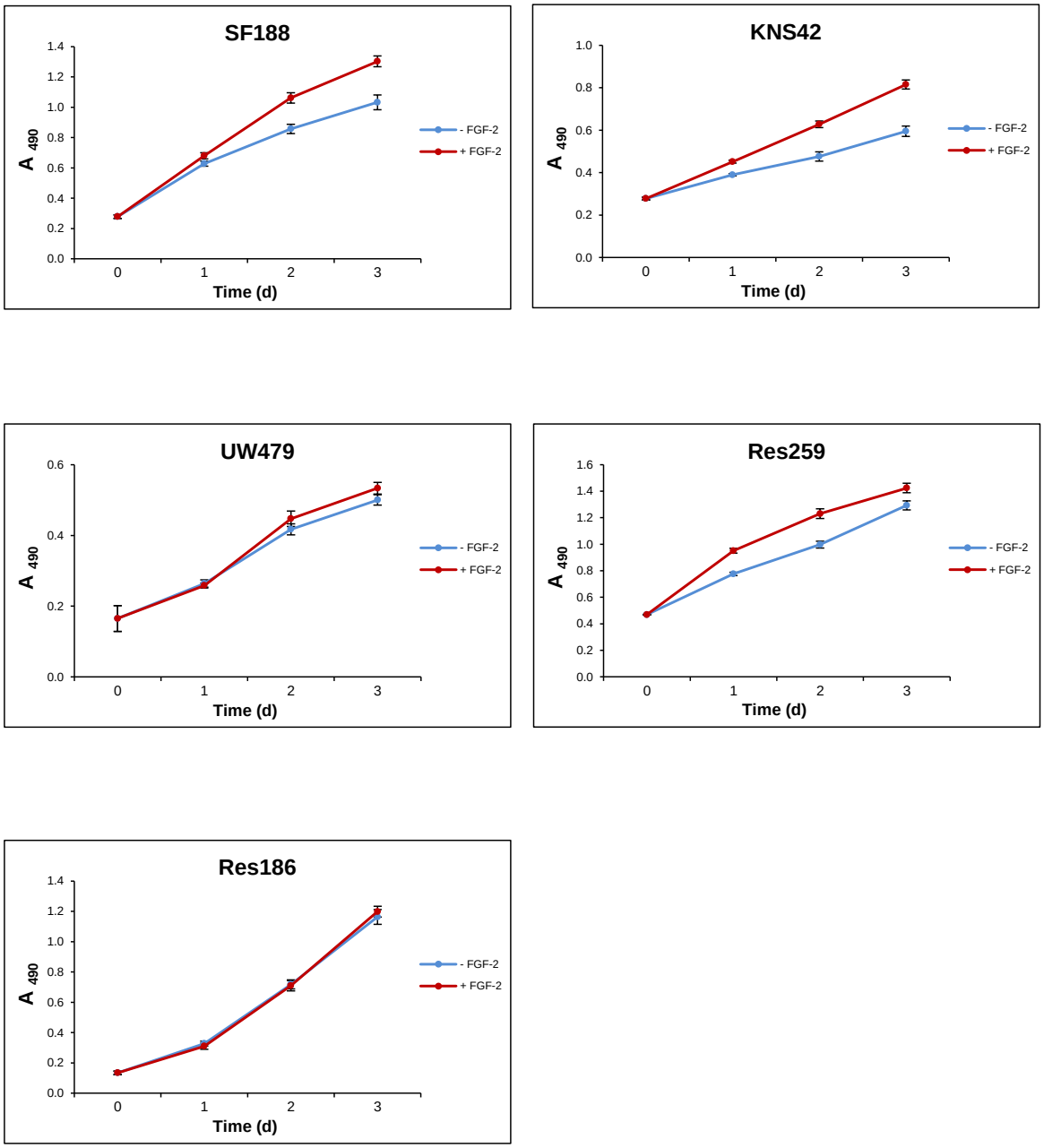

Figure 4.30. Effects of FGF-2 treatment on pediatric glioma cell proliferation. Pediatric glioma cells grown in medium containing 0.5% FBS were treated with FGF-2 (10 ng/ml) for 1, 2 and 3 days and cell number measured by the MTS assay. Each point represents mean ± standard deviation of a representative experiment performed with triplicate samples.

4.13 ERK1/2 activation by TIMP-2 in pediatric glioma cells

In MCF-7 cells and other human tumor cell lines MT1-MMP binding to its physiological protein inhibitor, TIMP-2, results in ERK1/2 activation by a proteolysis independent mechanism mediated by the cytoplasmic tail of MT1-MMP [43]. We therefore investigated whether this effect also occurs in pediatric glioma cells. For this purpose we first characterized our glioma cell lines for TIMP-2 expression by Western blotting. All the glioma cells expressed low TIMP-2 levels comparable to that of MCF-7 cells, with SF188 and UW479 cells showing lower levels than the other cell lines (Fig. 4.31).

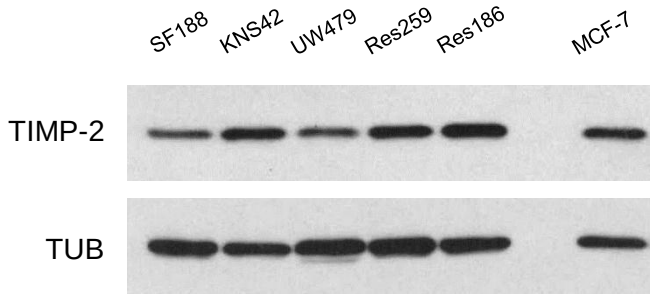

Figure 4.31. TIMP-2 expression in pediatric glioma cells. TIMP-2 was detected in pediatric glioma cell extracts by Western blotting. TIMP-2 expression in MCF-7 cells was used as positive control. Tubulin was used as a loading control.

Addition of exogenous, recombinant TIMP-2 (100 ng/ml for 15 min) to the culture medium induced ERK1/2 phosphorylation in all cell lines, and in particular the activation was stronger in SF188, Res259 and Res186 cells than in the other cell lines. However, no correlation between ERK1/2 activation and MT1-MMP expression was apparent. In fact, TIMP-2 induced ERK1/2 activation in cells that expressed MT1-MMP as efficiently as in cells without MT1-MMP (Fig. 4.32).

In MCF-7 cells the synthetic MMP inhibitor Ilomastat causes detachment of TIMP-2 from MT1-MMP and thus blocks TIMP-2 induction of ERK1/2 activation [43]. To investigate whether this effect also occurred in the glioma cell lines, UW479 and Res186 cells, which expressed MT1-MMP, were treated with TIMP-2 in the presence or absence of Ilomastat. In Res186 cells Ilomastat had the same effect as in MCF-7 cells. However, in UW479 cells Ilomastat alone induced strong ERK1/2 activation, which was partially reduced in the presence of TIMP-2. Conversely, no differences in ERK1/2 activation by TIMP-2 were detected in UW479 cells in the presence or absence of Ilomastat (Fig. 4.33).

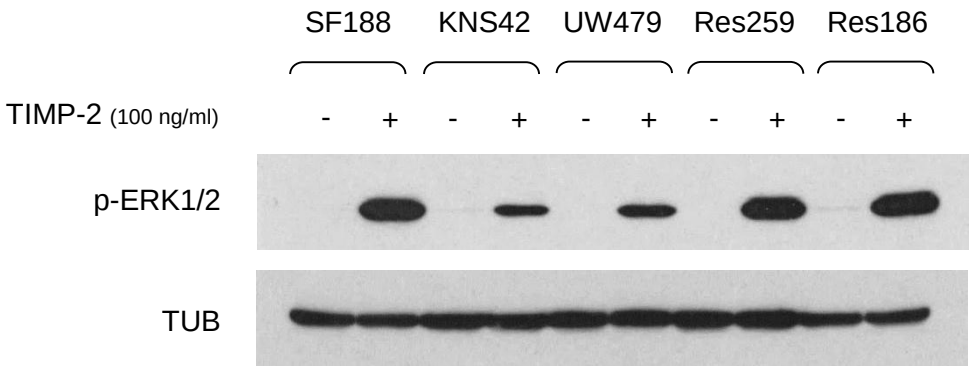

Figure 4.32. ERK1/2 activation by TIMP-2 in pediatric glioma cells. Pediatric glioma cells grown for 24 h in medium containing 0.5% FBS were treated with recombinant TIMP-2 (100 ng/ml for 15 min). ERK1/2 activation was detected by Western blotting. Tubulin was used as a loading control.

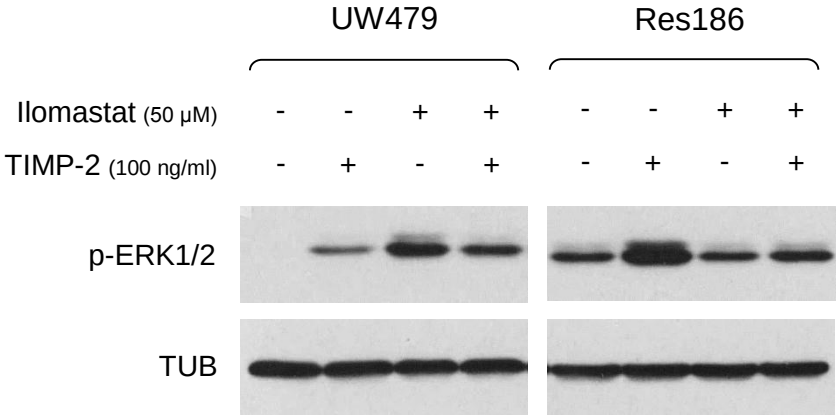

Figure 4.33. ERK1/2 activation by TIMP-2 in UW479 and Res186 cells treated with Ilomastat. UW479 and Res186 cells grown for 24 h in medium containing 0.5% FBS were treated with Ilomastat (50 μM) and TIMP-2 (100 ng/ml) for 15 min. ERK1/2 activation was detected by Western blotting. Tubulin was used as a loading control.

Chapter 5: Discussion

Primary human brain tumors represent the principal cause of solid cancer-related mortality in childhood [2]. Gliomas, the most frequent primary brain tumors, comprise a heterogeneous group of neoplasms that originate from glial cells, the supportive and most abundant cellular component of the brain. Children affected by gliomas, especially the more aggressive forms, have a poor clinical outcome and, although tumors do not metastasize, they can diffusely penetrate throughout the brain [27]. Furthermore, brain is a terminally differentiated organ protected by the blood-brain barrier, which prevents the entry of numerous drugs; therefore, tumors arising in this area are clearly different from any other malignant lesion [4]. The particular cellular composition of gliomas, together with their diffuse invasiveness and ability to escape therapies has challenged researchers for decades. Over the past 20 years the cytogenetic and molecular characterization of gliomas has been intensely investigated in association with tumor formation and progression [13,83]. Since the majority of the studies conducted so far are focused on adult gliomas, which show different genetic, molecular and clinical features from their pediatric counterparts, it is important to seek new advances for the complete understanding of childhood tumors, in order to improve their diagnosis and prognosis, as well as the development of new specific therapies for pediatric patients.

The biological mechanisms underlying glioma cell invasion in the normal brain tissue are numerous and complex. Glioma cell invasion is mainly characterized by the detachment of single tumor cells from the primary tumor mass, adhesion of cells to the ECM, degradation of the ECM and subsequent migration of cells, with the generation of neoplastic lesions distinct from the primary tumor mass [31]. Tumor cell dissemination may occur along definite structures, for example the basement membranes of blood vessels or the glial limitans externa, which contain ECM proteins. Frequently, invasive glioma cells can also migrate along myelinated fiber tracts of white matter. The extracellular space in anatomic structures, such as blood vessel basement membranes or between myelinated axons, is profoundly different, suggesting that glioma cells can use a variety of matrix ligands and activate distinct mechanisms for invasion. The enzymatic modification of the extracellular space or deposition of ECM by tumor cells may also create a more permissive environment for tumor spread into the adjacent brain [28]. The degradation of different components of the ECM involves both proteolytic and glycosidic enzymes whose activity can regulate many physiological processes, but most importantly mediate several changes in the microenvironment during tumor invasion and metastasis [84-86].

The expression of ECM-degrading enzymes and their potential role in glial tumors were investigated in this experimental study by using *in vitro* models of pediatric glioma. In particular, among the ECM-degrading enzymes, the heparan sulfate-degrading enzyme heparanase (HPSE) and membrane-type 1 matrix metalloproteinase (MT1-MMP) were the focus of our investigation.

All the pediatric glioma cell lines used in our study were derived from astrocytomas of differing grades (I, II, III and IV) arisen in patients aged 3-16 years. In particular, the cells included two glioblastoma multiforme (SF188 and KNS42), one anaplastic astrocytoma (UW479), one diffuse astrocytoma (Res259) and one pilocytic astrocytoma (Res186) cell line. These tumors originate from astrocytes, glial cells characterized by a star-like morphology that are responsible for the structural and metabolic support of neurons, and regulate the environment where they function.

The principal, detailed molecular and phenotypic characterization of these pediatric cell lines was recently carried out by Bax and colleagues [81].

Unlike the large number of MMPs, a single functional heparanase is used by cells to degrade the HS side chains of HSPGs [53]. In contrast to its widely reported overexpression in a variety of tumors, the heparan sulfate-degrading enzyme heparanase was found to be decreased in gliomas in one published study [63]. On the contrary, more recently Hong and colleagues have described heparanase upregulation in human gliomas [64]. Since the results of these few studies are still controversial, heparanase expression was investigated in all our pediatric glioma cell lines in order to understand its possible role in modulating glioma tumor growth.

Quantitative Real-Time PCR analysis showed different levels of *HPSE* expression. In order to determine the role of HPSE in pediatric gliomas, we silenced HPSE expression in SF188 cells, which produce high levels of this enzyme. Among the five stably silenced clones obtained, the one with the best silencing rate (73%) was characterized for mRNA expression of *MMP-2*, *MT1-MMP* and *VEGF*.

Zcharia and colleagues have recently shown that HPSE knock-out mice have increased expression of MMPs [74]. Consistent with this observation, we found that the SF188 HPSE silenced cells had *MMP-2* and *MT1-MMP* mRNA levels 35 and 50% higher, respectively, than non-silenced SF188 cells. This finding suggests that the upregulation of MMPs expression may compensate for the reduced *HPSE* expression.

HPSE exhibits also non-enzymatic activities independent of its involvement in ECM remodeling, and in particular it contributes to the regulation of VEGF signaling [56]. Therefore, we characterized *VEGF* mRNA expression in SF188 non-silenced and silenced cells; however, we found no differences in *VEGF* expression between the two cell lines. These results also contrast with a report by Zetser and colleagues, who provided evidence that *HPSE* overexpression and silencing in different tumor cell lines resulted in increased and reduced *VEGF* expression levels, respectively, suggesting that

VEGF expression can be regulated by HPSE [61]. Conversely, consistent with the knowledge that several growth factors, including FGF-2, upregulate *VEGF* expression [88], SF188 cells treated with FGF-2 showed 2.5-fold higher *VEGF* mRNA levels than untreated cells.
We found no statistically significant differences in cell proliferation between SF188 non-silenced and silenced cells, indicating that cell proliferation is not affected by HPSE silencing in these cells. Moreover, FGF-2 treatment induced a 25 and 20% increase in cell proliferation in non-silenced and silenced cells, respectively, an effect that can be mediated by FGF-2 directly and indirectly also by the upregulation of VEGF expression.

Before studying the involvement of MT1-MMP in the determination of the malignant phenotype of pediatric gliomas, the role of MT1-MMP was first examined in an *in vitro* model with a completely different origin, the human MCF-7 breast adenocarcinoma cell line. Since these cells do not express MT1-MMP, they represent an ideal model for the regulation of its expression as they offer the possibility to generate - by transient or stable transfection - cells that express wt or mutant MT1-MMP, and to use the parental cells with no MT1-MMP expression as control. In this study we also used a stably transfected MCF-7 cell line (MCF-7 clone 8), in which MT1-MMP expression is controlled by an inducible promoter.
The specific multi-domain structure of MT1-MMP consisting of the extracellular catalytic and hemopexin domains, a transmembrane sequence and a short cytoplasmic tail enables MT1-MMP proteolytic activity in the ECM and facilitates intracellular interactions with the transduction machinery involved in the cell response to extracellular signals [35].
In addition, MCF-7 cells do not express FGF-2 but do express three of the four FGF receptor tyrosine kinases (*FGFRs*); for this reason, they also offer a convenient model to study potential links between MT1-MMP and activation of intracellular signaling by FGF-2.
It is known that FGF-2 binding to FGFRs as well as MT1-MMP overexpression can activate several intracellular signaling pathways that control a variety of biological processes, including tumor cell proliferation and migration [65, 89], but no correlation between MT1-MMP and FGF-2 - FGFRs has been identified so far.
The results reported in this thesis show for the first time that the proteolytic activity of MT1-MMP reduces FGF-2 binding to the surface of MCF-7 cells and decreases ERK1/2 activation by FGF-2. These conclusions are based on numerous experimental evidences.
We initially observed that ERK1/2 activation by FGF-2 was lower in MT1-MMP-expressing MCF-7 cells than in cells with no MT1-MMP expression. Subsequent experiments performed with MCF-7 cells transiently transfected with plasmids encoding wt or mutant MT1-MMP cDNAs confirmed this initial observation and showed which domain of MT1-MMP was involved in the control of the cell response to FGF-2. In

particular, ERK1/2 activation by FGF-2 in MCF-7 cells transfected with the empty vector or with a plasmid encoding proteolytically inactive MT1-MMP mutated in the catalytic domain (E240A) was more elevated than in cells transfected with wt MT1-MMP. MCF-7 cells expressing MT1-MMP mutants lacking either the hemopexin (Δpex) or the cytoplasmic (Δcyt) domain but proteolytically active showed levels of ERK1/2 activation comparable to that of cells that expressed wt MT1-MMP. Therefore, this experiment showed that the proteolytic activity of MT1-MMP is responsible for the inhibition of ERK1/2 activation by FGF-2. The involvement of MT1-MMP catalytic domain was further supported by the finding that in MCF-7 cells treated with Ilomastat, a broad spectrum and potent inhibitor of the catalytic activity of MMPs, ERK1/2 activation by FGF-2 was higher than in cells that expressed proteolytically active MT1-MMP.

A recent report has shown that MT1-MMP can potentiate corneal neovascularization induced by FGF-2, by modulating FGF-2 signal transduction pathways. In particular, fibroblast cell lines expressing or not expressing MT1-MMP were treated with FGF-2, and the phosphorylation levels of the MAP kinases p38, JNK and ERK1/2 were analyzed. The Authors observed that both p38 and JNK activation by FGF-2 was higher in MT1-MMP-expressing cells than in cells with no MT1-MMP, whereas no differences were detected in ERK1/2 phosphorylation levels [90]. Although the cells used were not tumor cells and the observations contrast with the results we obtained with MCF-7 breast adenocarcinoma cells, it remains unclear how MT1-MMP can affect FGF-2 signaling.

We not only observed a difference in ERK1/2 phosphorylation levels between cells that expressed or lacked MT1-MMP but also found that the amount of cell-associated FGF-2 was reduced in MCF-7 cells expressing MT1-MMP relative to cells devoid of MT1-MMP.

Since the proteolytic activity of MT1-MMP targets numerous components of the ECM, cell adhesion molecules, and other pericellular non-matrix proteins, resulting in the regulation of cell behavior, tissue development and remodeling [91], we hypothesized that MT1-MMP could directly degrade FGF-2 or, alternatively, its low and/or high affinity cell membrane receptors (HSPGs and/or FGFRs). FGF-2 signaling is activated by the interaction of FGF-2 with both FGFRs and HSPGs; therefore, the degradation of one or more of these molecules can interfere with the intracellular response.

Although MT1-MMP-mediated degradation of FGF-2 has not been demonstrated, it would be not surprising. This hypothesis was first supported by the finding that the C-terminal region of FGF-2 can be cleaved *in vitro* by trypsin and chymotrypsin [92]. Moreover, Goodman and colleagues have reported that the cell surface peptidase neprilysin can cleave FGF-2, with its subsequent inactivation, loss of any detectable receptor binding activity, and inhibition of angiogenesis both *in vitro* and *in vivo* [93].

In addition, a study published in 1996 showed that FGFR-1 is a specific target for MMP-2 on the cell surface. MMP-2 can specifically hydrolyze the Val^{368}-Met^{369} peptide bond in

the FGFR-1 ectodomain, eight amino acids upstream of the transmembrane domain, and thus release the entire extracellular domain in the form of a soluble FGF receptor [94].
Finally, since soluble and membrane-bound HSPGs also act as co-receptors for FGF-2, their degradation by proteolytic or glycosidic degrading enzymes can modify FGF-2 signaling, affecting cell proliferation and migration [60,95].
The findings reported in this thesis show that MT1-MMP does not degrade FGF-2, but downregulates FGF-2 binding to the cell surface.
To test the hypothesis that MT1-MMP degrades FGF-2 by MT1-MMP we first performed a time-course experiment with MCF-7 cells. We found that whereas maximum ERK1/2 activation occurred after 5 min of FGF-2 treatment and rapidly decreased, the amount of cell-associated FGF-2 increased in a time-dependent manner. The discrepancy between level of ERK1/2 activation and amount of cell-associated FGF-2 can be explained by the typical FGF-2 - FGFR interaction and by the concentration of FGF-2 used in the experiment. As expected, the binding of a growth factor to its receptor rapidly activates intracellular signal transduction pathways, which are subsequently downregulated by cytoplasmic phosphatases. This effect explains why the levels of phosphorylation of intracellular signaling proteins normally decrease in a time-dependent manner. In addition, although 30 ng/ml is the best working concentration to detect FGF-2 binding to cells by Western blotting, it is about 3 times as high as the concentration required to saturate all cell surface receptors.
Our experiments showed that ERK1/2 phosphorylation levels and the amount of cell-associated FGF-2 were lower in MT1-MMP-expressing cells than in cells devoid of MT1-MMP. However, we did not find any MT1-MMP-dependent difference in the level of FGF-2 present in the conditioned medium of the treated cells. Notably, if the hypothesis that MT1-MMP degrades FGF-2 were correct, one or more degradation products and/or bands with lower molecular weight than native FGF-2 should have been detected by Western blotting. We found no evidence of such degradation products.
Taken together, these initial observations showed that MT1-MMP-expressing cells bound less FGF-2 on their surface than cells devoid of MT1-MMP, but did not show any FGF-2 degradation by MT1-MMP. Since the monoclonal anti-FGF-2 antibody we used for our Western blotting analysis interacts with a specific region of FGF-2, if this region is cleaved the binding between antibody and FGF-2 could be prevented, and no FGF-2 could be identified by Western blotting. Moreover, the antibody detects both intracellular and cell surface associated FGF-2. To obviate these limitations, we labeled recombinant FGF-2 with biotin. This approach offered at least two advantages: first, biotin could react with the numerous lysine and arginine residues of FGF-2; in addition, the sulfated-biotin we used did not permeate cell membranes, therefore only extracellular, membrane-bound FGF-2 was labeled. However, the finding that in our experiments biotin alone activated ERK1/2 as well as biotinylated FGF-2 complicated our approach. This experimental

problem could be explained by the fact that the amount of FGF-2 biotinylated (10 µg) was approximately 100-fold smaller than the quantity (1 mg) usually suggested for the labeling reaction with biotin; the small amount of FGF-2 available for labeling prevented the purification of the biotinylated FGF-2 (which would be lost during the purification procedures) and therefore the labeled protein contained an excess of biotin. Moreover, the biotinylated FGF-2 activated ERK1/2 less efficiently than the unlabeled molecule. These limitations prevented the use of biotinylated FGF-2 for our subsequent experiments.

We therefore adopted an alternative strategy. MCF-7 clone 8 cells were treated with FGF-2, after which all cell surface proteins including FGF-2 bound to HSPGs and FGFRs were biotinylated. Subsequently the biotinylated FGF-2 was immunoprecipitated and detected by Western blotting using streptavidin, which binds biotin with high affinity. The amount of biotinylated FGF-2 detected by this method was lower in MT1-MMP-expressing cells than in cells with no MT1-MMP. This result was consistent with our previous observations using anti-FGF-2 antibody; however, the difference between cells with or without MT1-MMP was much more evident because the cell biotinylation approach allowed us to detect only cell surface-associated FGF-2, whereas Western blotting of cell extracts with anti-FGF-2 antibody detects both cell surface-associated and intracellular FGF-2. These experiments therefore showed that catalytically active MT1-MMP inhibits FGF-2 binding to the surface of MCF-7 cells.

To investigate whether MT1-MMP controls FGF-2 binding to its low- or high-affinity receptors, we sought to detach FGF-2 from the cell surface by washing FGF-2 treated cells with either 2 M NaCl, pH 7.5 or 2 M NaCl, pH 4.0. Because of their different ionic strength, these solutions remove FGF-2 from HSPGs or FGFRs, respectively [82]. The effective detachment of FGF-2 from the cell surface was demonstrated by the presence of very faint bands corresponding to FGF-2 in extracts of the cells after the 2 M NaCl washings. Interestingly, when the cells were washed with 2 M NaCl at pH 7.5, FGF-2 was detected in the washings only if the cells did not express MT1-MMP, indicating that the amount of FGF-2 bound to the HSPGs in these cells was higher than in cells expressing MT1-MMP and that MT1-MMP activity controls FGF-2 binding to HSPGs. Conversely, when the cells were washed with 2 M NaCl at pH 4.0, no FGF-2 was detected in the washings, probably because the number of FGFRs was much lower than that of HSPGs molecules, and - under these experimental conditions - the amount of the FGF-2 detached from the FGFRs was possibly below the sensitivity limit of the Western blotting.

Further work is warranted to identify the FGF-2 binding sites degraded by MT1-MMP and understand the effect of decreased FGF-2 binding on tumor cell functions such as proliferation, migration and apoptosis.

However, we performed a preliminary experiment to investigate whether decreased FGF-2 binding affects cell proliferation. MCF-7 cells treated for 3 days with FGF-2 showed a

50% increase in proliferation relative to the untreated cells; however, no differences in cell proliferation were observed between MT1-MMP expressing and non-expressing cells.

It is important to consider here that HSPGs are not only necessary to facilitate the formation of the FGF-2 - FGFRs complex, but can positively or negatively regulate FGF-2 signaling. The HS-binding regions of FGF-2 and FGFRs require different structural motifs within the HS chains for binding. These differences explain why HS can modulate signaling in multiple ways. A particular HS that binds both FGF-2 and FGFR(s) acts as a stimulator, whereas a HS that only binds FGF-2 inhibits the signaling by sequestering the growth factor. Tight regulation is achieved by a balance of HSPGs that either stimulate or inhibit FGF-2 binding to its FGFRs [96]. HSPGs can have important functions in tumor biology, by regulating mediators of tumor cell survival, proliferation, migration and invasion. The specific effects of both cell surface and soluble HSPGs also depend on tumor cell type, so that they can stimulate cell growth, survival and migration in some cells but elicit apoptosis or additional cell functions in others [97].

In breast carcinoma syndecan-1 and -4, the most abundant cell surface HSPGs in this tumor, have an increased ability to promote the assembly of the FGF-2 - FGFR-1 complex compared with normal mammary epithelial cells [98].

Syndecans can also function as soluble HSPGs as their extracellular domain, consisting of the HS chains, can be released from the cell surface by a process known as ectodomain shedding [99]. Syndecan shedding can be induced by both MMPs [100,101] and the HS-degrading enzyme HPSE [102].

Among the MMPs, MT1-MMP expressed by stromal fibroblasts can directly cleave syndecan-1 on the cell surface and release the ectodomain, which in turn stimulates breast carcinoma cell proliferation [103]. The shedding of syndecan-1 mediated by MT1-MMP can also stimulate cell migration in a fibrosarcoma tumor model [95].

In conclusion, the data reported here show that, in an *in vitro* model of breast adenocarcinoma, MT1-MMP can affect FGF-2 activation of ERK1/2 signaling, an effect resulting from decreased FGF-2 binding to its low- and perhaps also high-affinity receptors.

Subsequently, the link between MT1-MMP and FGF-2 signaling was investigated in the pediatric glioma cell lines. The purpose of this investigation was to study whether the novel mechanism of control of FGF-2 by MT1-MMP observed in the MCF-7 breast carcinoma cell line was also effective in these cells.

Although it is known that both MT1-MMP [47,104] and FGF-2 [105] are expressed in adult gliomas, no information regarding the pediatric counterparts was available. For this reason, we first characterized the expression of these proteins in all the pediatric cell lines.

UW479 and Res186 cells expressed high levels of MT1-MMP, whereas in SF188 and Res259 cells the expression levels were moderate, and in KNS42 cells no protein was detected. In all MT1-MMP positive cells MT1-MMP migrated in SDS PAGE as a single band of approximately 57 kDa, and no degradation products with lower molecular weight were detected. This observation indicated that in these cells MT1-MMP was expressed in its inactive, proenzyme form.

The analysis of FGF-2 expression showed that Res186 cells produce high levels of both the low- and high-molecular weight forms (17 kDa and 22 kDa, respectively) of this growth factor. Conversely, KNS42 cells expressed low levels of FGF-2, and the other cell lines showed no detectable FGF-2 expression.

No correlation was apparent between MT1-MMP and/or FGF-2 expression and the aggressiveness of the original tumors. Interestingly, Res186 cells, which derive from a benign, grade I pilocytic astrocytoma, expressed high levels of HPSE, MT1-MMP and FGF-2. This finding contrasts with previous reports [39,59,106] demonstrating that the expression of HPSE, MT1-MMP and FGF-2 generally correlates with a more aggressive tumor phenotype and poor prognosis.

Since MT1-MMP is the physiological membrane activator of proMMP-2 [107], MMP-2 activation can be used as an indirect method to understand whether MT1-MMP is expressed by cells in its activated form. Gelatin zymography analysis of glioma cell culture supernatants showed that SF188, Res259 and Res186 cells express proMMP-2, whereas no MMP-2 was detected in the other cell lines. To understand whether MT1-MMP is produced by UW479 and Res186 cells in its active form, these cells were incubated with medium conditioned by BCE cells, which contains proMMP-2, and the culture supernatant was analyzed for MMP-2 activation by gelatin zymography. The results showed that neither cell line activates MMP-2.

The Western blotting finding of only one band corresponding to MT1-MMP and the absence of MMP-2 activation demonstrate unequivocally that UW479 and Res186 cells express inactive MT1-MMP.

The subsequent aim of the study was to analyze ERK1/2 activation and understand whether it correlates with MT1-MMP expression similarly to what was observed in MCF-7 cells. For this purpose we first characterized the mRNA expression levels of the four *FGFRs*. In adult gliomas at least three FGFRs are expressed [77]. We found that each pediatric cell line expressed the mRNA of at least one *FGFR*; *FGFR-1* being the only FGF receptor expressed in all the cell lines.

In SF188, KNS42 and Res259 cells, the levels of ERK1/2 activation by FGF-2 were very high and more elevated than in the other cell lines, which do not express MT1-MMP. In agreement with the results obtained with MCF-7 cells, ERK1/2 activation inversely correlated with MT1-MMP expression, although MT1-MMP was in its inactive form. However, unlike in MCF-7 cells, in all glioma cell lines the levels of ERK1/2 activation

by FGF-2 were decreased in cells in which MMPs, including MT1-MMP, were inhibited by Ilomastat or 1,10-phenantroline. Moreover, the amount of cell-associated FGF-2 was similarly decreased in Res186 cells treated with an MMP inhibitor. These results contrast with those obtained with MCF-7 cells. Since both Ilomastat and 1,10-phenantroline are selective inhibitors of the catalytic activity of MMPs, our findings suggest that MMP activity can enhance ERK1/2 activation by FGF-2 in pediatric gliomas. In addition, in these cells MT1-MMP is either not expressed or is expressed in its inactive, proenzyme form, indicating that other MMPs could be involved in this process. Among the MMPs, MMP-3 and -10 were shown to be implicated in the pathogenesis of astrocytomas [108,109]. To investigate whether MT1-MMP contributes to ERK1/2 activation, MT1-MMP expression should be inhibited, for example by silencing, in the glioma cell lines that express this proteinase.

Interestingly, in KNS42 and Res259 cells transiently transfected with wt MT1-MMP, MT1-MMP degradation products generated by auto-catalysis were detected by Western blotting. In addition, medium conditioned by these cells showed partial activation of MMP-2, indicating that the transfected MT1-MMP was expressed in its active form. However, both cell lines showed no differences in ERK1/2 activation by FGF-2 after transfection with wt or a proteolytically inactive MT1-MMP mutant (E240A). Furthermore, in KNS42 cells transfected with the E240A MT1-MMP mutant, the amount of cell-associated FGF-2 was higher than in cells transfected with wt MT1-MMP, as occurs in MCF-7 cells. The opposite result was obtained with Res259 cells.

All the glioma cell lines showed a very high growth rate both in the presence and in the absence of FGF-2. SF188 and KNS42 cells were the most responsive to this growth factor, whereas the effect of FGF-2 on the UW479 and Res259 cell proliferation was moderate, and absent on Res186 cells, probably because these cells expressed high levels of FGF-2. With the exception of Res259 cells, the increase in cell proliferation induced by FGF-2 was more pronounced in cells that do not express MT1-MMP.

The expression of TIMP-2 - the physiological inhibitor of MT1-MMP [110] - in the glioma cell lines was comparable to that of MCF-7 cells, in which it is not sufficiently high to inhibit MT1-MMP activity. Since in MCF-7 cells it is known that MT1-MMP - TIMP-2 interaction induces ERK1/2 activation [43], all the glioma cell lines were treated with recombinant TIMP-2. This treatment induced ERK1/2 activation in all the cell lines, but no correlation was apparent between ERK1/2 activation and MT1-MMP expression.

To further characterize the MT1-MMP – TIMP-2 interaction in glioma cell lines, the MT1-MMP expressing UW479 and Res186 cells were treated with TIMP-2 in the presence of Ilomastat. With UW479 cells no differences in ERK1/2 activation by TIMP-2 were observed in the presence or in the absence of Ilomastat. In contrast Ilomastat reduced ERK1/2 activation by TIMP-2 in Res186 cells, with an effect similar to that obtained in MCF-7 cells [43]. These results indicate that TIMP-2 can also have MMP-

independent functions, including binding to cell surface proteins other than MT1-MMP and thereby activating intracellular signaling [111].

In conclusion, the data reported in this thesis show that the proteolytic activity of MT1-MMP inhibits ERK1/2 activation by FGF-2 and reduces FGF-2 binding to the cell surface of human MCF-7 breast adenocarcinoma cells. Although preliminary experiments highlight the possible involvement of HSPGs, more experimental evidences is warranted in order to identify the FGF-2 binding sites degraded by MT1-MMP and understand the effect of decreased FGF-2 binding on tumor cell functions.

The characterization of five pediatric astrocytoma cell lines has also provided new insights into the knowledge of this poorly studied group of tumors. We could find no clear correlation between HPSE, MT1-MMP or FGF-2 expression and the aggressiveness of these tumor cells. Our results showed that *HPSE* silencing in a pediatric glioblastoma cell line does not affect cell proliferation, but upregulates *MMP-2* and *MT1-MMP* expression, probably to compensate for the reduced HPSE activity. In these pediatric glioma cells ERK1/2 activation appears to inversely correlate with MT1-MMP expression, although endogenous MT1-MMP was expressed in its inactive, proenzyme form. In all the glioma cell lines, ERK1/2 activation by FGF-2 was higher in cells in which MMP activities were not inhibited, suggesting a possible involvement of MMPs other than MT1-MMP. Although cells transfected with wt MT1-MMP expressed this proteinase in its active form, we detected no differences in ERK1/2 activation by FGF-2. In addition, our results indicated that in these cells TIMP-2 may have signaling functions independent of MT1-MMP.

The significant differences between the pediatric glioma cell lines and the breast adenocarcinoma cell line used in this study are likely to reflect the different origin of glial and epithelial tumors, as well as the profoundly different composition of the extracellular environment within the brain, and the expression of proteases, heparanase, growth factors, receptors, HSPGs, and other molecules. Therefore, a detailed understanding of the specific mechanisms that control glioma cells proliferation and invasion can have important implications for the development of novel therapeutic strategies for the management of pediatric gliomas.

Bibliography

1. Ohgaki H, Kleihues P. Epidemiology and etiology of gliomas. Acta Neuropathol. (2005) 109:93-108.
2. Pollack IF. Brain tumors in children. N Engl J Med. (1994) 331:1500-1507.
3. Buckner JC, Brown PD, O'Neill BP, Meyer FB, Wetmore CJ, Uhm JH. Central nervous system tumors. Mayo Clin. Proc. (2007) 82(10):1271-1286.
4. Pollack IF, Jakacki RI. Childhood brain tumors: epidemiology, current management and future directions. Nat Rev Neurol. (2011) 7:495-506.
5. Louis DN, Ohgaki H, Wiestler OD, Cavenee WK, Burger PC, Jouvet A *et al*. The 2007 WHO classification of tumours of the central nervous system. Acta Neuropathol. (2007) 114:97-109.
6. Kaatsch P, Rickert C, Kühl J, Schüz J, Michaelis J. Population based epidemiologic data on brain tumors in German children. Cancer. (2001) 92(12):3155-3164.
7. Pfister S, Hartmann C, Korshunov A. Histology and molecular pathology of pediatric brain tumors. J Child Neurol. (2009) 24:1375-1386.
8. Westphal M, Lamszus K. The neurobiology of gliomas: from cell biology to the development of therapeutic approaches. Nat Rev Neurosci. (2011) 12(9):495-508.
9. Burkhard C, Di Patre PL, Schüler D, Schüler G, Yaşargil MG, Yonekawa Y *et al*. A population-based study of the incidence and survival rates in patients with pilocytic astrocytoma. J Neurosurg. (2003) 98(6):1170-4.
10. Riemenschneider MJ, Reifenberger G. Molecular neuropathology of gliomas. Int J Mol Sci. (2009) 10:184-212.
11. Reddy AT. Advances in biology and treatment of childhood brain tumors. Curr Neurol Neurosci Rep. (2001) 1(2):137-143.
12. Sievert AJ, Fisher MJ. Pediatric low-grade gliomas. J Child Neurol. (2009) 24(11): 1397-1408.
13. Reddy AT, Wellons JC. Pediatric high-grade gliomas. Cancer J. (2003) 9(2):107-112.
14. Gutmann DH. Using neurofibromatosis-1 to better understand and treat pediatric low-grade glioma. J Child Neurol. (2008) 23(10):1186-1194.
15. Dasgupta B, Yi Y, Chen DY, Weber JD, Gutmann DH. Proteomic analysis reveals hyperactivation of the mammalian target of rapamycin pathway in neurofibromatosis 1-associated human and mouse brain tumors. Cancer Res. (2005) 65(7):2755-2760.
16. Janzarik WG, Kratz CP, Loges NT, Olbrich H, Klein C, Schäfer T *et al*. Further evidence for a somatic KRAS mutation in a pilocytic astrocytoma. Neuropediatrics. (2007) 38(2):61-63.
17. Felix CA, Slavc I, Dunn M, Strauss EA, Phillips PC, Rorke LB *et al.* p53 gene mutations in pediatric brain tumors. Med Pediatr Oncol. (1995) 25(6):431-436.
18. Pfister S, Janzarik WG, Remke M, Ernst A, Werft W, Becker N *et al*. BRAF gene duplication constitutes a mechanism of MAPK pathway activation in low-grade astrocytomas. J Clin Invest. (2008) 118(5):1739-1749.

19. Mariani L, Deiana G, Vassella E, Fathi AR, Murtin C, Arnold M *et al*. Loss of heterozygosity 1p36 and 19q13 is a prognostic factor for overall survival in patients with diffuse WHO grade 2 gliomas treated without chemotherapy. J Clin Oncol. (2006) 24(29):4758-4763.
20. Rickert CH, Strater R, Kaatsch P, Wassmann H, Jürgens H, Dockhorn-Dworniczak B *et al*. Pediatric High-Grade Astrocytomas Show Chromosomal Imbalances Distinct from Adult Cases. Am J Pathol. (2001) 158(4):1525-1532.
21. Raffel C, Frederick L, O'Fallon JR, Atherton-Skaff P, Perry A, Jenkins RB *et al*. Analysis of oncogene and tumor suppressor gene alterations in pediatric malignant astrocytomas reveals reduced survival for patients with PTEN mutations. Clin Cancer Res. (1999) 5(12):4085-4090.
22. Wang Y, Yang J, Zheng H, Tomasek GJ, Zhang P, McKeever PE *et al*. Expression of mutant p53 proteins implicates a lineage relationship between neural stem cells and malignant astrocytic glioma in a murine model. Cancer Cell. (2009) 15(6):514-526.
23. Sung T, Miller D, Hayes R, Alonso M, Yee H, Newcomb EW. Preferential inactivation of the p53 tumor suppressor pathway and lack of EGFR amplification distinguish de novo high grade pediatric astrocytomas from de novo adult astrocytomas. Brain Pathol. (2000) 10(2):249-259.
24. Faury D, Nantel A, Dunn SE, Guiot MC, Haque T, Hauser P *et al*. Molecular profiling identifies prognostic subgroups of pediatric glioblastoma and shows increased YB-1 expression in tumors. J Clin Oncol. (2007) 25(10):1196-1208.
25. Fisher PG, Tihan T, Goldthwaite PT, Wharam MD, Carson BS, Weingart JD *et al*. Outcome analysis of childhood low-grade astrocytomas. Pediatr Blood Cancer. (2008) 51(2):245-250.
26. Karajannis M, Allen JC, Newcomb EW. Treatment of pediatric brain tumors. J Cell Physiol. (2008) 217(3):584-589.
27. MacDonald TJ, Aguilera D,Kramm CM. Treatment of high-grade glioma in children and adolescents. Neuro-Oncol. (2011) 13(10):1049-1058.
28. Giese A, Westphal M. Glioma invasion in the central nervous system. Neurosurgery. (1996) 39(2):235-250; discussion 250-252.
29. Gundelfinger ED, Frischknecht R, Choquet D, Heine M. Converting juvenile into adult plasticity: a role for the brain's extracellular matrix. Eur J Neurosci. (2010) 31:2156-2165.
30. Dityatev A, Seidenbecher CI, Schachner M. Compartmentalization from the outside: the extracellular matrix and functional microdomains in the brain. Trends Neurosci. (2010) 33(11):503-512.
31. Onishi M, Ichikawa T, Kurozumi K, Date I. Angiogenesis and invasion in glioma brain tumor. Pathol (2011) 28:13-24.
32. Tate MC, Aghi MK. Biology of Angiogenesis and Invasion in Glioma Neurotherapeutics. (2009) 6(3):447-457.
33. Kessenbrock K, Plaks v, Werb Z. Matrix Metalloproteinases: Regulators of the tumor microenvironment. Cell. (2010) 141(1):52-67.
34. Bourboulia D, Stetler-Stevenson WG. Semin Cancer Biol. Matrix metalloproteinases (MMPs) and tissue inhibitors of metalloproteinases (TIMPs):

positive and negative regulators in tumor cell adhesion. Semin Cancer Biol. (2010) 20(3):161-168.
35. Nagase H, Visse R, Murphy G. Structure and function of matrix metalloproteinases and TIMPs. Cardiovasc Res. (2006) 69(3):562-573.
36. Egeblad M, Werb Z. New functions for the matrix metalloproteinases in cancer progression. Nat Rev Cancer. (2002) 2(3):161-174.
37. Barbolina MV, Stack MS. Membrane type 1-matrix metalloproteinase: substrate diversity in pericellular proteolysis. Semin Cell Dev Biol. (2008) 19(1):24-33.
38. Holmbeck K, Bianco P, Yamada S, Birkedal-Hansen H. A Tethered Collagenase. J Cell Physiol. (2004) 200(1):11-19.
39. Itoh Y, Seiki M. MT1-MMP: a potent modifier of pericellular microenvironment. J Cell Physiol. (2006) 206(1):1-8.
40. Strongin AY. Proteolytic and non-proteolytic roles of membrane type-1 matrix metalloproteinase in malignancy. Biochim Biophys Acta. (2010) 1803(1):133-141
41. Remacle A, Murphy G, Roghi C. Membrane type I-matrix metalloproteinase (MT1-MMP) is internalised by two different pathways and is recycled to the cell surface. J Cell Sci (2003) 116:3905-3916.
42. Gingras D, Béliveau R. Emerging concepts in the regulation of membrane-type 1 matrix metalloproteinase activity. Biochim Biophys Acta. (2010) 1803(1):142-150.
43. D'Alessio S, Ferrari G, Cinnante K, Scheerer W, Galloway AC, Roses DF *et al*. Tissue inhibitor of metalloproteinases-2 binding to membrane-type 1 matrix metalloproteinase induces MAPK activation and cell growth by a non-proteolytic mechanism. J Biol Chem. (2008) 283(1):87-99.
44. Zarrabi K, Dufour A, Li J, Kuscu C, Pulkoski-Gross A, Zhi J *et al*. Inhibition of matrix metalloproteinase 14 (MMP-14)-mediated cancer cell migration. J Biol Chem. (2011) 286(38):33167-33177.
45. Cho JA, Osenkowski P, Zhao H, Kim S, Toth M, Cole K *et al*. The inactive 44-kDa processed form of membrane type 1 matrix metalloproteinase (MT1-MMP) enhances proteolytic activity via regulation of endocytosis of active MT1-MMP. J Biol Chem. (2008) 283(25):17391-17405.
46. Sato H, Takino T. Coordinate action of membrane-type matrix metalloproteinase-1 (MT1-MMP) and MMP-2 enhances pericellular proteolysis and invasion. Cancer Sci. (2010) 101(4):843-847.
47. Xie H, Xue YX, Liu LB, Wang P, Liu YH, Ying HQ. Expressions of matrix metalloproteinase-7 and matrix metalloproteinase-14 associated with the activation of extracellular signal-regulated kinase1/2 in human brain gliomas of different pathological grades. Med Oncol. (2011) 1:433-438.
48. Snuderl M, Chi SN, De Santis SM, Stemmer-Rachamimov AO, Betensky RA, De Girolami U *et al*. Prognostic value of tumor microinvasion and metalloproteinases expression in intracranial pediatric ependymomas. J Neuropathol Exp Neurol. (2008) 67(9):911-920.
49. Bernfield M, Götte M, Park PW, Reizes O, Fitzgerald ML, Lincecum J *et al*. Functions of cell surface heparan sulfate proteoglycans. Annu Rev Biochem. (1999) 68:729-777.
50. Watanabe A, Mabuchi T, Satoh E, Furuya K, Zhang L, Maeda S *et al*. Expression of syndecans, a heparan sulfate proteoglycan, in malignant gliomas: participation of

nuclear factor-kappaB in upregulation of syndecan-1 expression. J Neurooncol. (2006) 77(1):25-32.
51. Steck PA, Moser RP, Bruner JM, Liang L, Freidman AN, Hwang TL *et al*. Altered expression and distribution of heparan sulfate proteoglycans in human gliomas. Cancer Res. (1989) 49(8):2096-2103.
52. Toyoshima M, Nakajima M. Human heparanase. Purification, characterization, cloning, and expression. J Biol Chem. (1999) 274(34):24153-24160.
53. Vlodavsky I, Friedmann Y, Elkin M, Aingorn H, Atzmon R, Ishai-Michaeli R *et al*. Mammalian heparanase: gene cloning, expression and function in tumor progression and metastasis. Nat Med. (1999) 5(7):793-802.
54. McKenzie EA. Heparanase: a target for drug discovery in cancer and inflammation. Br J Pharmacol. (2007) 151(1):1-14.
55. Parish CR, Freeman C, Hulett MD. Heparanase: a key enzyme involved in cell invasion. Biochim Biophys Acta. (2001) 1471(3):M99-108.
56. Ilan N, Elkin M, Vlodavsky I. Regulation, function and clinical significance of heparanase in cancer metastasis and angiogenesis. Int J Biochem Cell Biol. (2006) 38(12):2018-2039.
57. Vlodavsky I, Ilan N, Nadir Y, Brenner B, Katz BZ, Naggi A *et al*. Heparanase, heparin and the coagulation system in cancer progression. Thromb Res. (2007) 120(2):S112-120.
58. Xu X, Quiros RM, Maxhimer JB, Jiang P, Marcinek R *et al*. Inverse correlation between heparan sulfate composition and heparanase-1 gene expression in thyroid papillary carcinomas: a potential role in tumor metastasis. Clin Cancer Res. (2003) 9:5968-5979.
59. Vlodavsky I, Elkin M, Abboud-Jarrous G, Levi-Adam F, Fuks L, Shafat I *et al*. Heparanase: one molecule with multiple functions in cancer progression. Connect Tissue Res. (2008) 49(3):207-210.
60. Xu X, Rao G, Quiros RM, Kim AW, Miao HQ, Brunn GJ *et al*. In vivo and in vitro degradation of heparan sulfate (HS) proteoglycans by HPR1 in pancreatic adenocarcinomas. Loss of cell surface HS suppresses fibroblast growth factor 2-mediated cell signaling and proliferation. J Biol Chem. (2007) 282(4):2363-2373.
61. Zetser A, Bashenko Y, Edovitsky E, Levy-Adam F, Vlodavsky I, Ilan N. Heparanase induces vascular endothelial growth factor expression: correlation with p38 phosphorylation levels and Src activation. Cancer Res. (2006) 66(3):1455-1463.
62. Nadir Y, Brenner B, Gingis-Velitski S, Levy-Adam F, Ilan N, Zcharia E. Heparanase induces tissue factor pathway inhibitor expression and extracellular accumulation in endothelial and tumor cells. Thromb Haemost. (2008) 99(1):133-141.
63. Ueno Y, Yamamoto M, Vlodavsky I, Pecker I, Ohshima K, Fukushima T. Decreased expression of heparanase in glioblastoma multiforme. J Neurosurg. (2005) 102(3):513-521.
64. Hong X, Nelson KK, de Carvalho AC, Kalkanis SN. Heparanase expression of glioma in human and animal models. J Neurosurg. (2010) 113(2):261-269.
65. Beenken A, Mohammadi M. The FGF family: biology, pathophysiology and therapy. Nat Rev Drug Discov. (2009) 8(3):235-253.

66. Mignatti P, Morimoto T, Rifkin DB. Basic fibroblast growth factor, a protein devoid of secretory signal sequence, is released by cells via a pathway independent of the endoplasmic reticulum-Golgi complex. J Cell Physiol. (1992) 151(1):81-93.
67. Mignatti P, Rifkin DB. Release of basic fibroblast growth factor, an angiogenic factor devoid of secretory signal sequence: a trivial phenomenon or a novel secretion mechanism? J Cell Biochem. (1991) 47(3):201-207.
68. Mignatti P, Morimoto T, Rifkin DB. Basic fibroblast growth factor released by single, isolated cells stimulates their migration in an autocrine manner. Proc Natl Acad Sci USA. (1991) 88(24):11007-11011.
69. Chlebova K, Bryja V, Dvorak P, Kozubik A, Wilcox WR, Krejci P. High molecular weight FGF2: the biology of a nuclear growth factor. Cell Mol Life Sci. (2009) 66(2):225-235.
70. Wesche J, Haglund K, Haugsten EM. Fibroblast growth factors and their receptors in cancer. Biochem J. (2011) 437(2):199-213.
71. Zhou M, Sutliff RL, Paul RJ, Lorenz JN, Hoying JB, Haudenschild CC, *et al*. Fibroblast growth factor 2 control of vascular tone. Nat Med (1998) 4:201-207.
72. Presta M, Dell'Era P, Mitola S, Moroni E, Ronca R, Rusnati M. Fibroblast growth factor/fibroblast growth factor receptor system in angiogenesis. Cytokine Growth Factor Rev. (2005) 16(2):159-178.
73. Jiang X, Couchman JR. Perlecan and tumor angiogenesis. J Histochem Cytochem. (2003) 51(11):1393-1410.
74. Ribatti D, Vacca A, Rusnati M, Presta M. The discovery of basic fibroblast growth factor/fibroblast growth factor-2 and its role in haematological malignancies. Cytokine Growth Factor Rev. (2007) 18(3-4):327-334.
75. Bremnes RM, Camps C, Sirera R. Angiogenesis in non-small cell lung cancer: the prognostic impact of neoangiogenesis and the cytokines VEGF and bFGF in tumours and blood. Lung Cancer. (2006) 51(2):143-158.
76. Yetgin S, Yenicesu I, Cetin M, Tuncer M. Clinical importance of serum vascular endothelial and basic fibroblast growth factors in children with acute lymphoblastic leukemia. Leuk Lymphoma. (2001) 42(1-2):83-88.
77. Loilome W, Joshi AD, ap Rhys CM, Piccirillo S, Vescovi AL, Gallia GL *et al*. Glioblastoma cell growth is suppressed by disruption of fibroblast growth factor pathway signaling. J Neurooncol. (2009) 94(3):359-366.
78. Bredel M, Pollack IF, Campbell JW, Hamilton RL. Basic fibroblast growth factor expression as a predictor of prognosis in pediatric high-grade gliomas. Clin Cancer Res. (1997) 3(11):2157-2164.
79. Tao J, Xiang JJ, Li D, Deng N, Wang H, Gong YP. Selection and characterization of a human neutralizing antibody to human fibroblast growth factor-2. Biochem Biophys Res Commun. (2010) 394(3):767-773.
80. Brown PD, Bloxidge RE, Anderson E, Howell A. Expression of activated gelatinase in human invasive breast carcinoma. Clin Exp Metastasis. (1993) 11(2):183-189.
81. Bax DA, Little SE, Gaspar N, Perryman L, Marshall L, Viana-Pereira M *et al*. Molecular and phenotypic characterisation of paediatric glioma cell lines as models for preclinical drug development. PLoS One. (2009) 4(4):e5209.
82. Moscatelli D. High and low affinity binding sites for basic fibroblast growth factor on cultured cells: absence of a role for low affinity binding in the stimulation of

plasminogen activator production by bovine capillary endothelial cells. J Cell Physiol. (1987) 131(1):123-130.
83. Tatevossian RG, Lawson AR, Forshew T, Hindley GF, Ellison DW, Sheer D. MAPK pathway activation and the origins of pediatric low-grade astrocytomas. J Cell Physiol. (2010) 222(3):509-514.
84. Gialeli C, Theocharis AD, Karamanos NK. Roles of matrix metalloproteinases in cancer progression and their pharmacological targeting. FEBS J. (2011) 278(1):16-27.
85. Arvatz G, Shafat I, Levy-Adam F, Ilan N, Vlodavsky I. The heparanase system and tumor metastasis: is heparanase the seed and soil? Cancer Metastasis Rev. (2011) 30(2):253-268.
86. Rowe RG, Weiss SJ. Navigating ECM barriers at the invasive front: the cancer cell-stroma interface. Annu Rev Cell Dev Biol. (2009) 25:567-595.
87. Zcharia E, Jia J, Zhang X, Baraz L, Lindahl U, Peretz T *et al*. Newly generated heparanase knock-out mice unravel co-regulation of heparanase and matrix metalloproteinases. PLoS One. (2009) 4(4):e5181.
88. Ferrara N, Gerber HP, LeCouter J. The biology of VEGF and its receptors. Nat Med. (2003) 9(6):669-676.
89. Gingras D, Bousquet-Gagnon N, Langlois S, Lachambre MP, Annabi B, Béliveau R. Activation of the extracellular signal-regulated protein kinase (ERK) cascade by membrane-type-1 matrix metalloproteinase (MT1-MMP). FEBS Lett. (2001) 507(2):231-236.
90. Onguchi T, Han KY, Chang JH, Azar DT. Membrane type-1 matrix metalloproteinase potentiates basic fibroblast growth factor-induced corneal neovascularization. Am J Pathol. (2009) 174(4):1564-1571.
91. Strongin AY. Mislocalization and unconventional functions of cellular MMPs in cancer. Cancer Metastasis Rev. (2006) 25(1):87-98.
92. Sommer A, Rifkin DB. Interaction of heparin with human basic fibroblast growth factor: protection of the angiogenic protein from proteolytic degradation by a glycosaminoglycan. J Cell Physiol. (1989) 138(1):215-220.
93. Goodman OB Jr, Febbraio M, Simantov R, Zheng R, Shen R, Silverstein RL *et al*. Neprilysin inhibits angiogenesis via proteolysis of fibroblast growth factor-2. J Biol Chem. (2006) 281(44):33597-33605.
94. Levi E, Fridman R, Miao HQ, Ma YS, Yayon A, Vlodavsky I. Matrix metalloproteinase 2 releases active soluble ectodomain of fibroblast growth factor receptor 1. Proc Natl Acad Sci USA. (1996) 93(14):7069-7074.
95. Endo K, Takino T, Miyamori H, Kinsen H, Yoshizaki T, Furukawa M *et al*. Cleavage of syndecan-1 by membrane type matrix metalloproteinase-1 stimulates cell migration. J Biol Chem. (2003) 278(42):40764-40770.
96. Guimond S, Maccarana M, Olwin BB, Lindahl U, Rapraeger AC. Activating and inhibitory heparin sequences for FGF-2 (basic FGF). Distinct requirements for FGF-1, FGF-2, and FGF-4. J Biol Chem. (1993) 268(32):23906-23914.
97. Teng YH, Aquino RS, Park PW. Molecular functions of syndecan-1 in disease. Matrix Biol. (2012) 31(1):3-16.

98. Mundhenke C, Meyer K, Drew S, Friedl A. Heparan sulfate proteoglycans as regulators of fibroblast growth factor-2 receptor binding in breast carcinomas. Am J Pathol. (2002) 160(1):185-194.
99. Hayashida K, Bartlett AH, Chen Y, Park PW. Molecular and cellular mechanisms of ectodomain shedding. Anat Rec. (2010) 293(6):925-937.
100. Brule S, Charnaux N, Sutton A, Ledoux D, Chaigneau T, Saffar L *et al*. The shedding of syndecan-4 and syndecan-1 from HeLa cells and human primary macrophages is accelerated by 101. SDF-1/CXCL12 and mediated by the matrix metalloproteinase-9. Glycobiology. (2006) 16(6):488-501.
101. Fears CY, Woods A. The role of syndecans in disease and wound healing. Matrix Biol. (2006) 25(7):443-456.
102. Purushothaman A, Chen L, Yang Y, Sanderson RD. Heparanase stimulation of protease expression implicates it as a master regulator of the aggressive tumor phenotype in myeloma. J Biol Chem. (2008) 283(47):32628-32636.
103. Su G, Blaine SA, Qiao D, Friedl A. Membrane type 1 matrix metalloproteinase-mediated stromal syndecan-1 shedding stimulates breast carcinoma cell proliferation. Cancer Res. (2008) 68(22):9558-9565.
104. Fillmore HL, VanMeter TE, Broaddus WC. Membrane-type matrix metalloproteinases (MT-MMPs): expression and function during glioma invasion. J Neurooncol. (2001) 53(2):187-202.
105. Maxwell M, Naber SP, Wolfe HJ, Hedley-Whyte ET, Galanopoulos T, Neville-Golden J *et al*. Expression of angiogenic growth factor genes in primary human astrocytomas may contribute to their growth and progression. Cancer Res. (1991) 51(4):1345-1351.
106. Korc M, Friesel RE. The role of fibroblast growth factors in tumor growth. Curr Cancer Drug Targets. (2009) 9(5):639-651.
107. Nagase H. Cell surface activation of progelatinase A (proMMP-2) and cell migration. Cell Res. (1998) 8(3):179-186.
108. Mercapide J, Lopez De Cicco R, Castresana JS, Klein-Szanto AJ. Stromelysin-1/matrix metalloproteinase-3 (MMP-3) expression accounts for invasive properties of human astrocytoma cell lines. Int J Cancer. (2003) 106(5):676-682.
109. Bodey B, Bodey B Jr, Siegel SE, Kaiser HE. Matrix metalloproteinase expression in childhood astrocytomas. Anticancer Res. (2000) 20(5A):3287-3292.
110. Visse R, Nagase H. Matrix metalloproteinases and tissue inhibitors of metalloproteinases: structure, function, and biochemistry. Circ Res. (2003) 92(8):827-839.
111. Walsh LA, Cepeda MA, Damjanovski S. Analysis of the MMP-dependent and independent functions of tissue inhibitor of metalloproteinase-2 on the invasiveness of breast cancer cells. J Cell Commun Signal. (2012) [Epub ahead of print].

Publications

1. **Tassone E**, Maran C, Masola V, Bradaschia A, Garbisa S, Onisto M. Antidepressant hyperforin up-regulates VEGF in CNS tumour cells. Pharmacol Res. (2011) 63(1):37-43.

2. Fassan M, **Tassone E**, Onisto M, Perilongo G, D'Avella D, Gardiman MP. MGMT promoter methylation in pediatric high-grade gliomas. Childs Nerv Syst. (2011) 27:7-8.

3. Masola V, Maran C, **Tassone E**, Zin A, Rosolen A, Onisto M. Heparanase activity in alveolar and embryonal rhabdomyosarcoma: implications for tumor invasion. BMC Cancer. (2009) 9:304.

4. Maran C, **Tassone E**, Masola V, Onisto M. The story of SPATA2 (Spermatogenesis-associated protein 2): from sertoli cells to pancreatic beta-cells. Curr Genomics. (2009) 10(5):361-363.